1971

Investigation of steady-state performance of bistable and proportional fluid amplifiers

Ramesh Gupta
Lehigh University

INVESTIGATION OF STEADY-STATE PERFORMANCE OF BISTABLE AND PROPORTIONAL FLUID AMPLIFIERS

Ramesh Gupta

ABSTRACT

A test-rig has been built which allows the determination of the steady-state performance of proportional and bistable amplifiers. The effect of supply pressure on the steady-state performance characteristics of two bistable amplifiers and one proportional amplifier has been investigated. Also investigated were the effects of acoustic noise on the performance characteristics of a bistable amplifier. One of the amplifiers tested was a commercially available standard element, two other amplifiers tested were of experimental type built by Harry Diamond Laboratories.

In the range of supply pressures tested, the best operating characteristics were found to correspond to the lowest supply pressure. There was a very slow deterioration of the performance of the amplifiers as the supply pressure was increased. By externally applying sound, the performance of a bistable amplifier was markedly changed.

INVESTIGATION OF STEADY-STATE PERFORMANCE OF BISTABLE AND PROPORTIONAL FLUID AMPLIFIERS

by

Ramesh Gupta

A Thesis

Presented to the Graduate Committee

of Lehigh University

in Candidacy for the Degree of

Master of Science

in

Mechanical Engineering

Lehigh University

1970

CERTIFICATE OF APPROVAL

This thesis is accepted and approved in partial fulfillment of the requirements for the degree of Master of Science in Mechanical Engineering.

October 16, 1970
(date)

James A. Bucknell
Professor in Charge

Ferdinand P. Beer
Chairman of Department

ACKNOWLEDGEMENTS

I wish to express my gratitude to my thesis advisor, Professor Jerzy A. Owczarek, for his guidance and valuable suggestions during the course of this work.

Also, I would like to express my thanks to Professor Donald O. Rockwell for his helpful suggestions, Frank J. Pechacek, Jr., for the construction of the apparatus and Grant Horn for the maintenance of the electrical equipment.

Thanks are due to Barbara DeLazaro for the typing of the thesis.

TABLE OF CONTENTS

LIST OF FIGURES

NOMENCLATURE

P_s	supply pressure
P_c	control pressure
P_o	output pressure
P_t	total pressure
P_{atm}	atmospheric pressure
m	mass flow rate
Q	volumetric flow rate
R	gas constant, impedance of the loudspeaker
Re	Reynolds number
S	Strouhal number
w	width of power jet
A	area of power jet
T_t	total temperature (absolute)
f	frequency, cycles/second
$\overline{U}$	average velocity of power jet

Suffixes

s	supply nozzle
o	output port
c	control port
ℓ, L	left port
r, R	right port

ABSTRACT

A test-rig has been built which allows the determination of the steady-state performance of proportional and bistable amplifiers. The effect of supply pressure on the steady-state performance characteristics of two bistable amplifiers and one proportional amplifier has been investigated. Also investigated were the effects of acoustic noise on the performance characteristics of a bistable amplifier. One of the amplifiers tested was a commercially available standard element, two other amplifiers tested were of experimental type built by Harry Diamond Laboratories.

In the range of supply pressures tested, the best operating characteristics were found to correspond to the lowest supply pressure. There was a very slow deterioration of the performance of the amplifiers as the supply pressure was increased. By externally applying sound, the performance of a bistable amplifier was markedly changed.

1. INTRODUCTION

The performance characteristics of one proportional and two bistable amplifiers are presented. The purpose of the performance curves is to provide performance data which can be used in fluid circuit design. The curves obtained permit the determination of steady state operating points of the amplifier, and of the gain.

Fluidic elements have been used in large numbers as system components. In order to ensure proper operation of fluidic circuits, it is necessary to use performance characteristics to match two or more devices properly. The most practical approach in obtaining the characteristics is to treat the amplifier as a black-box having one supply and two control inputs and two outputs. At a particular supply pressure the behavior of a fluidic device can be adequately described by three characteristic curves: control port input curve which defines the particular load that a control input signal feels when it is applied at the control ports, transfer curve which determines what happens to the output when a control signal is applied, and the output characteristic curve which shows the effect on the output signal on an externally applied load.

Numerous parameters affect the performances of fluidic elements. These have been extensively studied by various authors (1,2,3). When a black-box approach is used, one of

the parameters involved in the performance of fluidic elements is the supply pressure. Yong and Lapisa (4), in 1969, investigated the performance of amplifiers using a black-box approach. They obtained output characteristics for a zero control pressure differential at various supply pressures of a single proportional amplifier and of a three-stage device. The three-stage device had a much higher gain than the single element while the output flow was considerably less than that from the single element. For supply pressure varying from 5 psig to 25 psig, the pressure recovery of the element at a deadhead load (blocked output ports) was about 30% of the supply gage pressure. At higher supply pressures the losses increased and the pressure recovery decreased.

Taplin (5), analyzed a proportional amplifier by dividing it into simpler sections and then combining the simpler equivalent circuits into an overall circuit satisfying coupling requirements. The flow through the output ports was modeled by an equivalent circuit having a source stagnation pressure generator (stagnation tank) and an orifice-type restriction of some given area. Thus the output flow characteristics could be described by an equation used for flow through an orifice, that is a constant, say "k", multiplied by the square root of the pressure drop across the orifice. At various supply pressures and zero control pressure differential, a value of the constant "k" was computed which was used to calculate the flow through the output ports. The calculated values of the flows

agreed well with the experimental values. However, as the load pressure approached the stagnation pressure, the value of the stagnation pressure digressed from the predicted value. He developed a procedure that made it possible to calculate the no-load receiver flow for various control pressure differentials when the no-load receiver flow was known for zero control pressure differential together with the supply pressure. Using the value of "k", it was possible to evaluate the stagnation pressure with receiver blocked.

It would be very helpful to an engineer if a single parameter could be defined that can provide useful information from the system engineering and operating point of view. Boros and Helm (6), in 1970, introduced a complex characteristic index called the "quality index" that is a function of the fan-out, power jet mass flow rate, and of the switching time. It is a general practice in describing the geometry of the elements to give all dimensions as functions of the power jet width; similarly, the quantities involved in the quality index are all functions of the supply pressure. From their investigations, carried out on a commercially available element, they have found that the quality index has at least one maximum value at a particular supply pressure.

The fact that free jets are sensitive to sound has been known for about a hundred years. Sensitivity of jets has been mainly associated with laminar jets but recent developments have shown that jets at high Reynolds numbers can also be af-

fected by sound. A large part of the research on sound-sensitive jet has been conducted in the field of free jets or attached jet flows. Unfried (7) has shown on a Reynolds number-Strouhal number plot the sound-sensitive regions of wall jets. Roffman and Toda (8), in 1969, investigated the effect of sound on free jets and flueric devices. Their investigation involved introducing sound at right angles to a free jet and obtaining the velocity profiles of the jet. They observed that a spreading of the jet occurred on application of sound. For the range of Reynolds numbers observed, the spread could be increased with the influx of sound. At a given power jet pressure, the increase in the spread angle appeared to be dependent on the sound amplitude. In the range of frequencies for which a given jet is sensitive, a value of frequency exists at which the jet is most sensitive. In the case of attached jet flows, sound is known to affect the jet reattachment point to a Coanda wall. Weigner (9), in 1965, found that a sensitive frequency of very small amplitude may disturb an attached jet. In his experiments, increasing the sound amplitude moved the reattachment point upstream (towards the nozzle) until further increases of the sound amplitude resulted in the reattachment point moving downstream. Unfried investigated the switching of a bistable jet between two boundaries. The experiments were conducted with the jet marginally stable on one boundary. The author successfully operated acoustically activated flueric switches at sound frequencies of 400 to 4000 c.p.s. The velocity of the jets used

in the experiments was lower than that encountered in fluidic elements, and the cross-sectional areas of the jets were several times larger than those used in fluidic elements.

Since jets are sensitive to sound, it was decided to study the effects of sound on a fluid amplifier and to compare any changes in the characteristics determined without an external sound source.

2. EXPERIMENTAL EQUIPMENT AND PROCEDURES

2.1 Experimental Equipment

The amplifiers tested were:

1. Bistable amplifier Number 190471 of Corning Glass Works,

2. Bistable amplifier made at the Harry Diamond Laboratories,

3. Proportional amplifier made at the Harry Diamond Laboratories.

The nozzle dimensions of the bistable amplifier Number 190471 were .0254 ins. by .078 ins., for which the nominal aspect ratio could be taken as 3. The other bistable amplifier from the Harry Diamond Laboratories, had a convergent-divergent power nozzle. The dimensions of the throat were approximately .028 ins. by .060 ins., and at the exit of the nozzle were .030 ins. by .060 ins., which gives a nominal aspect ratio of 2. It was not possible to measure the dimensions of the proportional amplifier without destroying the amplifier.

A sketch of a proportional and of a bistable amplifier is shown in Figure 1. The schematics of the test rigs used are shown in Figures 2, 3, 4 and 5. The test rigs were positioned in a horizontal plane on a table. Each of the three amplifier

input ports was connected to a supply line that had a series of valves and regulators, a flow meter and a stagnation tank. The regulators used were: Model 40-15, with a range of 0 to 15 psig, for the power jet supply line, and Model 40-2, with a range of 0 to 50 inches of water, for the control port supply lines. Flow meters, made by S and K Instruments Company, in the supply lines gave a rough indication of the volumetric flow rates. The stagnation tanks placed upstream of the amplifier were used for stagnation pressure measurements. The stagnation tanks were one foot long, and had an inside diameter of 6 inches. The velocity of air in the tanks was very small so that the static pressure measured could be taken as the stagnation pressure without introducing any significant error. The load at the output ports was applied using two valves. When the valves were fully open there was no-load applied at the output ports.

A Venturi tube, made by the Fox Valve Development Company, was used to measure the flow rates. The pressure difference between the inlet to the Venturi tube and the throat is related to the flow rate. The stagnation pressure and the pressure difference related to the flow rate were recorded by an electromechanical method. Pressure transducers, Model 902-1 and Model 360 of the Decker Corporation, were used for these measurements. The output of the transducers was voltage that varied linearly with pressure over the experimental range of values. Digital voltmeters from Disa were connected to the

transducers to have accurate readouts. The outputs from the transducers were fed to an X-Y plotter, Model EAI-1125, manufactured by Electronic Associates, Incorporated, thus making it possible to record the variation of the flow rate with the stagnation pressure.

2.2 Experimental Procedures

Power Jet Characteristics

The schematic of the rig used in this test is shown in Figure 2. The output ports and the control ports were vented to the atmosphere. The supply pressure was varied from zero to 15 lbs/in^2, and the flow rate and supply pressure measured using water and mercury manometers. The temperature of the air was noted using a thermometer placed inside a stagnation tank.

Control Port Characteristics

The control jet characteristics were determined with a test set-up shown in Figure 3. The power jet supply pressure was held constant at a selected value and the control pressures varied. For proportional amplifiers, the inactive control port was held at a constant bias pressure. A bias pressure of 20% of supply pressure was selected for most of the tests. The value of the bias pressure selected allowed the amplifier to be tested over the full range of control input pressure differentials. In the case of bistable ampli-

fiers, the inactive control port was vented to the atmosphere. The variations of the active control port flow rate and of the control pressure were recorded on an X-Y plotter. The effect of loading the output ports, on the control jet characteristics, was also investigated at various supply pressures.

Output Characteristics

a) Proportional Amplifier

The output characteristics were obtained for the following operating conditions:

1. The control bias pressure was fixed at 20% of supply pressure.

2. The loading at the output ports was varied from zero to blocked-port conditions.

3. Power jet pressure was varied from 3.0 to 7.0 psig.

The schematic of the test-rig is shown in Figure 4. The supply pressure was fixed at a desired value and an equal bias pressure of 20% Ps was applied at each control port. At this zero control input pressure differential, the load was applied simultaneously at both output ports and the output pressure and flow rate recorded. The control input pressure differential was subsequently varied, while the bias pressure was held constant and a series of output characteristics were obtained at the particular supply pressure.

b) Bistable Amplifiers

The output characteristics of the bistable amplifiers were obtained under the following operating conditions:

1. Inactive control port was vented.

2. Resistance was varied from zero to blocked port conditions.

3. Active control port pressure was varied from zero to a maximum value.

4. Supply pressure was varied from 3.0 to 8.0 psig.

The schematic of the test rig is the same as shown in Figure 4, except that the inactive port was vented. At the beginning of each test the supply pressure was set at a desired value and the inactive control port vented. Then, the pressure in the active control port was increased until the jet switched; subsequently, the active control port gage pressure was decreased to zero again. Simultaneous equal loads were applied at the output ports until deadhead load was reached, and the variation of the output pressure with the flow recorded during the loading process. Subsequently additional tests were carried out keeping the active control port pressures at certain chosen values.

Differential Input-Output Curves

The test set-up used for obtaining the differential input-output curves is shown in Figure 5. These tests give an indication of the linearity and symmetry of proportional amplifiers and the hysteresis width for bistable amplifiers. In the case of proportional amplifiers, the supply pressure was fixed and an equal bias level applied at the control ports. For a fixed load, in our case for blocked ports, one control pressure was increased from the bias level to a maximum value and then reduced to the bias level again while the inactive control bias pressure was held constant. The variation of the pressure difference at the output ports with the pressure difference at the control ports was recorded. This test determined one-half of the input-output curve. The other half was obtained by reversing the role of the two control ports.

For bistable amplifiers the test set-up was the same, and the characteristic was obtained by venting the inactive control port and varying the pressure in the active control port from zero to a maximum and subsequently, after switching has occurred, reducing it back to zero.

Acoustic Tests

A speaker was placed inside an 8 inch internal diameter stagnation chamber as shown in the photograph (Figure 6). The speaker was connected to an amplifier and an oscil-

lator. The frequency and the amplitude of the signal were controlled using the oscillator. The output from the amplifier was fed to an oscilloscope and a trace of the input voltage to the speaker, monitored on the oscilloscope screen, was used to calculate the power supplied to the speaker.

a) Sound Introduced in the Power Jet

The stagnation chamber with the loudspeaker was connected to the power jet of the fluidic bistable amplifier, No. 190471. The supply pressure was fixed at a chosen value. To obtain the lower limit of frequencies that affected the performance of the fluid amplifier at a selected power input the frequency was increased continuously from 20 cycles/second until a significant change was observed in the performance characteristics when compared with that corresponding to no sound conditions. For the upper limit, the frequency was continuously decreased from 5000 c/s. With the sound introduced in the power jet the control jet and output port characteristics were recorded on an X-Y plotter as described previously.

b) Sound Introduced in a Control Jet

Sound was introduced in a control port by connecting the stagnation chamber with the loudspeaker to one of the control ports. It was not possible to obtain control jet characteristics because the Venturi tube used for the flow rate measurements acted as a damper of the acoustic signals.

Hence only the differential input-output curves were plotted.

The schematic of the test set-up is shown in Figure 5. The supply pressure was fixed and the differential input-output curves plotted without applying sound. The range of frequencies to which the fluidic amplifier tested was sensitive was determined in the following way: For the lower limit of the range, the pressure in the active left control port was increased until the jet switched to the right wall, and then reduced to zero again. The pressure in the right control port was increased to about three-quarters of that required to switch the jet. Sound was introduced through the right control port and the amplitude level on the oscillator was set at 40 and the frequency was increased from 20 c/s until the jet switched. To get the upper limit of the sensitive range, the frequency was decreased from 5000 c/s. As was mentioned previously, the differential input-output curves were first plotted without application of sound. On the same graph paper curves were subsequently plotted corresponding to a particular frequency chosen within the sensitive range and various amplitudes. A series of tests were carried out with supply pressures varying from 2.0 to 8.0 psig.

3. PARAMETERS USED IN DETERMINING PERFORMANCE CHARACTERISTICS

The mass flow rate was calculated using the standard equation of flow through Venturi tubes in reference 15. Compressibility effects were taken into consideration for the mass flow rate calculations. The characteristic curves have been plotted using dimensionless mass flow rate and dimensionless pressure. In the case of power jet the parameters plotted were (14):

$$\text{dimensionless mass flow rate} = \frac{\dot{m}_s \sqrt{RT_t}}{AP_t}$$

$$\text{dimensionless pressure} = \frac{P_s}{P_{atm}}$$

where P_s is the (absolute) supply pressure in pound per square inch.

For all other characteristics, the mass flow rate and the pressure were normalized with respect to the power jet mass flow rate and the supply pressure. The Reynolds numbers were calculated using the throat conditions and were based on the width of the power jet. The velocity at the throat was computed from the volumetric flow rate through the nozzle. The experimentally-determined power jet and control jet characteristic curves were compared with the curves calculated for compressible flow of a perfect fluid. In calculations in which incompressible fluid flow were assumed, the value of the den-

sity used was the average density corresponding to the supply and atmospheric pressures.

For the tests with sound, the Strouhal number S was defined as

$$S = \frac{fw}{\overline{U}}$$

Due to lack of sufficient equipment it was not possible to measure the frequency and the amplitude of the sound produced by the loudspeaker at the inlet to the power jet or the control jet of the fluidic amplifier. The frequencies used to calculate the Strouhal numbers were noted from the settings on the oscillator, and the average velocity, $\overline{U}$, at the exit of the supply nozzle was calculated using the measured volumetric flow rate. To obtain some indication of the power supplied to the air in the acoustic tests, measurements were made of the power supplied to the loudspeaker. The power supplied to the loudspeaker was defined as

$$\text{Power } E = \frac{V^2}{R}$$

where V = voltage (rms value)

R = impedance of the loudspeaker in ohms

The rms voltage supplied to the loudspeaker was calculated from the trace of the input voltage to the loudspeaker obtained on the oscilloscope. The impedance was assumed to be constant

and equal to 8 ohms as indicated on the loudspeaker. A photograph of the trace obtained on the oscilloscope is shown in Figure 7. As can be seen from the photograph, the sine wave input is distorted. The distortions were found to be very high frequency oscillations. When the loudspeaker was disconnected and a trace of the amplifier output obtained, there was no distortion of the sine wave output. Hence we can conclude that the distortions were due to the loudspeaker and the power supplied could be calculated assuming a sine wave input.

4. DISCUSSION AND RESULTS

4.1 Characteristic Curves of the Bistable Amplifier No. 190471 (Corning Glass Works)

Figure 8 shows the normalized power jet characteristics of the amplifier tested. The cross-sectional area of the power nozzle is one of the parameters used to normalize the mass flow rate. The dimensions of the nozzle throat were measured using a telescope. The throat of the nozzle was not in the form of a true rectangular section and the area calculated was about 25% greater than the nominal value given in the manufacturer's catalog. From the curve it can be seen that at pressures greater than about 9.0 psig ($P/P_{atm} = 1.6$), the mass flow rate parameter is nearly constant. For comparison, a curve corresponding to compressible flow of a perfect fluid in a convergent nozzle is superimposed on the supply characteristics. The difference between the two curves accounts for the losses between the stagnation tank and the amplifier inlet and in the nozzle. At the inlet to the amplifier the velocities of air were high and hence the inlet could account for a major share of the losses. The Reynolds numbers of the jet, based on the supply nozzle throat width and on the average flow speed at the nozzle exit, at supply pressures of 3.0, 5.0 and 8.0 psig were 625, 800 and 990, respectively.

Figure 9 shows the differential input-output characteristics at various supply pressures. These characteris-

tics were obtained under no-load conditions. The pressure difference at the output ports was nearly a constant fraction of the supply pressure, and was independent of the control input differential. Another interesting point about the curves is that they are symmetrical to a remarkable extent about both axes. As the load was increased, the pressure required to switch the jet decreased and at blocked ports the hysteresis loop virtually disappeared and the jet had a tendency to be unstable. The hysteresis effect in a fluidic bistable amplifier is a well defined phenomenon. It was found to be a function of the output loading.

Figure 10 is the input characteristic of the control port. When the active control port was closed a vacuum pressure of 20% to 30% of supply (gage) pressure existed due to the entrainment by the jet. At zero control port pressure the flow entrained by the jet was 15 to 20% of the supply flow rate. The figures show that during switching of the jet from one wall to the other, the pressure in the stagnation tank of the active control port remains constant as expected, while the mass flow rate decreases because the pressure at the control port exit becomes close to the atmospheric pressure. The decrease in the control port flow rate is due to decreased entrainment by the supply jet. Due to manufacturing imperfections the characteristics of the right and left control ports differ. The control port characteristics were found to be dependent on the load applied at the output ports.

When the output ports were blocked, the control port pressure required to switch the jet was very nearly equal to atmospheric pressure, and the jet had a tendency to be unstable at switching. Figure 16 shows the control port characteristics at a supply pressure of 3.0 psig as obtained on the X-Y plotter. The loading of the output ports results in an increase of the pressure in the interaction region. Thus a higher control port pressure is necessary to achieve the same mass flow rate when load is applied at the output ports as compared to the no-load conditions.

Figure 11, represents the output characteristics, obtained for both right and left output ports, of the bistable amplifier at various supply pressures. At a lower value of supply pressure ($P_s - P_{atm}$ = 3.0 psi) the variation of flow rate with output pressure was approximately linear except when the load applied at the output ports was nearly a deadhead load (no flow condition). At no load conditions, the mass flow rate through the output ports was in general greater than unity. The flow rates through the right and left output ports differ at corresponding control port pressures. The difference could be due to an asymmetry of the amplifier geometry. The maximum value of pressure recovered at zero control port (gage) pressures was about 26% of the supply pressure, and the value increased as the active control pressure was increased. Figure 17 shows the output characteristics as obtained on the X-Y plotter.

Figure 12 shows that the pressure recovered at the output ports decreases slightly with increasing supply pressure in the range tested. For the curves corresponding to zero control (gage) pressure, the variation of pressure recovered with supply pressure was somewhat smaller than that corresponding to the control pressure equal to $0.1(P_s - P_{atm})$. The decrease of the pressure recovery at the output ports with increasing supply pressure can be explained by increase in the losses of the interacting jets resulting from higher flow velocities. Figure 13 shows the variation, with the supply pressure, of the mass flow rate through the output ports at no load conditions. The mass flow rate is constant for supply pressures up to 6.0 psig and decreases gradually at higher supply (gage) pressures. The pressure recovered at the output port and the mass flow rate do not have maxima in the range of supply pressures tested. Figures 14 and 15 show the variation of the vacuum pressure created due to the entrainment produced by the jet and of the pressure required to switch the jet with the supply (gage) pressure, respectively. A vacuum (gage) pressure as high as $0.19(P_s - P_{atm})$ was observed in the right control port at a supply pressure 4.0 psig. It was caused by the entrainment effect of the jet. The control port pressure required to switch the jet has a maximum value at a supply pressure approximately equal to 6.5 psig. At the lowest operating supply pressure at which tests were made (3.0 psig) the losses, as well as the pressure required to switch the jet are smallest. From the performance

curves shown in Figures 12 to 15, it can be seen that the asymmetry in the geometry of the amplifier can have a significant effect on the amplifier characteristics. Hence, in the staging of elements it would be necessary to determine the input and output characteristics of each amplifier port to ensure proper matching of the elements. The effect of supply pressure on the performance characteristics of the bistable amplifier tested appears to be only marginal, except on the control port switching pressure (see Figures 12 to 15).

Figure 18 shows the control port characteristics, and Figure 19 shows the output characteristics of the amplifier tested evaluated assuming an incompressible flow. The volumetric flow rate is normalized using the power nozzle volumetric flow rate. On comparing the curves, with those obtained taking compressibility effects into consideration (Figures 10 and 11), it is found that the curves are similar. At corresponding pressures, the mass flow rate $(\frac{m_o}{m_s})$ is smaller than the volumetric flow rate $(\frac{Q_o}{Q_s})$. To calculate the volumetric flow rate through the supply nozzle the equation for incompressible flow through a Venturi tube was used, and the density was taken as the density corresponding to the average pressure based on the supply and atmospheric pressures. The performance curves based on the assumption that the flow is incompressible are not very accurate.

4.2 Characteristic Curves of Bistable Amplifier No. 2 (Made by the Harry Diamond Laboratories)

Figure 20 shows the power jet characteristics of the bistable amplifier No. 2. At supply pressures greater than 8.0 psig ($\frac{P_s}{P_{atm}} = 1.5$) the mass flow rate parameter was nearly constant. The maximum value of the mass flow rate was much closer to the value calculated for compressible flow of a perfect fluid in a convergent nozzle than in the case of amplifier No. 1. Figure 21 represents the differential input-output characteristics at various supply pressures under no load conditions. The pressure difference at the output ports was nearly constant. The control input pressure required to switch the jet decreases as the supply pressure was increased, and it was of the order of a few inches of water. When a dead-head load was applied at the output ports, the jet was unstable at a supply pressure of 3 psig and only marginally stable at higher supply pressures. The control port characteristics could not be obtained as the mass flow rate was very small and below the range that could be measured by our instruments. Thus, the power jet was switched from one wall to the other by the pressure applied at the control ports, rather than the momentum of the control jet. Figure 22 shows the output characteristics for both the left and right output ports of the amplifier at various supply pressures (3, 5 and 8 psig). The curves were obtained at three control pressures namely 0, 0.5 and 1.5 psig. As the control pressure was increased from zero the output pressure and the flow rate increased to a maximum,

and further increases in the control pressure resulted in a decrease of the output pressure and the flow rate. At a supply pressure of 5 psig, the output pressure at a deadhead load was greater at zero control port pressure than at a control pressure of 1.5 psig.

4.3 Characteristic Curves of the Proportional Amplifier (Made by the Harry Diamond Laboratories)

Figure 23, shows the power jet characteristics for the proportional amplifier tested. The mass flow rate is plotted in pounds per second as the cross-sectional area of the power nozzle was not known and could not be measured without destroying the element.

Figure 24 shows the differential input-output curves of the amplifier. Due to the asymmetry of the amplifier the curves do not pass through the origin which represents a null output pressure differential for zero control input pressure differential. The output differential pressure reaches a maximum at a control input differential pressure of about .15 ($P_s - P_{atm}$), and the characteristics are virtually independent of the supply pressure.

Figure 25 represents the input characteristics of the amplifier tested. The slope of the curves represent the input impedance of the amplifier. It is approximately constant at all supply pressures used. Also, the left and right control port characteristics are almost the same. This should be the

case for a good amplifier. Figure 26 shows the output characteristics of the proportional amplifier. At the left control port, the pressure recovery at a deadhead load is around 65% of the supply (gage) pressure at a zero pressure difference between the control ports, and is practically independent of the supply pressure. To obtain curves at various control port pressure differences, the following procedure was used. The pressure in one control port was increased by a certain value above the bias level and the pressure in the other control port was decreased below the bias level by the same amount. Thus the sum of the control pressure was always a constant. This procedure was used on the assumption that the amplifier tested was being driven by another amplifier. The output curves were obtained at a bias level of $.2(P_s - P_{atm})$ and at that bias level the control flows were 25 to 30% of the supply flow (see Figure 25). The sum of the dimensionless mass flow through the two output ports $(\frac{m_o}{m_s})$ was equal to the sum of the normalized supply and control flows, at all supply pressures. Thus virtually all the control flow went through the output ports and there was negligible flow through the vents.

4.4 Acoustic Tests on the Bistable Amplifier No. 1 (Corning Glass Works)

As was mentioned earlier, the amplitude and frequency of the applied sound could not be measured at the inlet to the amplifier. Figure 6 shows the loudspeaker in the stagnation chamber and the connections between the tank and the amplifier. The stagnation tank was connected to a $\frac{1}{2}$ inch I.D. tubing as shown. The length of the $\frac{1}{2}$ inch tubing between the tank and the amplifier was about one foot. Thus the acoustic noise at the inlet to the control port could be at a different frequency and amplitude than that at which the loudspeaker was driven.

a) Sound Applied in the Stagnation Tank of the Power Jet

Figure 27 shows the effect of sound on the output characteristics of the amplifier tested. The curves were obtained at a frequency of 500 c/s because at this frequency the jet was most sensitive to sound, at a supply pressure of 1.0 psig. At low amplitudes, the sound applied had very little effect on the output characteristics. At higher amplitudes the amplifier became unstable as the load was increased. Figure 28 shows the variation in the control port flow with the control port input pressure when sound at the frequency of 500 c/s was applied. As the amplitude of sound was increased the control port pressure required to switch the jet decreased. At low supply pressures (of the order of 1.0 psig) it was possible to switch the jet to either side of the ampli-

fier by applying sound (at 500 c/s) with both control ports vented. The amplifier characteristics were not affected by sound at higher supply pressures.

b) Sound Applied in the Stagnation Tank of the Control Port Jet

Figures 29, 30 and 31 are the differential input-output curves of the bistable amplifier tested at supply pressures of 2.0, 3.0 and 5.0 psig, respectively. The tests were conducted at various supply pressures over the sensitive range of frequencies. For supply pressures varying from 3.0 to 7.0 psig, the sound had an affect on the differential input-output curves, though it was more intense at lower supply pressures. The velocity of the power jet at the exit of the nozzle was in the range of 450 to 800 ft/sec.

The range of frequencies at which the amplifier is sensitive was observed to be between 350 to 560 cycles/second, at a maximum power input to the loudspeaker of about 4.5 watts, which corresponds to an amplitude setting of 40 on the oscillator. In the tests, sound was introduced through the right control port. From the figures, it can be seen that the effect of sound on switching the jet from the left wall to right wall is much greater than switching the jet from right to left. At an amplitude of 40 for frequencies of 350 and 400 c/s and an amplitude of 20 at 375 c/s, increasing the right control pressure switched the jet from the right wall to the

left and on decreasing the pressure the jet switched back to the right wall. Thus it was possible to control the switching from one control port only. At higher amplitudes and at supply pressures of 2.0, 3.0 and 5.0 psig, and frequencies of 375 cps, 500 cps and 370 cps, respectively, the differential input-output curves are completely changed. At the above frequencies the amplifier has no hysteresis loop and the jet could be stable attached to either wall. Figure 32 shows the characteristics as obtained on the X-Y plotter. When the application of sound produces no hysteresis loop, at zero control input pressure the pressure difference between the output ports was less than the corresponding pressure for the case when the hysteresis is present. At a certain value of control pressure the pressure difference at the output ports is zero in the case of no hysteresis loop. Possible explanation of this phenomenon could be that the jet spreading may be intense and the jet breaks up, thereby making it possible to obtain flow through both the output ports (9). If the jet is not attached to either wall it would strike the splitter and behave as in a proportional amplifier.

The Strouhal numbers corresponding to the sensitive range in our tests were of the order of .001 to .0025. These values are about a hundred times lower than those obtained by Rockwell and Toda (13) in the study of attached jet flows. Part of the explanation of this difference may be due to the fact that Rockwell and Toda, in their study, used wide jets which were not confined.

CONCLUSIONS

In the range investigated, the effect of the supply pressure on the performance characteristics was found to be small, except on the pressure required to switch the jet in one bistable amplifier. However, as the supply pressure was increased there was a definite deterioration of the performance characteristics. The variations of performance parameters with the supply pressure do not have maxima in the range of supply pressures tested. Thus it is possible that there exists an optimum operating supply pressure outside of the range of supply pressures used. There was a difference between the characteristics obtained for the left and the right ports, undoubtedly due to the asymmetry of the amplifier geometry. This indicates that the characteristics of each port of an element should be obtained, to ensure proper matching of elements in a fluidic circuit.

The performance of the bistable amplifier tested with sound was found to be affected by externally applied sound at certain sensitive frequencies. At low supply pressures, the power jet could be switched to either wall of the amplifier when sound was applied through the power jet. Applying sound through the power jet seemed to have an effect only at low supply pressures. It is possible that at higher supply pressures the amplifier is sensitive to sound at amplitudes higher than those used in the tests. The effect of sound was much more intense when the sound was introduced through the control

ports than when it was introduced through the power jet. A complete change of bistable amplifier characteristics took place at certain frequencies, and the switching of the power jet could be controlled by one control jet only or by varying the sound input.

REFERENCES

1. T. Sarpkaya and J. M. Kirshner, "The comparative performance characteristics of vented and unvented, cusped and straight and curved-walled bistable amplifier", Proceedings Third Cranfield Fluidics Conference, Turin, May 1968.

2. A. McCabe and D. L. Hughes, "Characteristics of proportional fluidic amplifiers", Proceedings Second Cranfield Fluidics Conference, 1967.

3. J. Walton, "Optimisation of the static and dynamic characteristics of a proportional amplifier", Proceedings Fourth Cranfield Fluidics Conference, 1970.

4. K. Yong and R. J. Lapisa, "Characteristics of fluidic proportional amplifier", Technical report No. 6908, Watervliet Arsenal, 1969.

5. L. B. Taplin, "The admittance properties of a jet proportional amplifier", SAE Transactions, 1969.

6. A. Boros and L. Helm, "On the complex/static and dynamic/ testing of fluid elements", Proceedings Fourth Cranfield Fluidics Conference, 1970.

7. H. H. Unfried, "Experiment and theory of acoustically controlled fluid switches", Proceedings of Fluid Amplification Symposium, 1965.

8. G. L. Roffman and K. Toda, "A discussion of the effects of sound of jets and flueric devices", Journal of Engineering for Industry, Trans. ASME, Vol. 91, November 1969.

9. S. D. Weigner, "The effect of sound on a reattaching jet at low Reynolds numbers", Proceedings of Fluid Amplification Symposium, Vol. IV, October 1965.

10. M. A. Madonna, "Investigation of environmental effects on pure fluid amplifier", Technical Report G102, Clearinghouse, 1968.

11. C. A. Belsterling, "Digital and proportional jet interaction devices and circuits", Fluidics Quarterly, Vol. 1, No. 4, 1968.

12. R. E. Norwood, "A performance criterion for fluid jet amplifiers", Symposium on Fluid Control Devices, 1962.

13. D. Rockwell and K. Toda, "Effect of applied acoustics fields on attached jet flows", Proceedings, Joint Automatic Control Conference, June 1970.

14. J. Owczarek, "Fundamentals of gas dynamics", International Textbook Company, June 1968.

15. "Flow Measurement", ASME, Flow Measurement, Part 5, 1959.

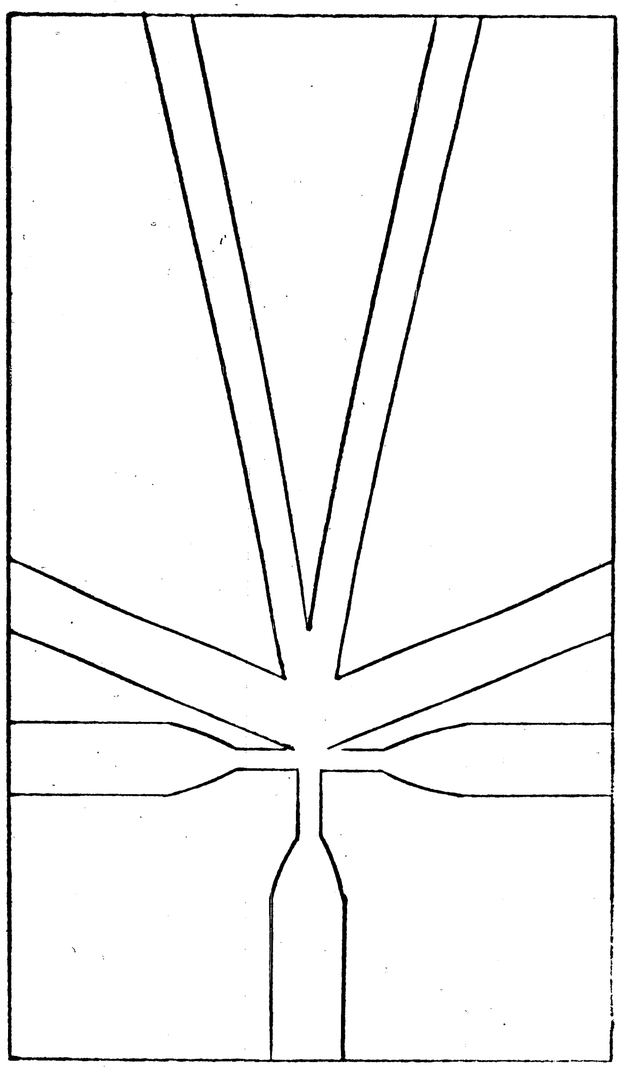

(a) Proportional Amplifier

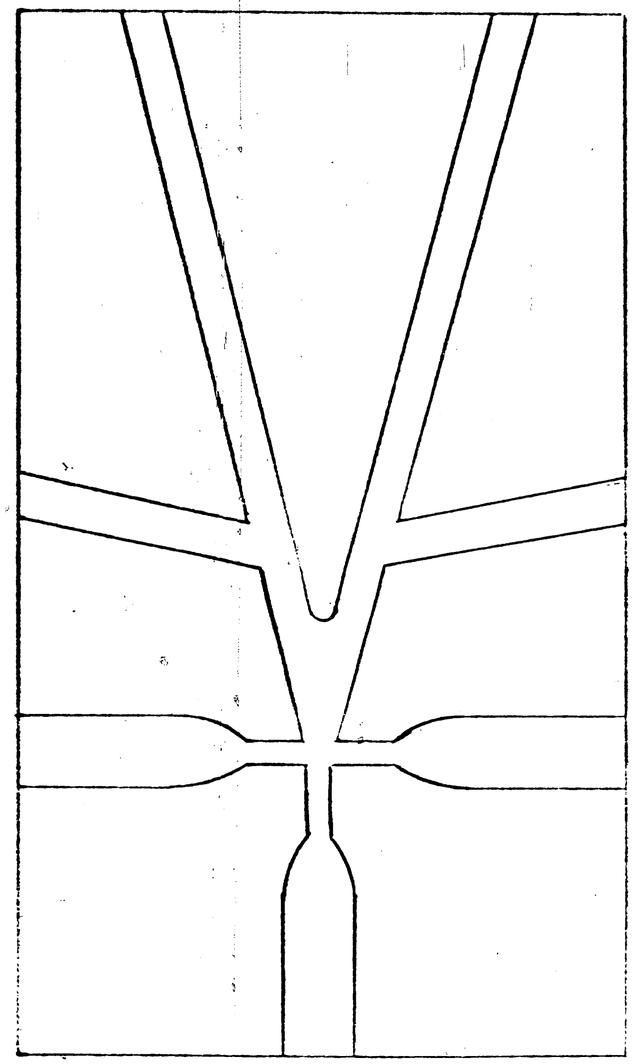

(b) Bistable Amplifier

Figure 1. Sketch of a Proportional and Bistable Amplifier

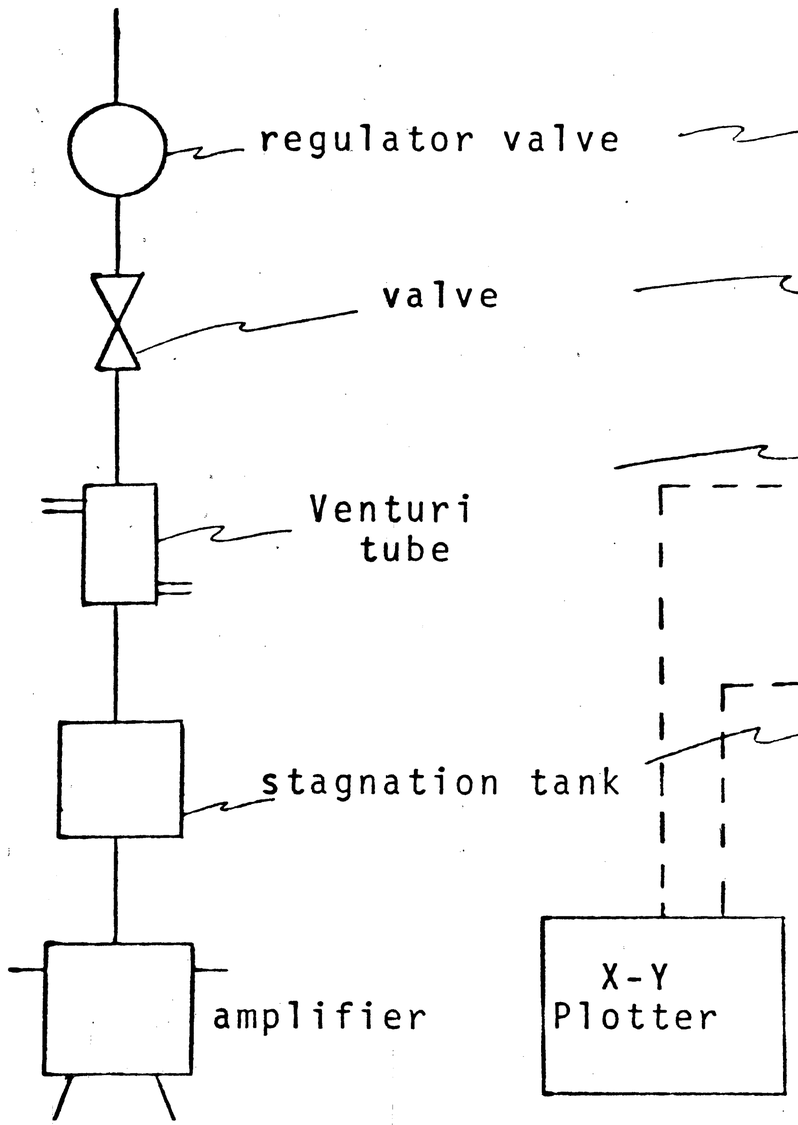

Figure 2. Schematic of test rig to determine power jet characteristics

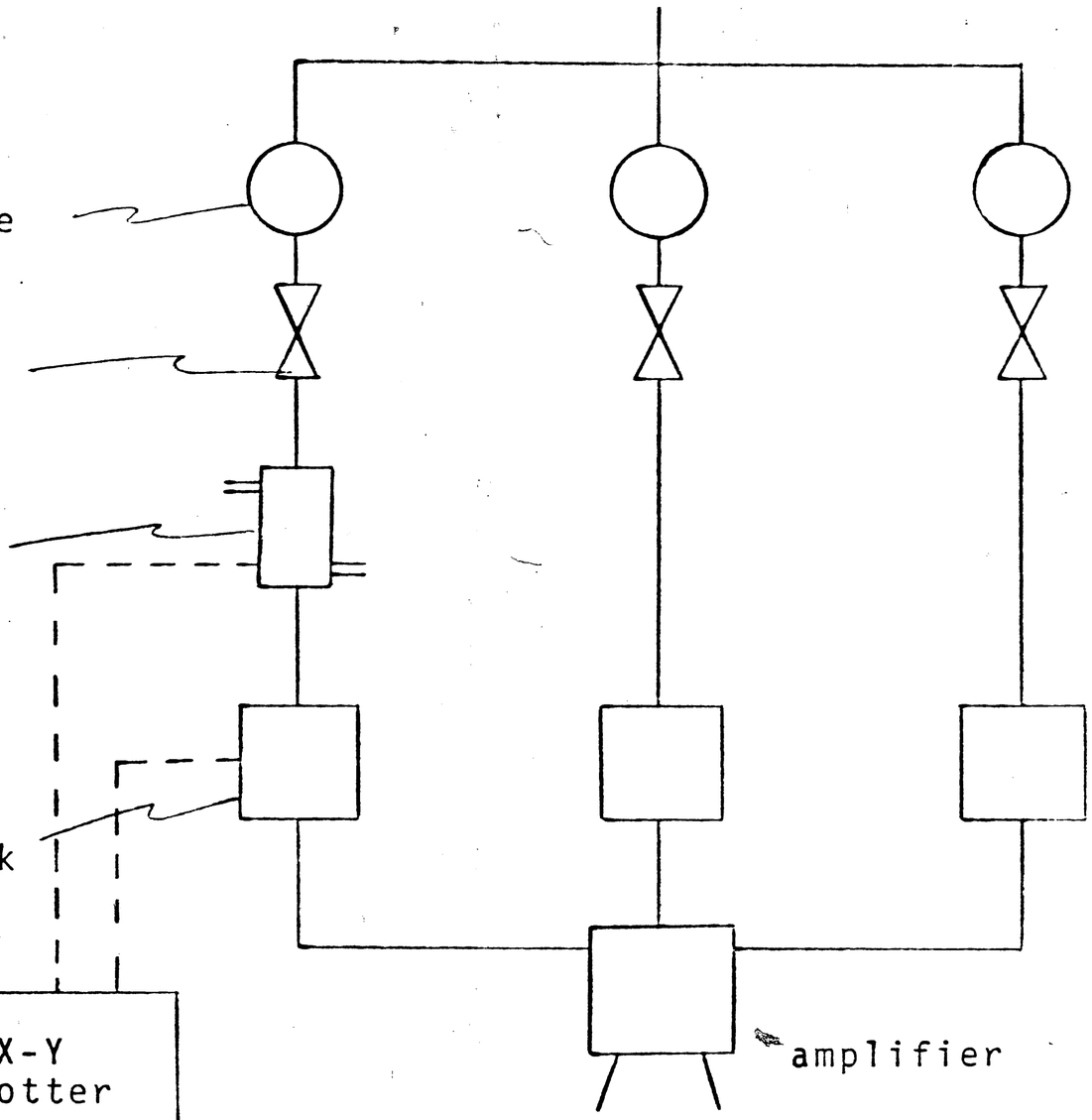

Figure 3. Schematic of test rig to determine control jet characteristics

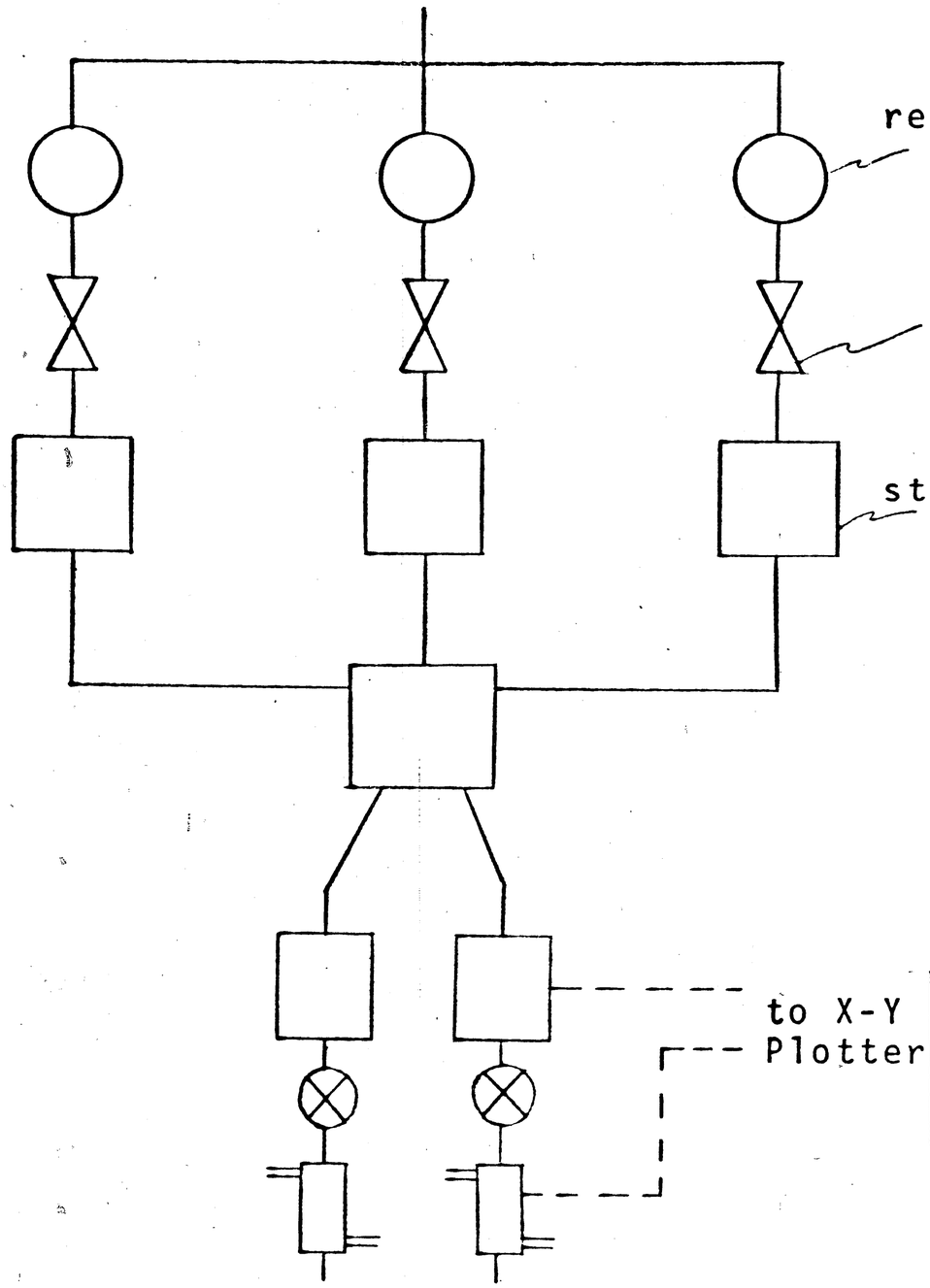

Figure 4. Schematic of test rig to determine out-put characteristics

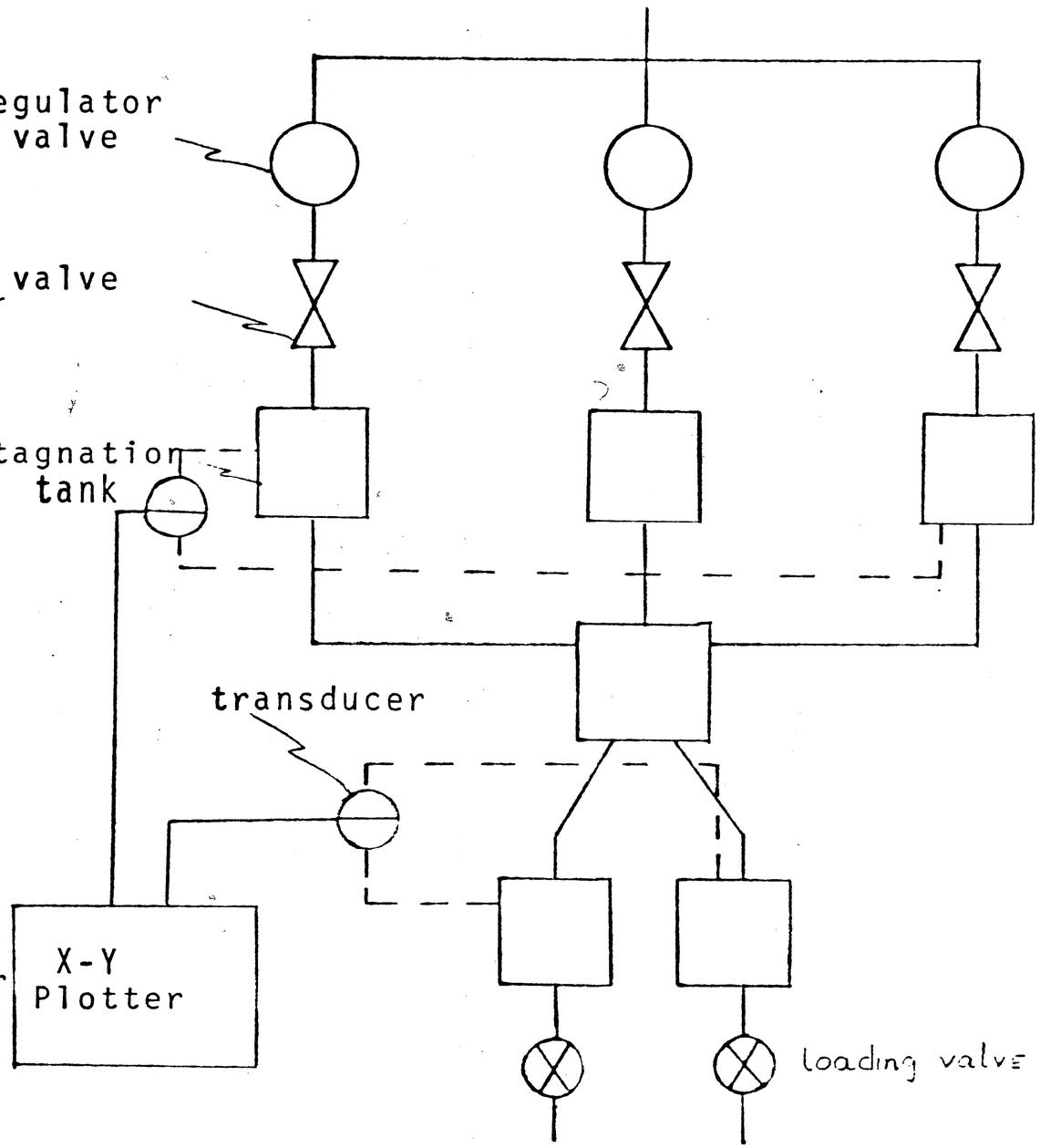

Figure 5. Schematic of test rig to determine differential input-output characteristics

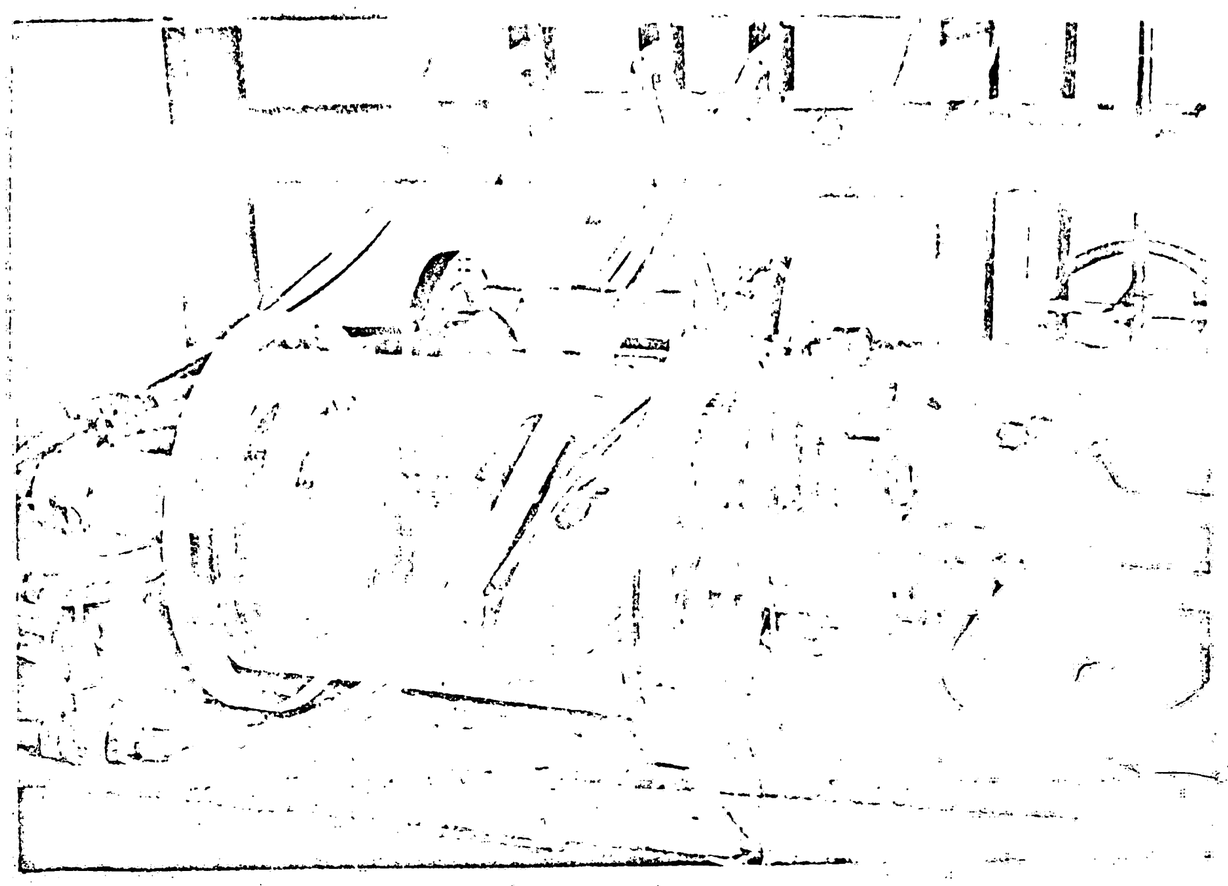

Figure 6. Loudspeaker in stagnation tank

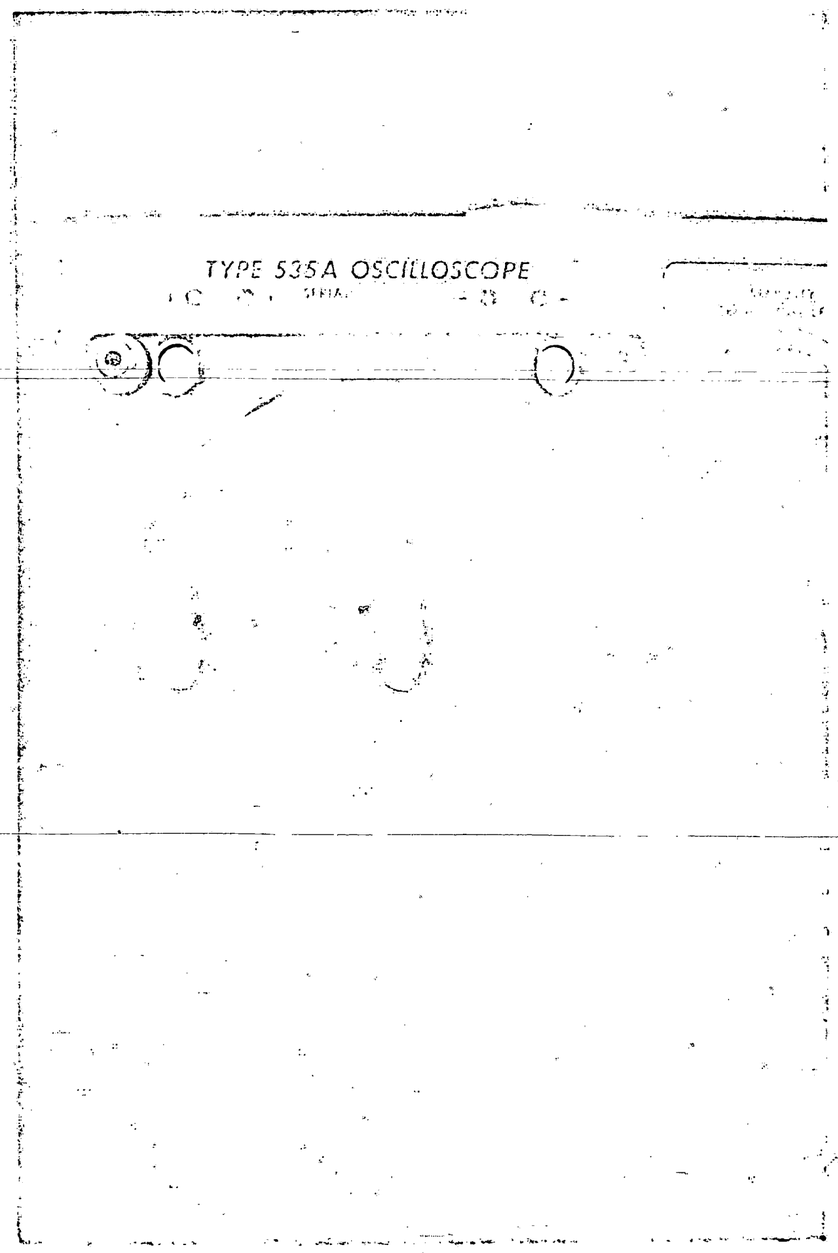

Figure 7. Trace of voltage input to speaker

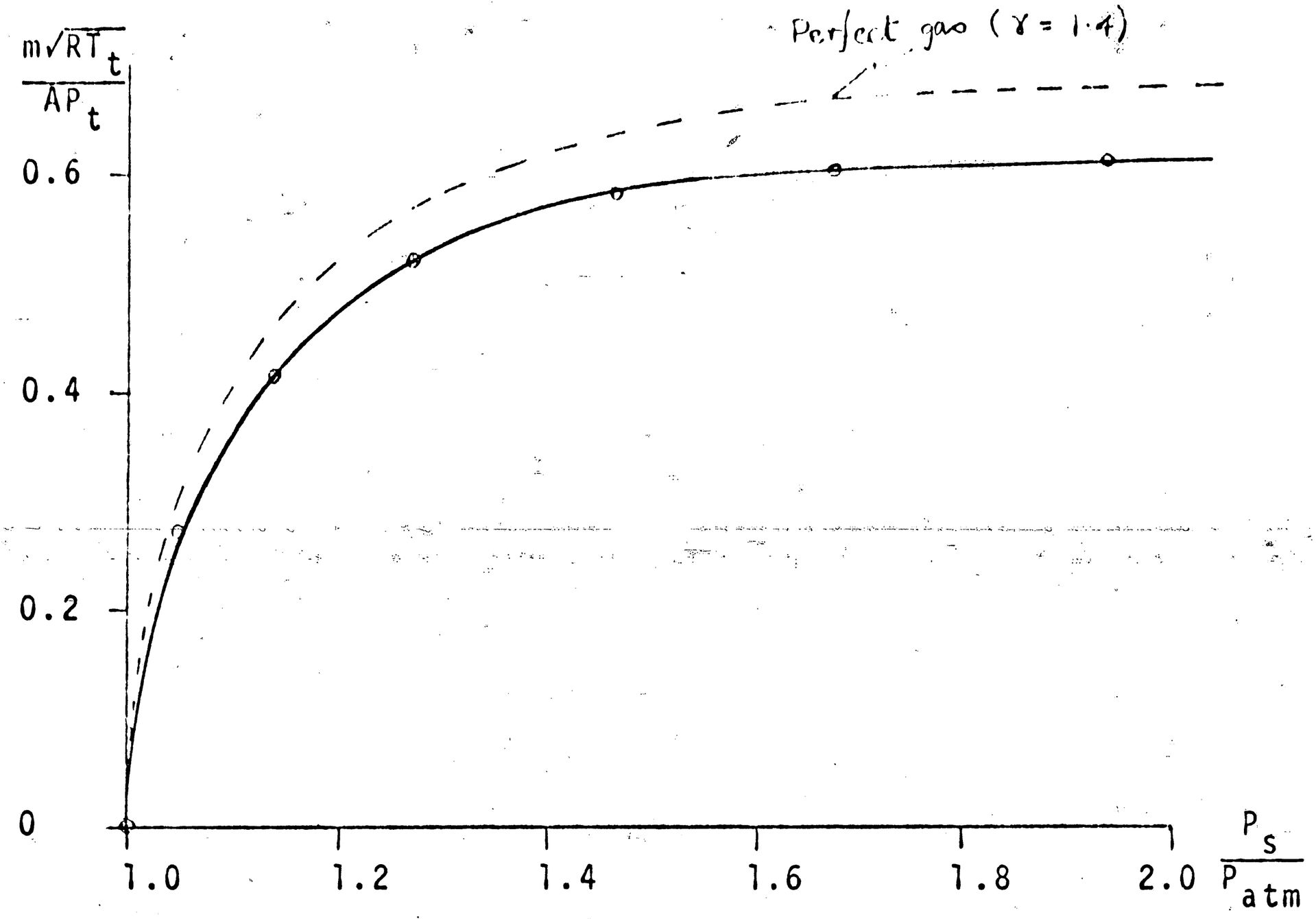

Figure 8. Power jet characteristics, Bistable Amplifier No. 1

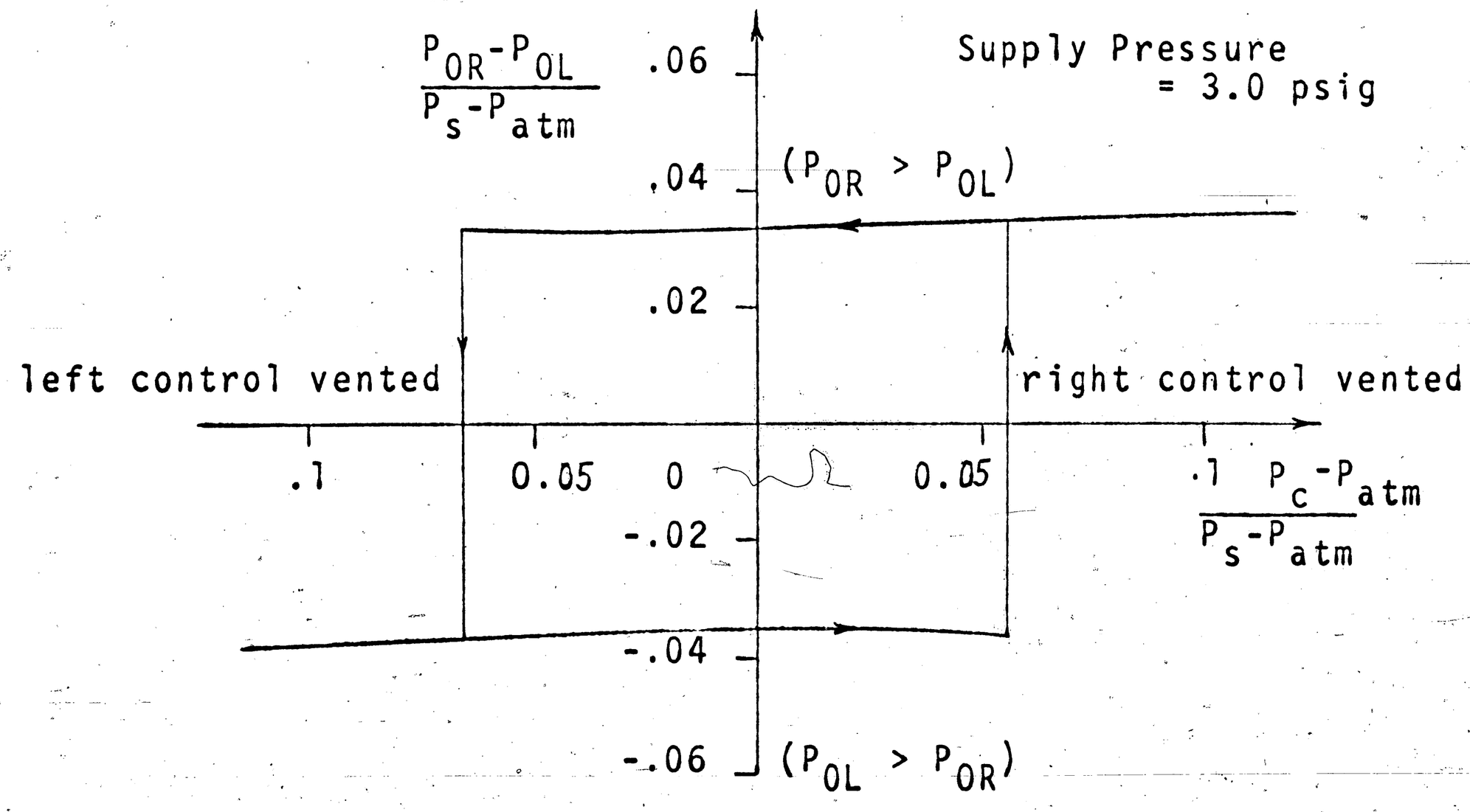

Figure 9(a)

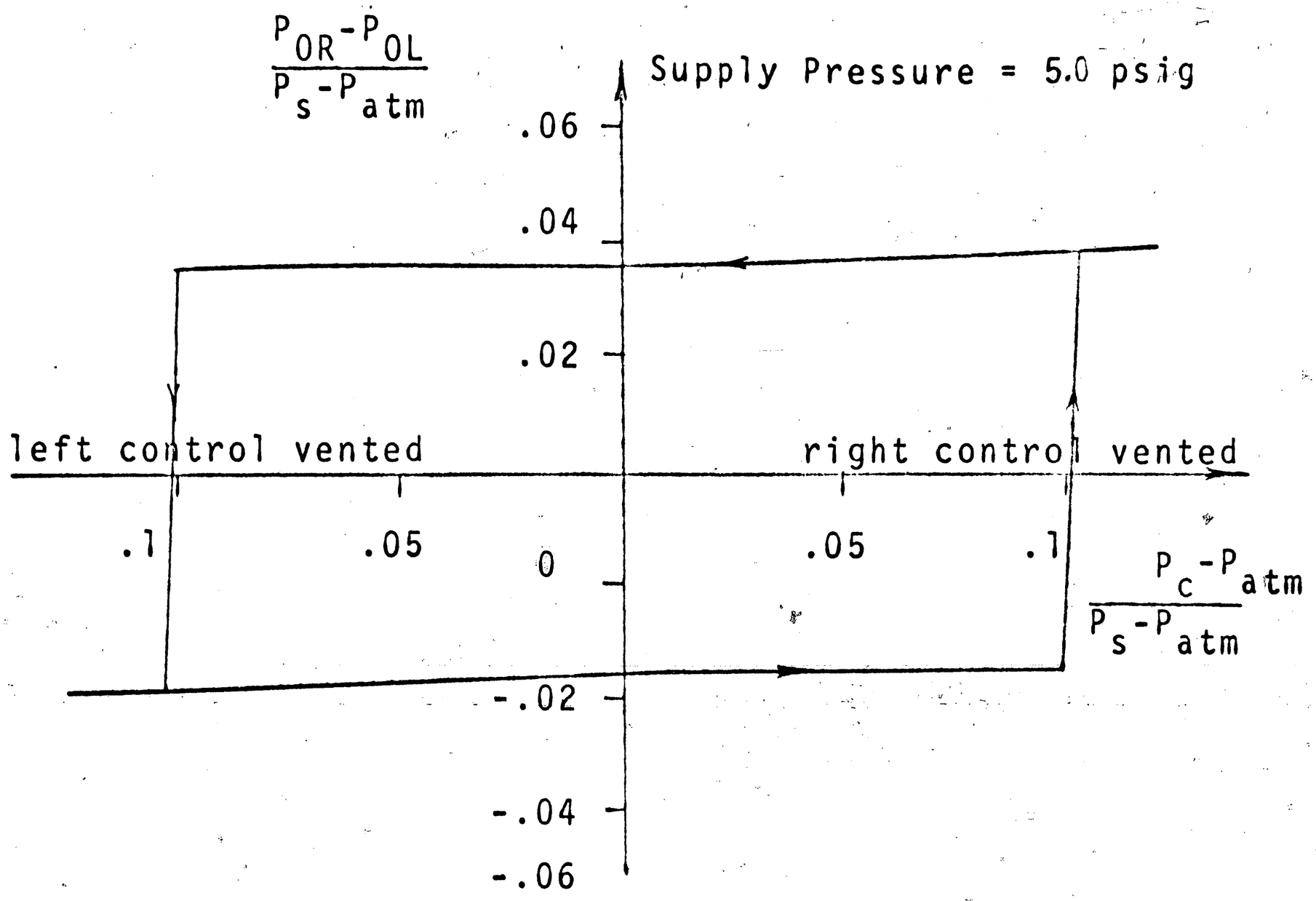

Figure 9(b)

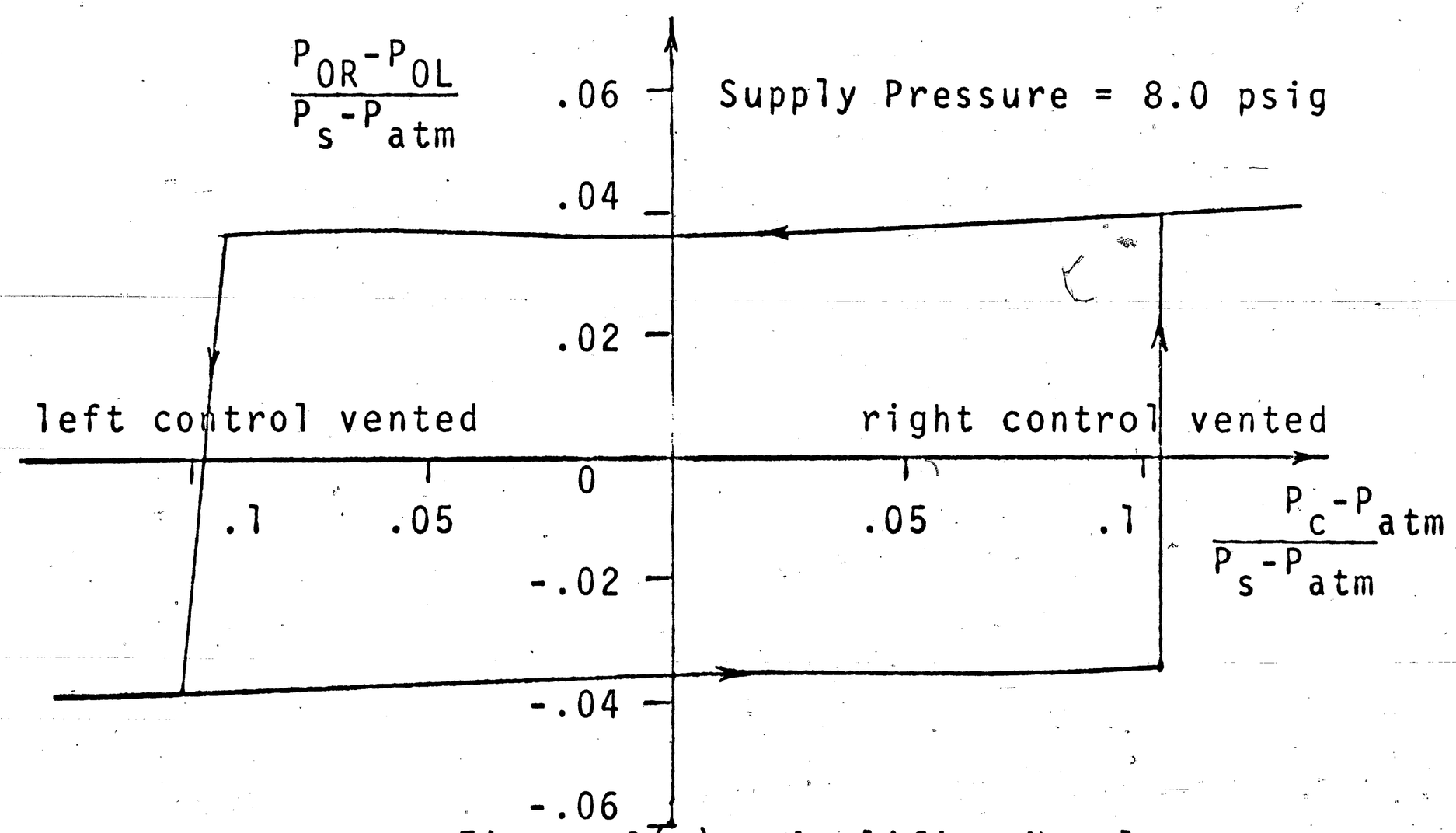

Figure 9(c) - Amplifier No. 1
Differential input-output-characteristics at no load conditions

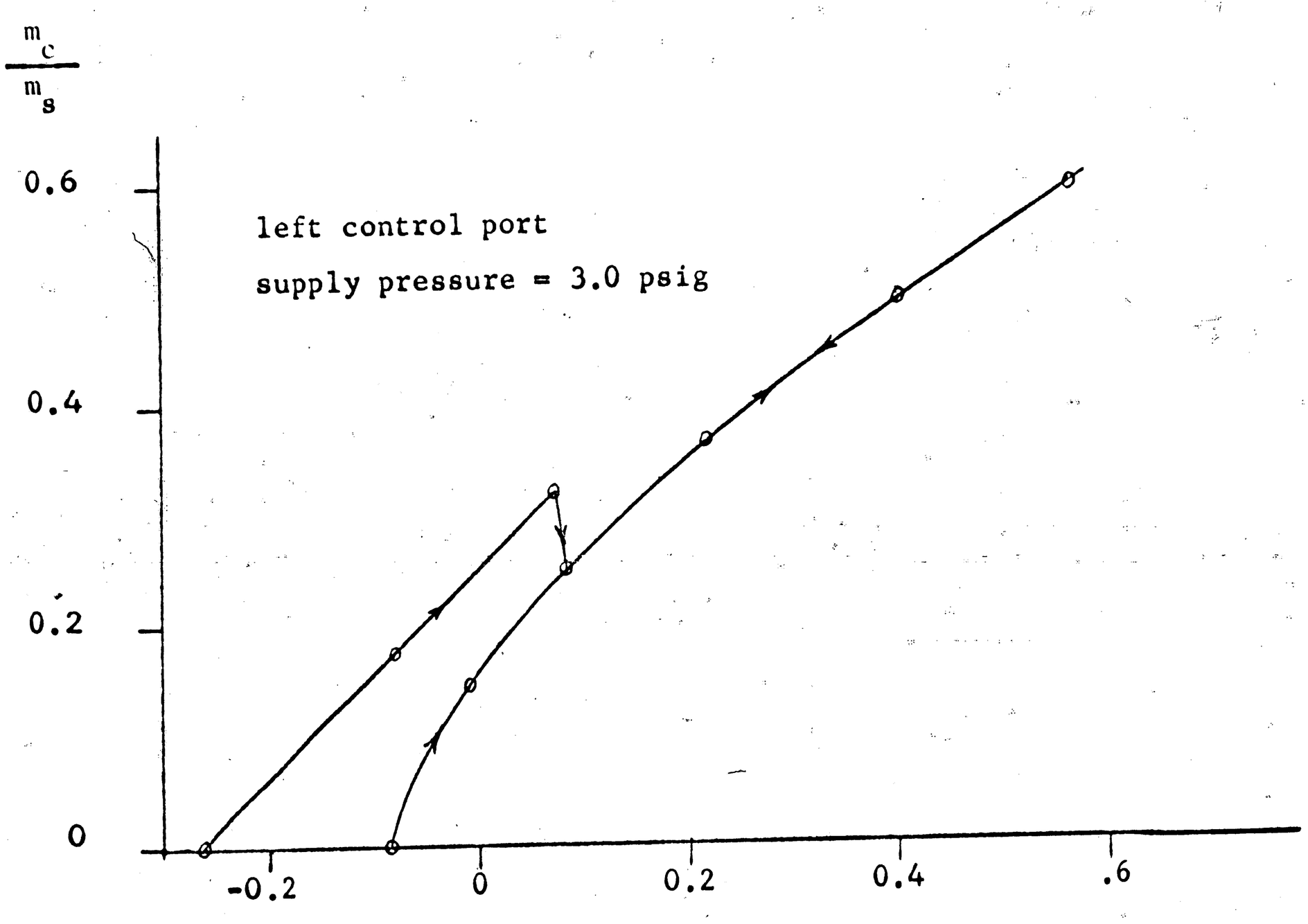

Figure 10 (a)

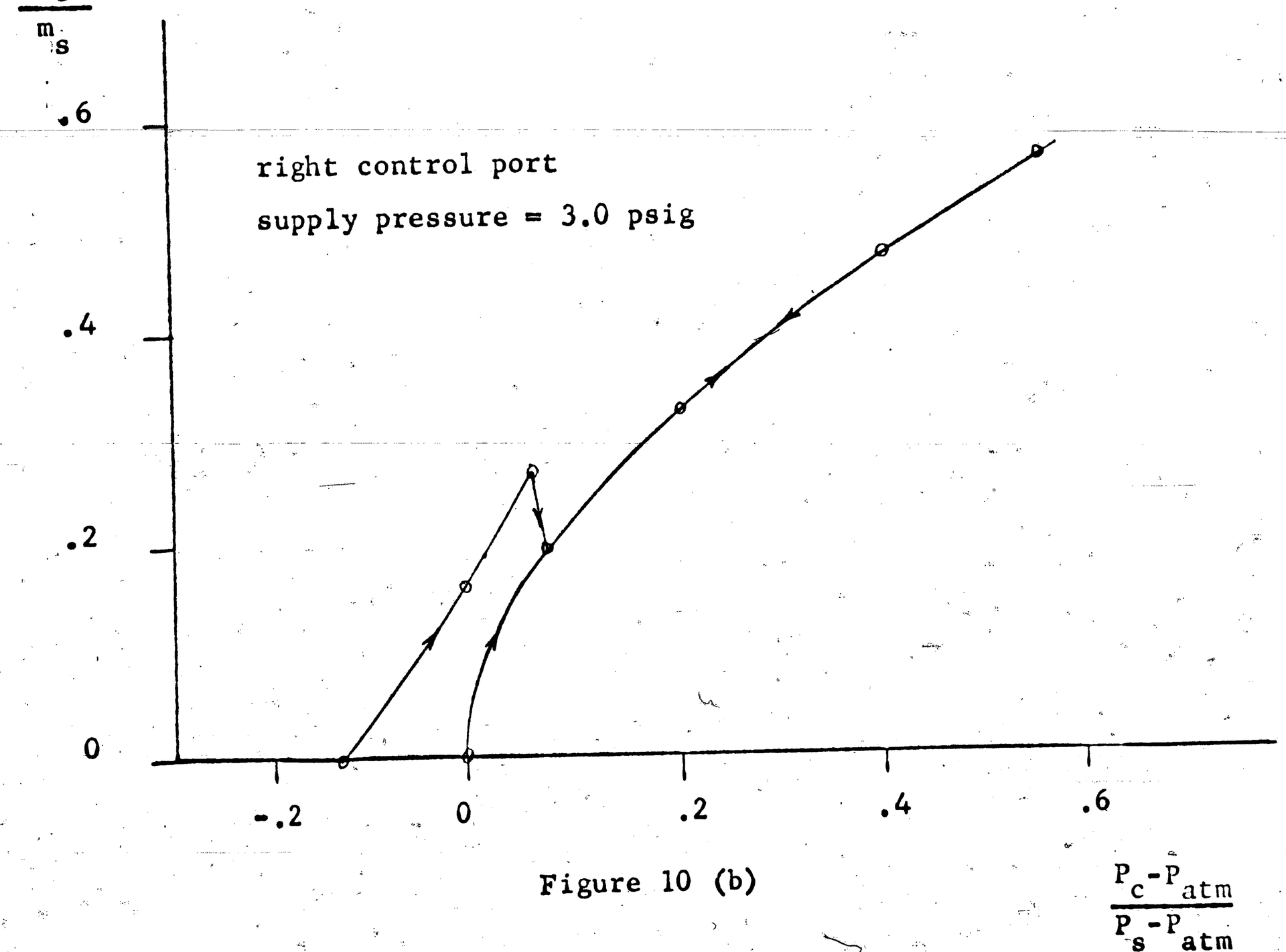

Figure 10 (b)

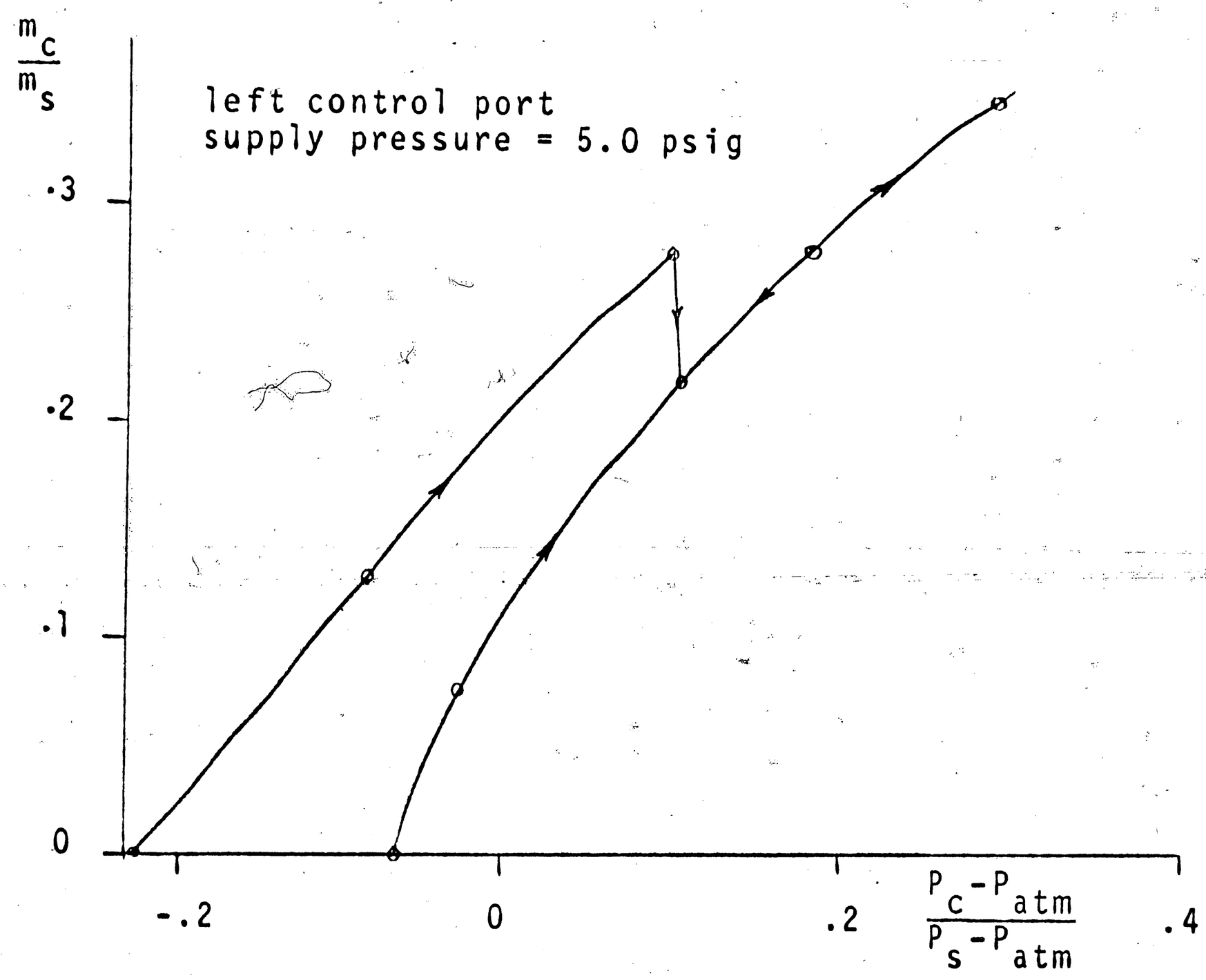

Figure 10(c)

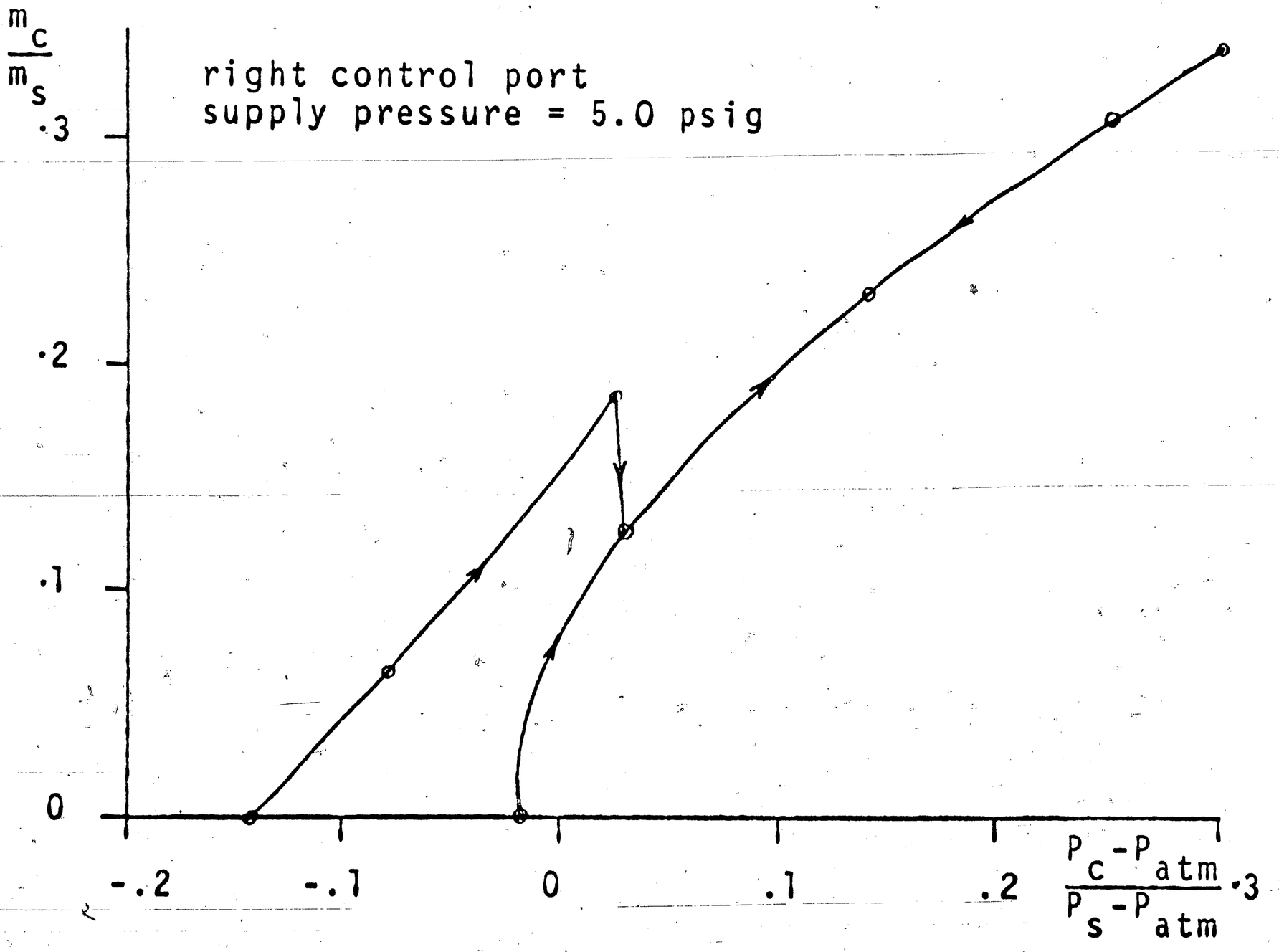

Figure 10(d)

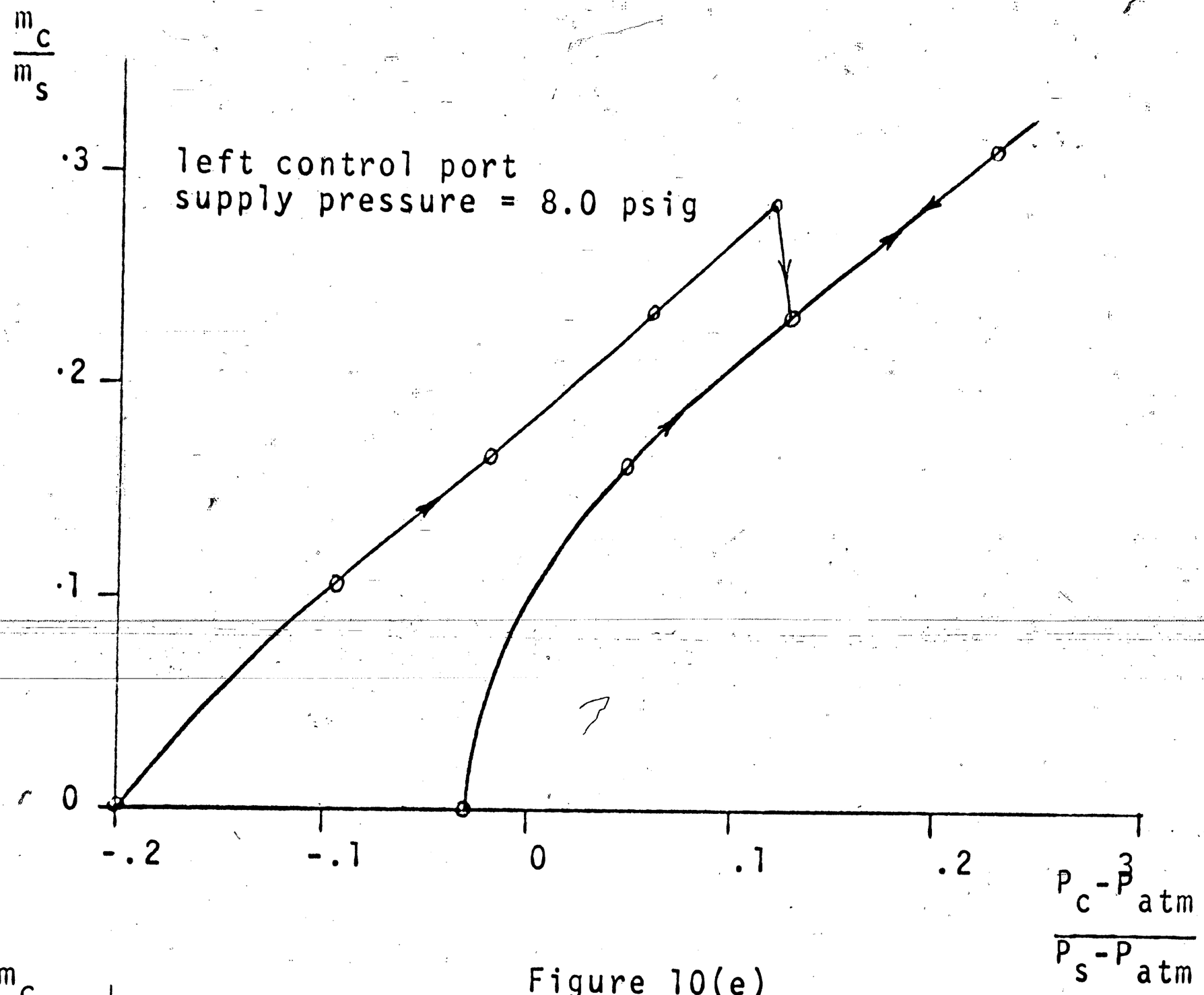

Figure 10(e)

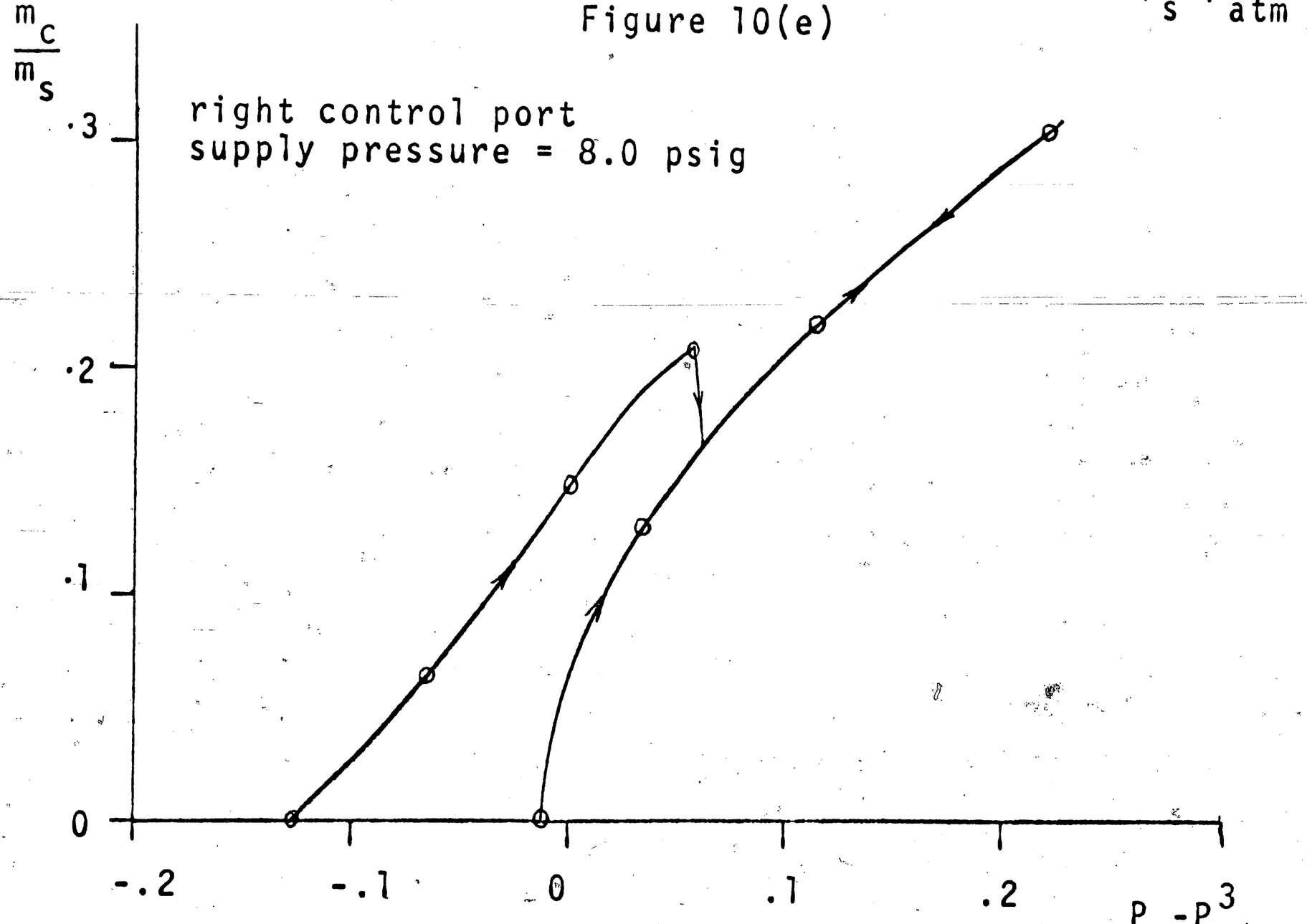

Figure 10(f)

Amplifier No. 1 - Control port characteristics at no load conditions

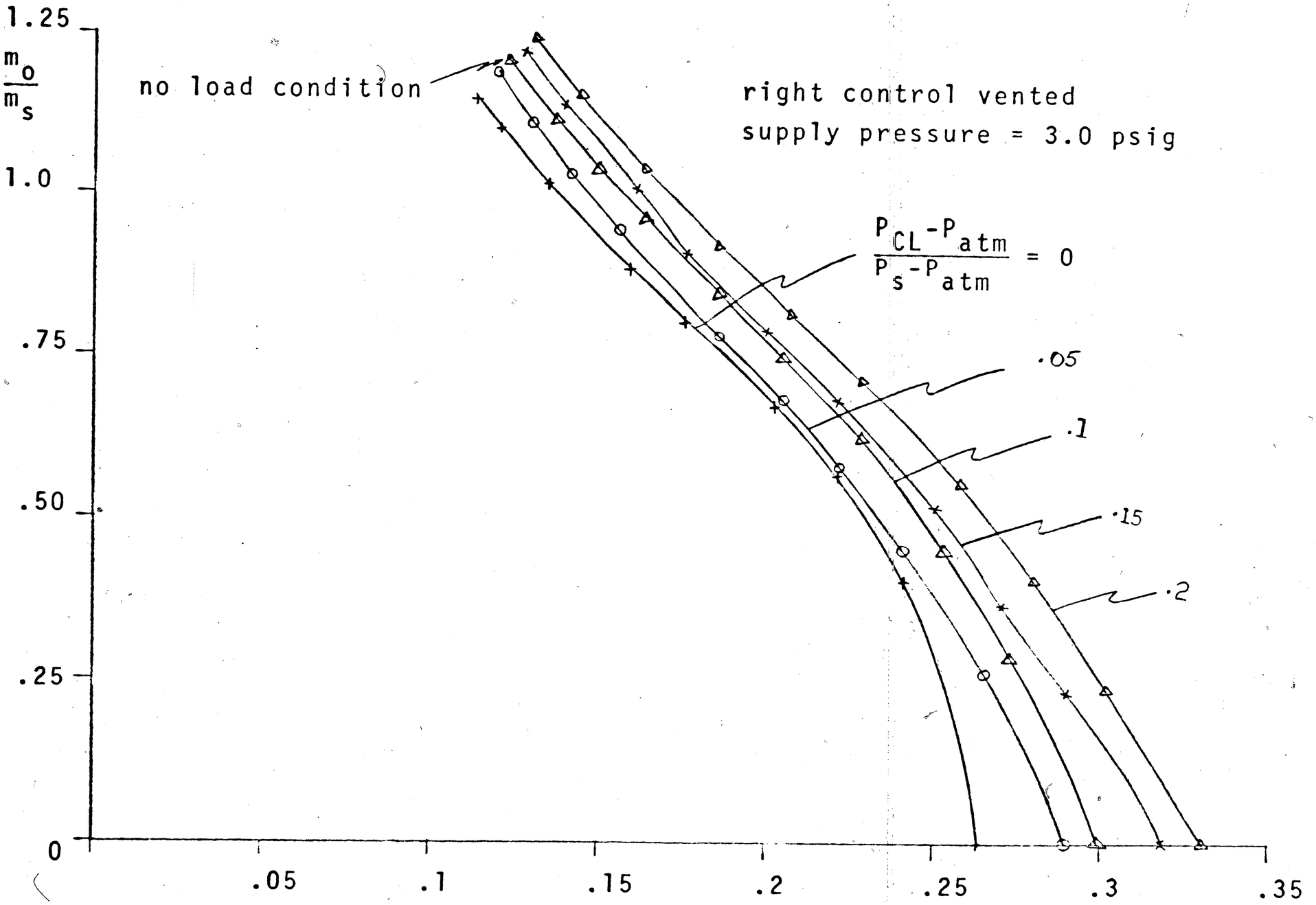

Figure 11(a). Right output characteristics

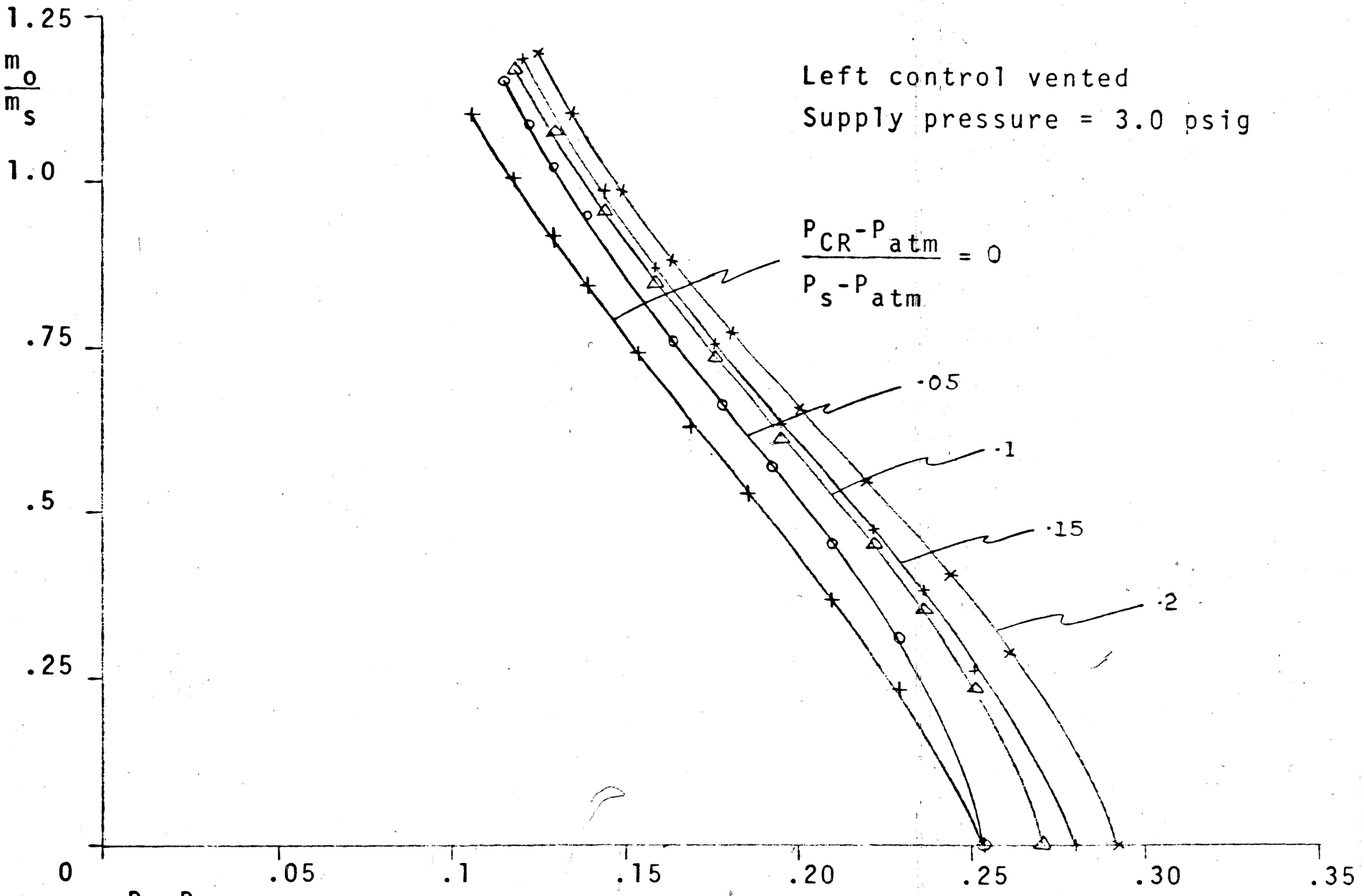

Figure 11(b). Left output characteristics

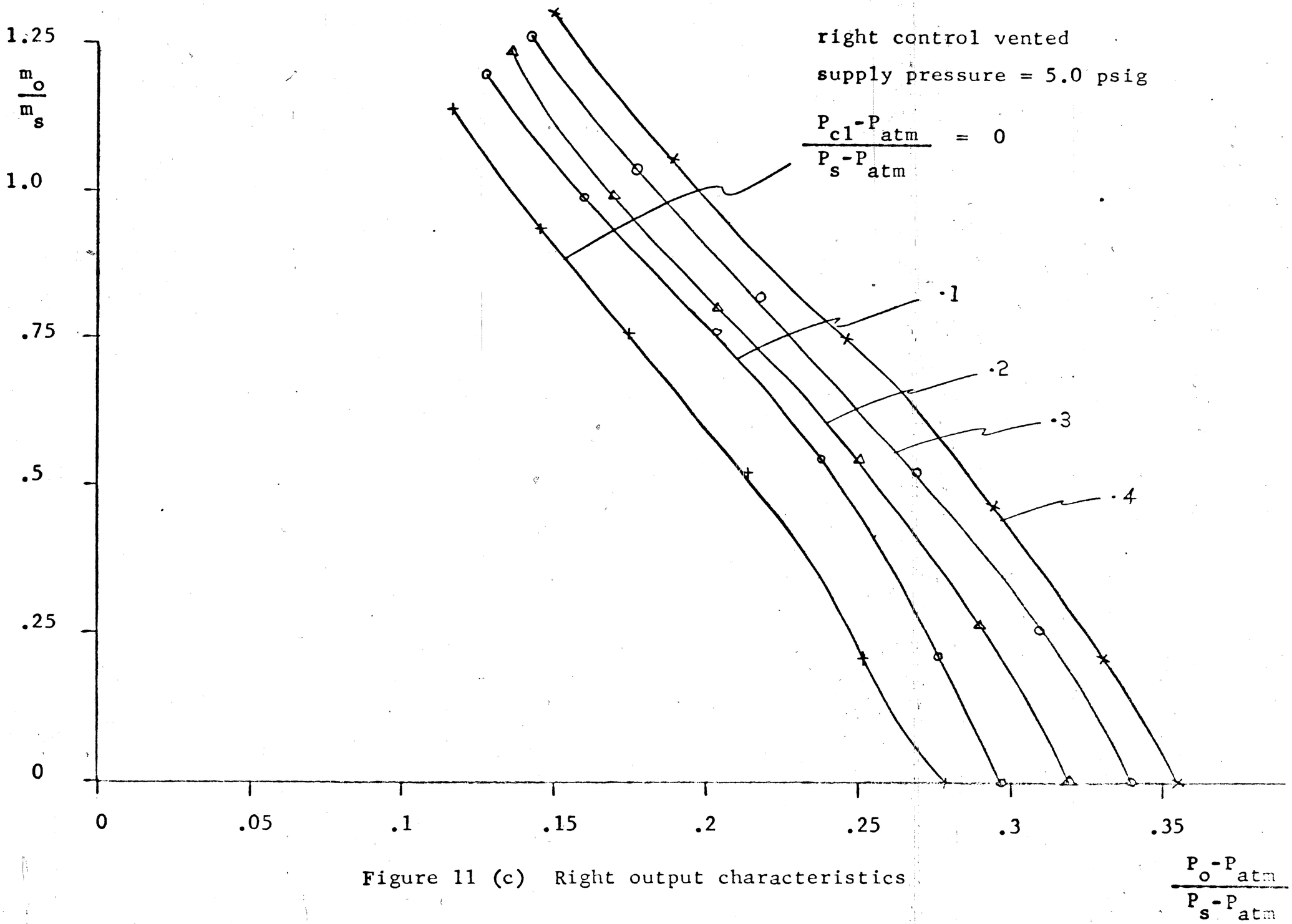

Figure 11 (c) Right output characteristics

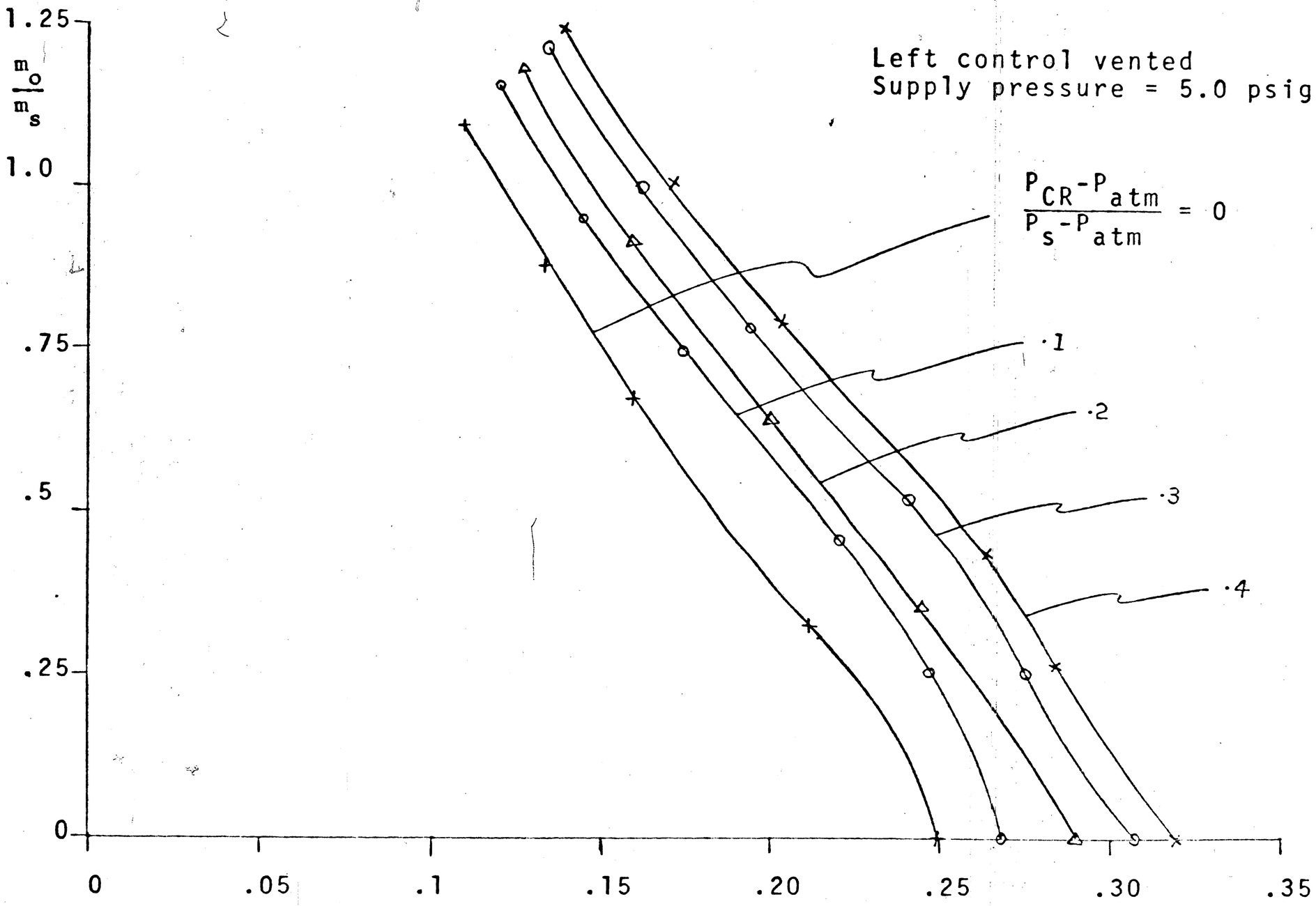

Figure 11(d). Left Output Characteristics

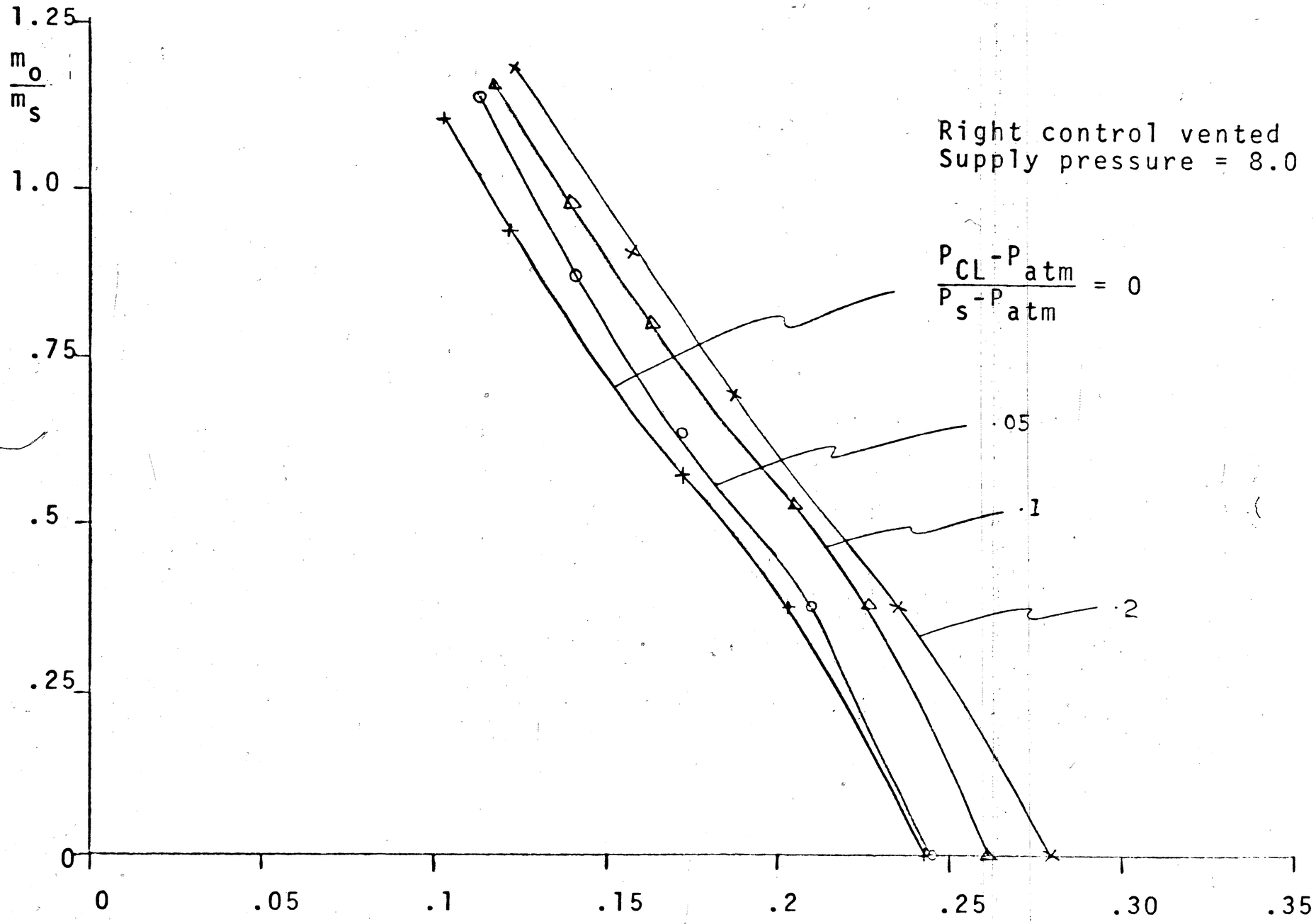

Figure 11(e). Right Output Characteristics

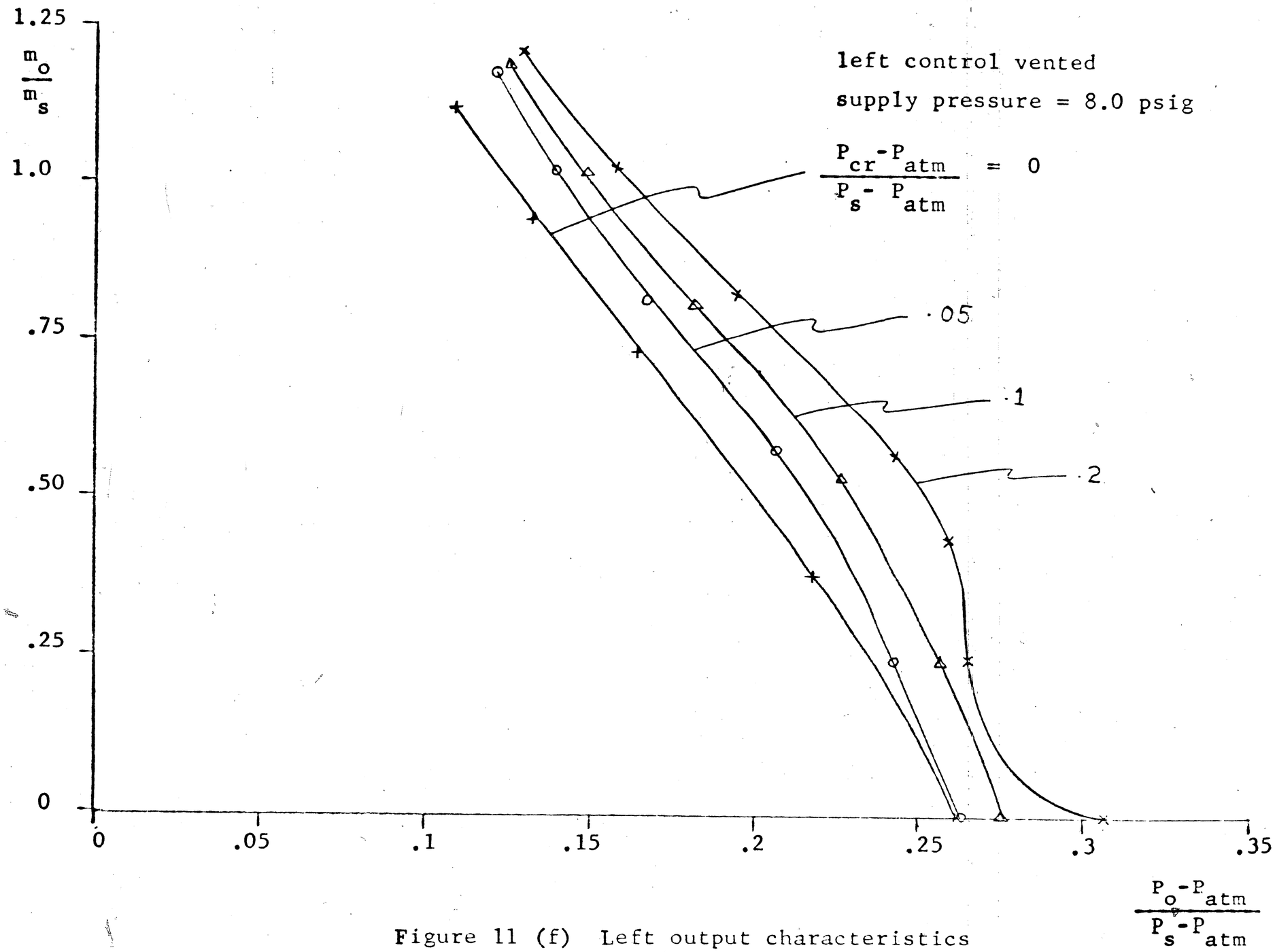

Figure 11 (f) Left output characteristics

Output characteristics Amplifier No. 1

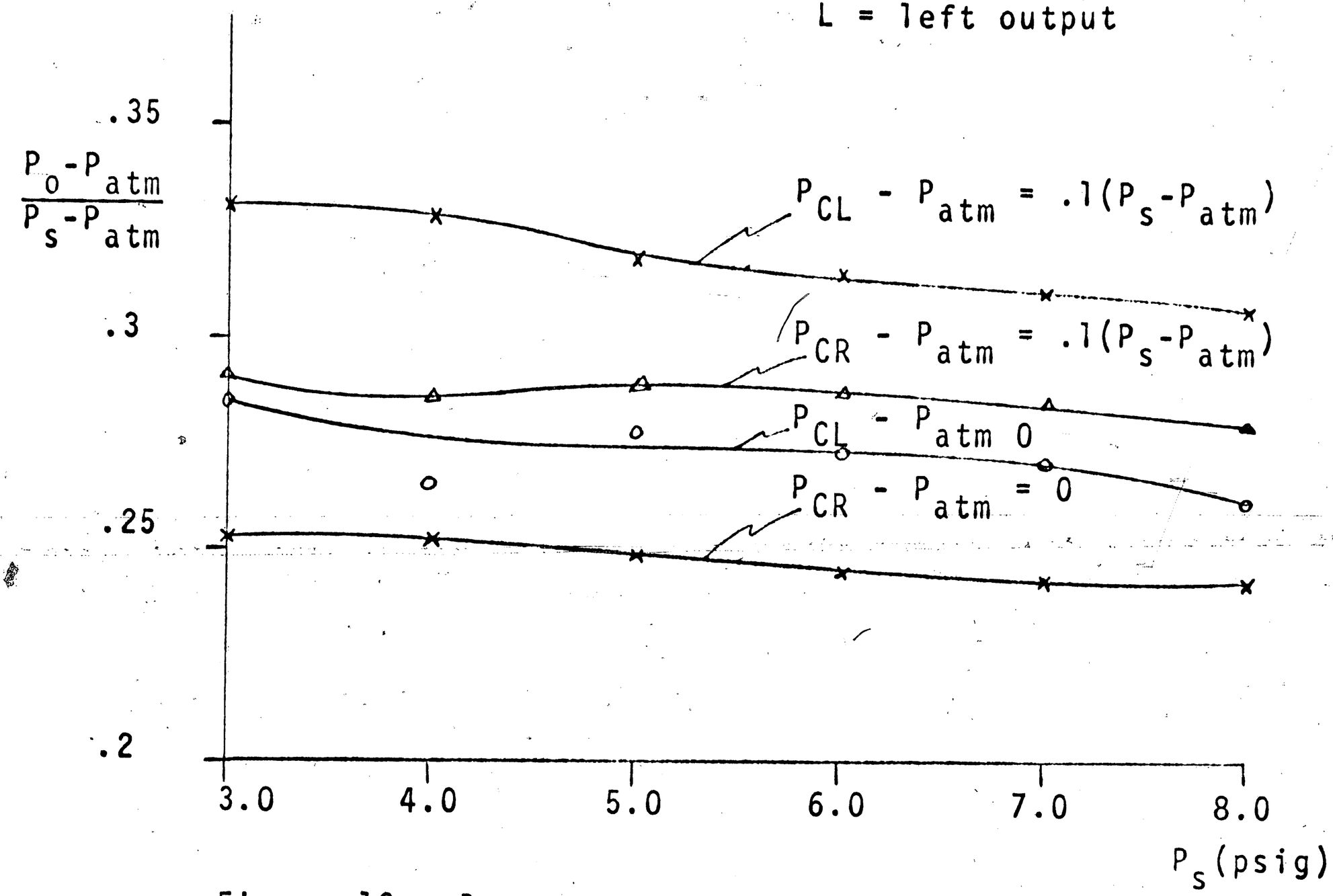

Figure 12. Pressure recovery versus supply pressure Amplifier No. 1

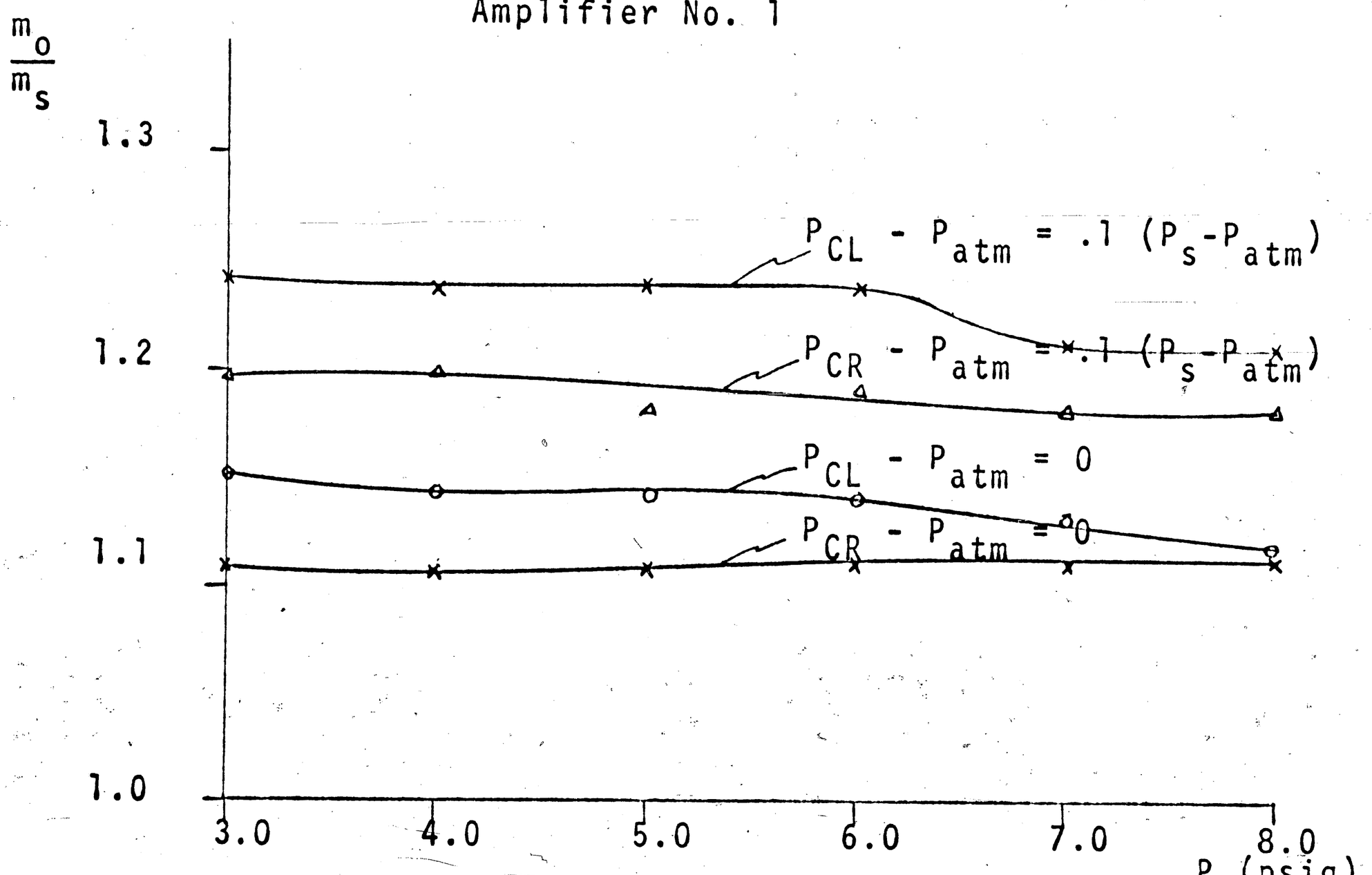

Figure 13. Mass flow rate at no load conditions versus supply pressure

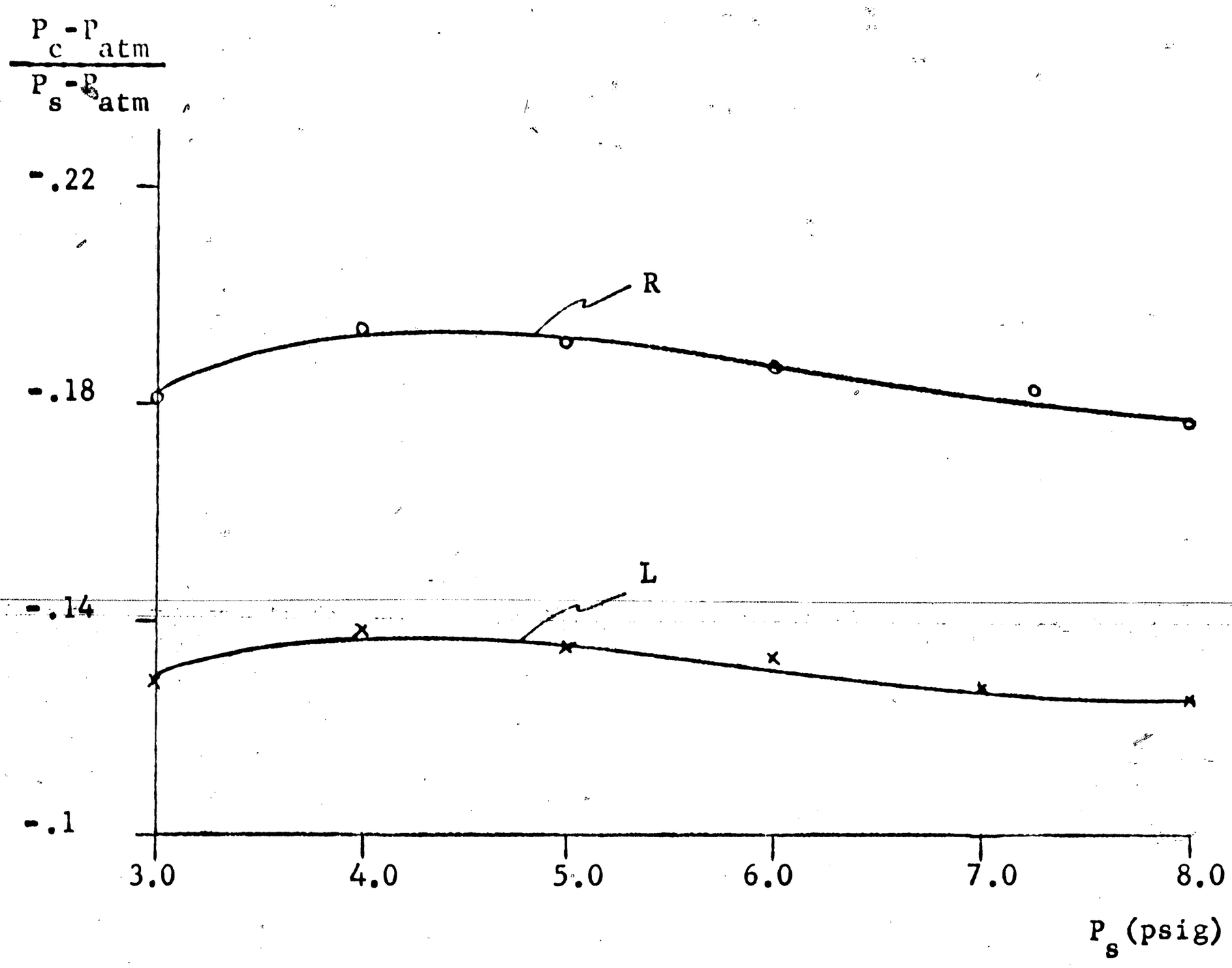

Figure 14. Control port pressure versus supply pressure
Amplifier No. 1

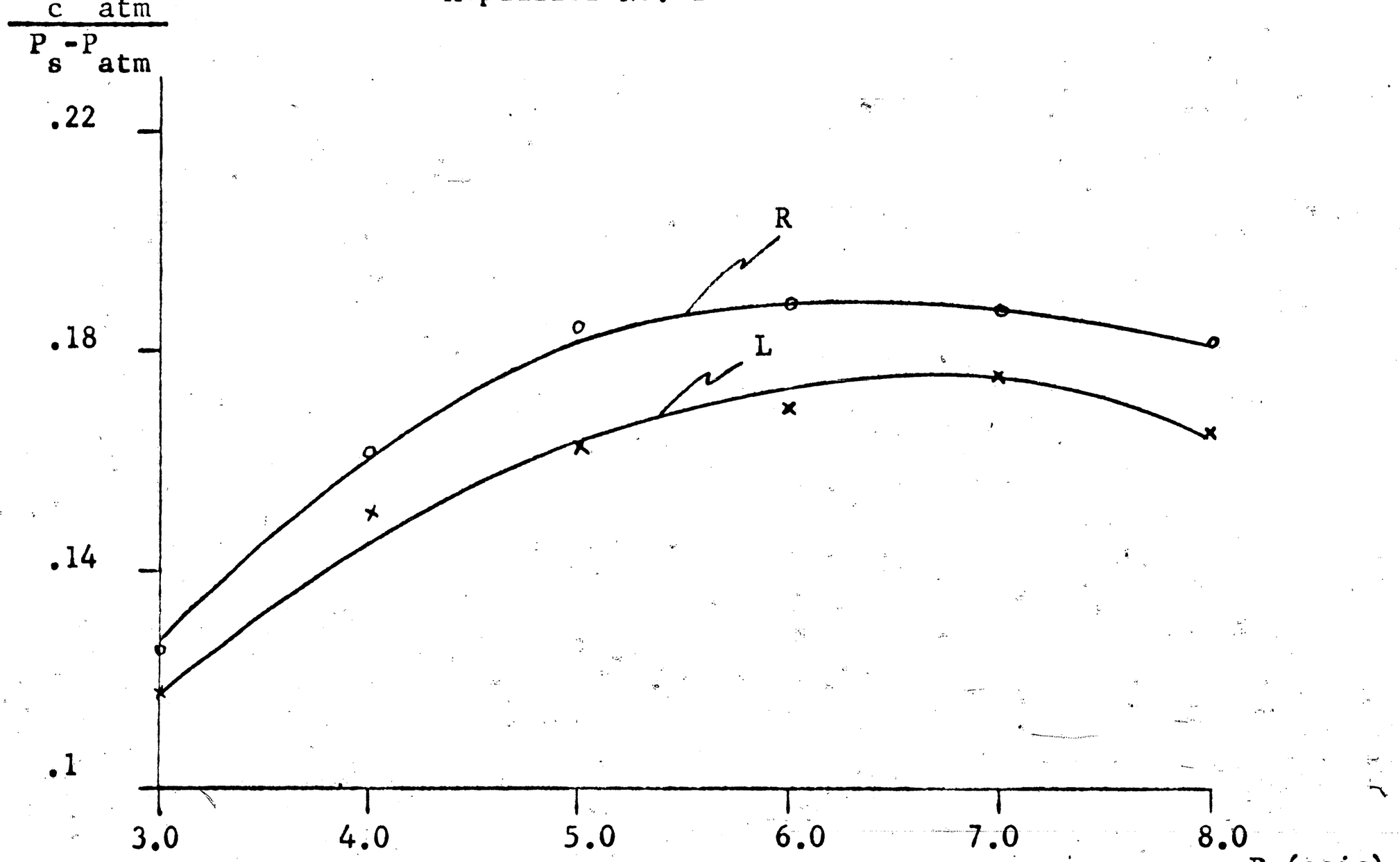

Figure 15. Control port pressure at switching versus supply pressure
Amplifier No. 1

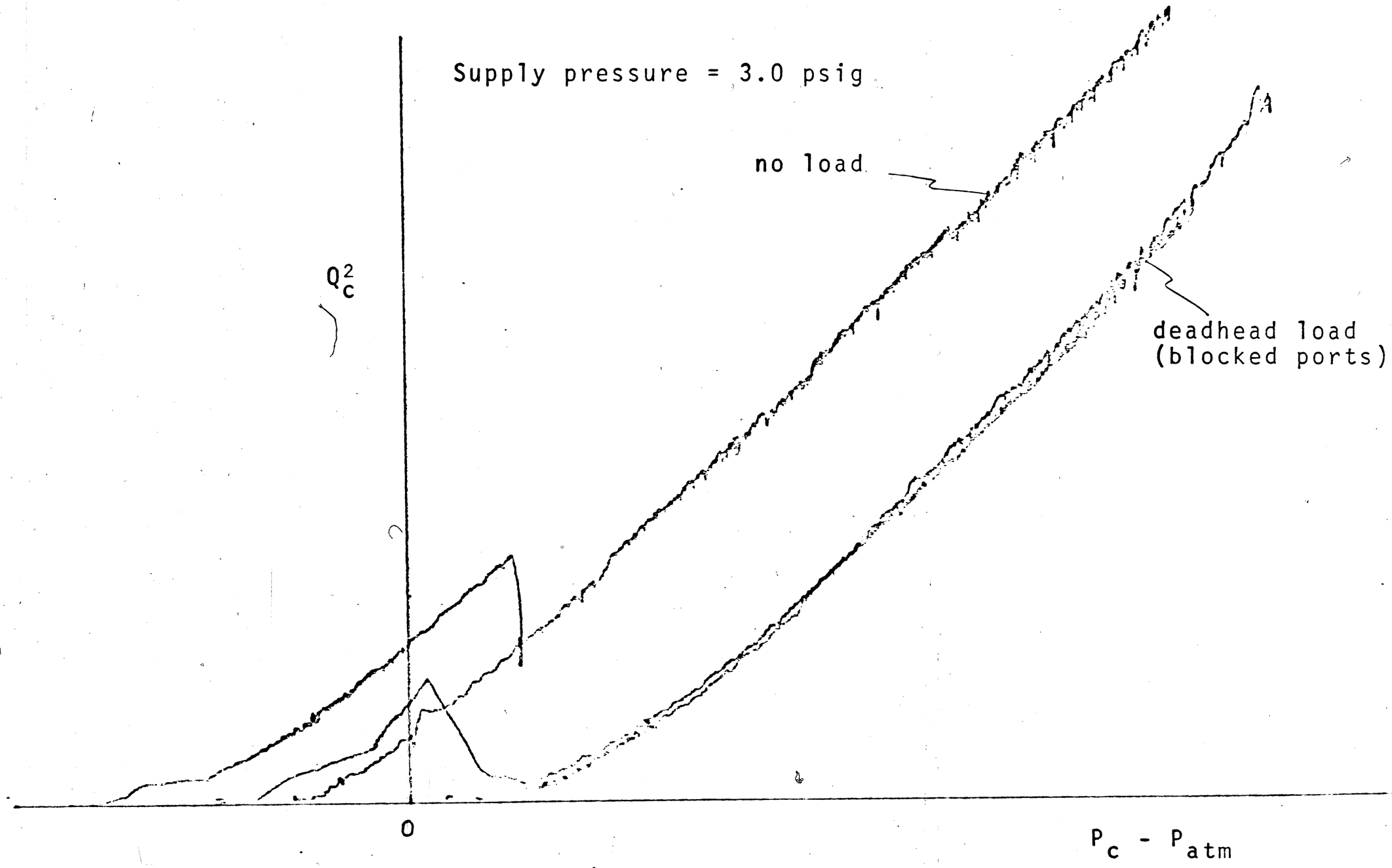

Figure 16. Control port characteristics as obtained on the X-Y plotter

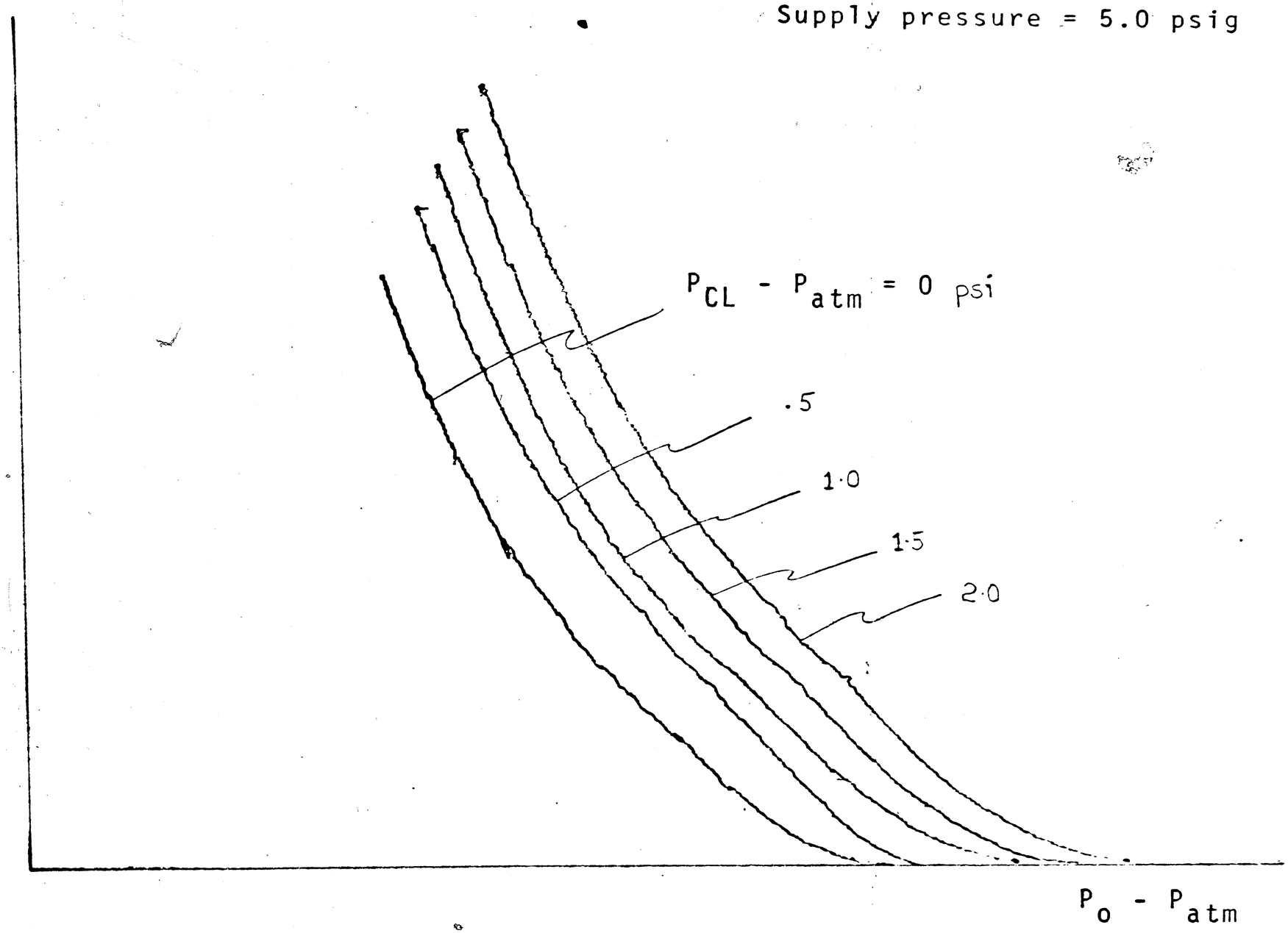

Figure 17. Output characteristics as obtained on X-Y plotter

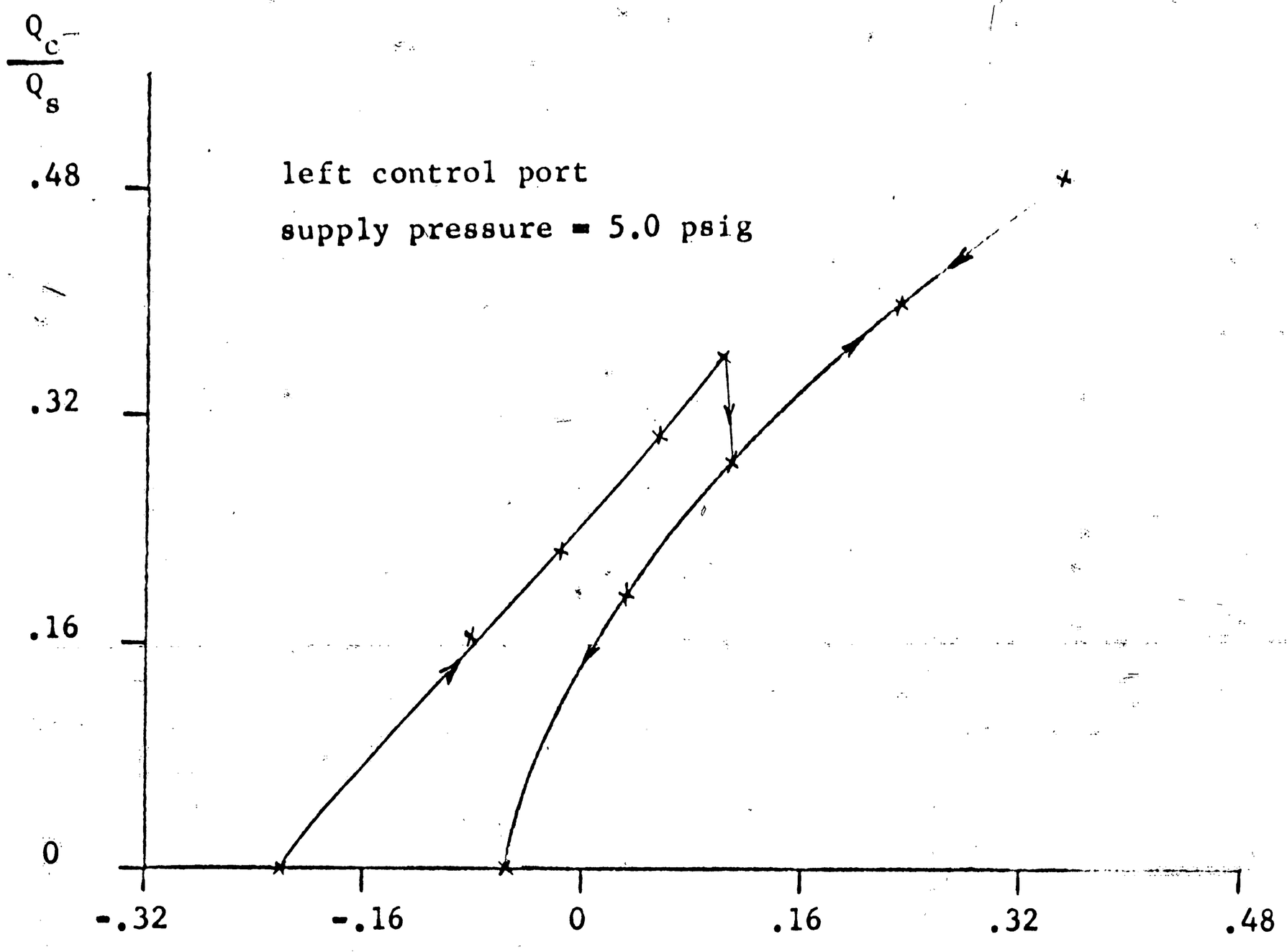

Figure 18 (a)

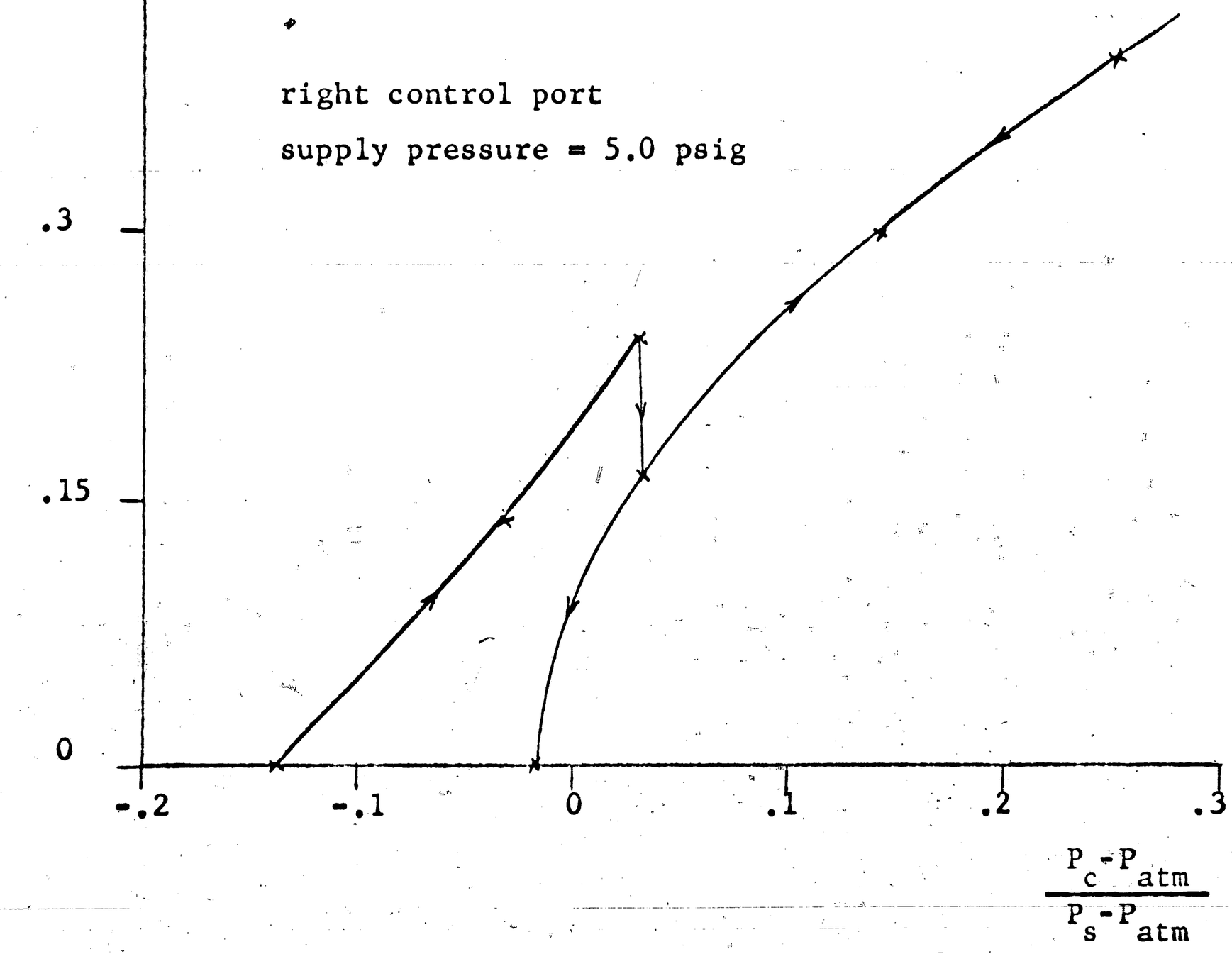

Figure 18 (b) Control port characteristics at no load conditions

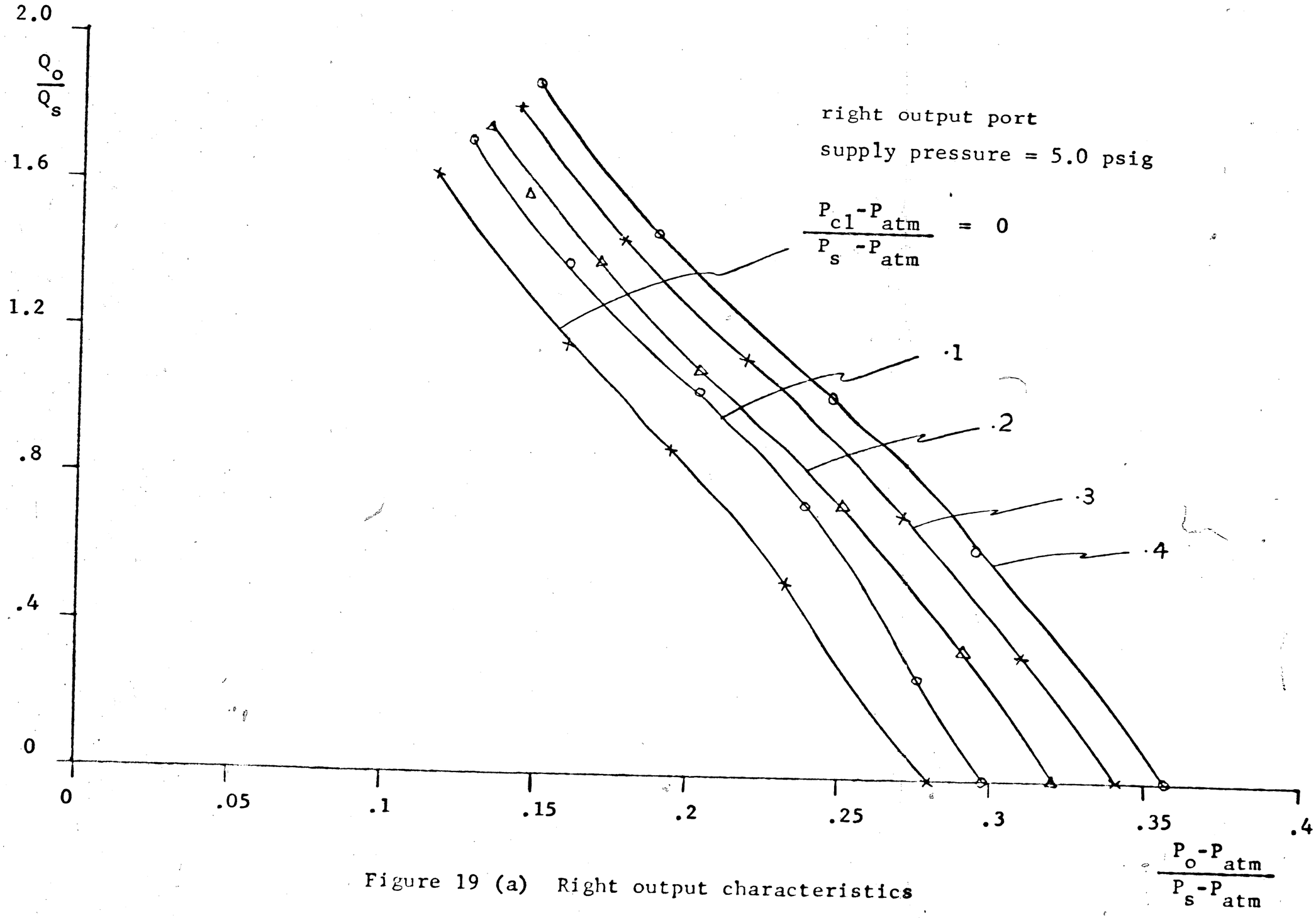

Figure 19 (a) Right output characteristics

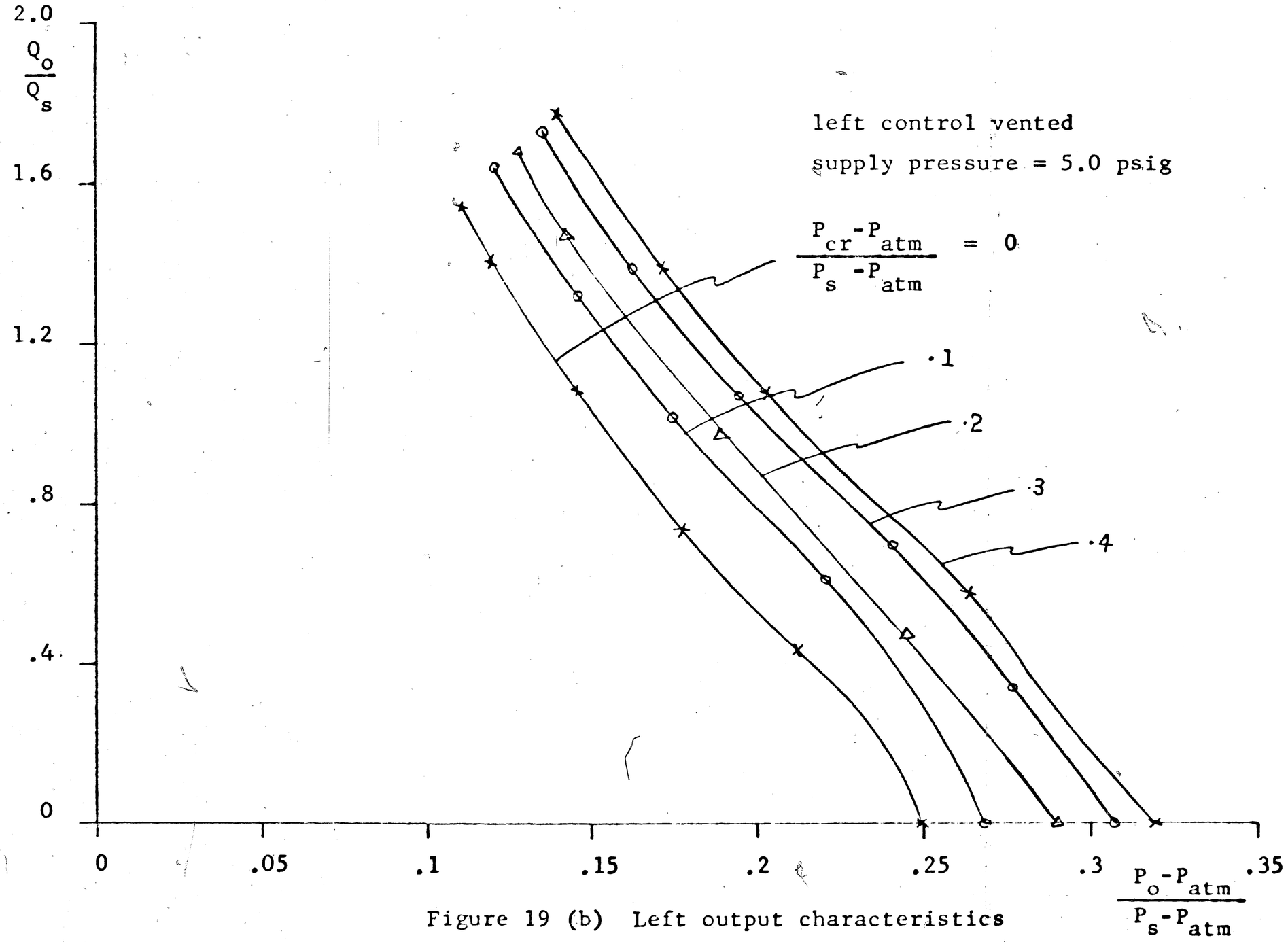

Figure 19 (b) Left output characteristics

Output characteristics Amplifier No. 1

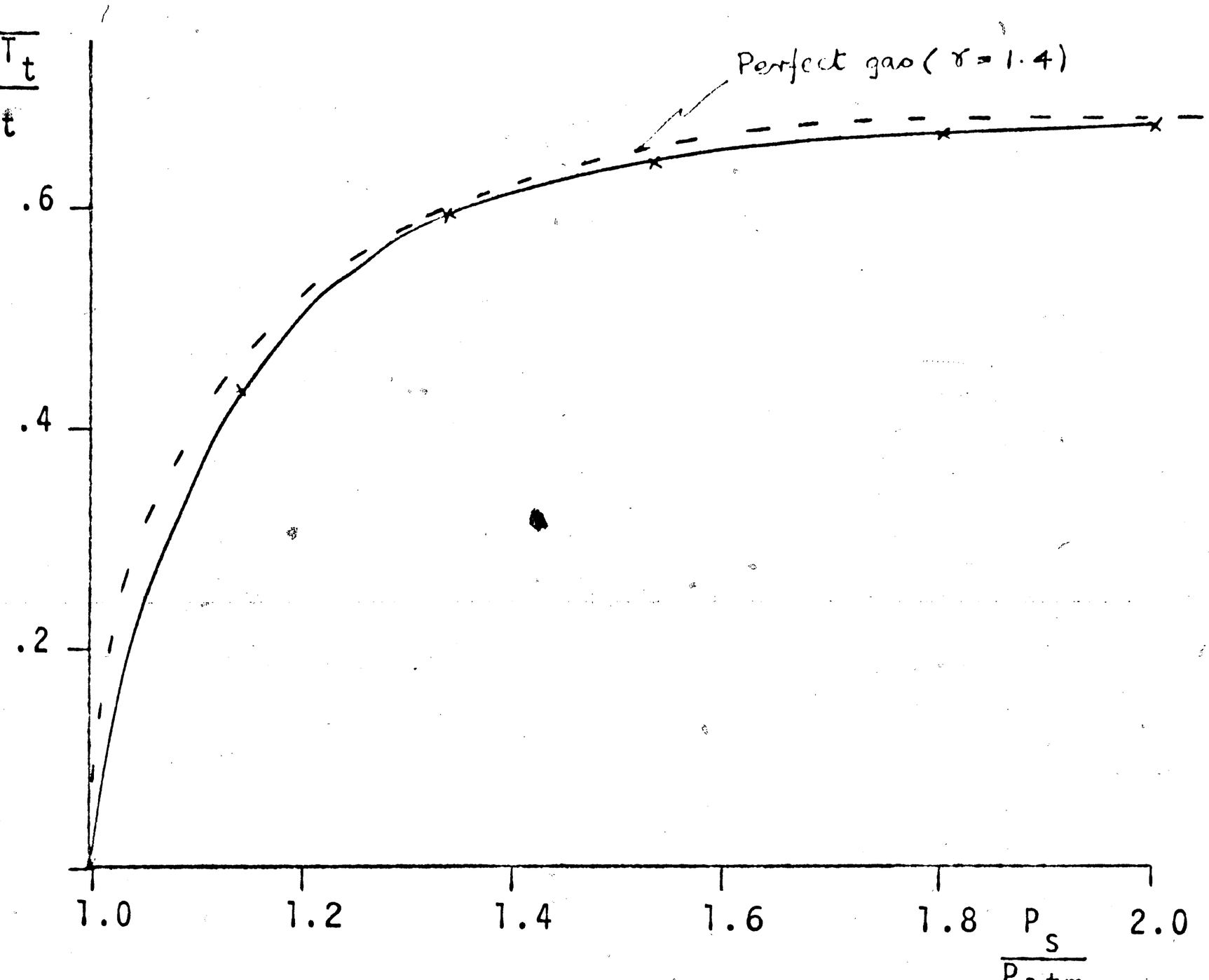

Figure 20. Power jet characteristics, Amplifier No. 2

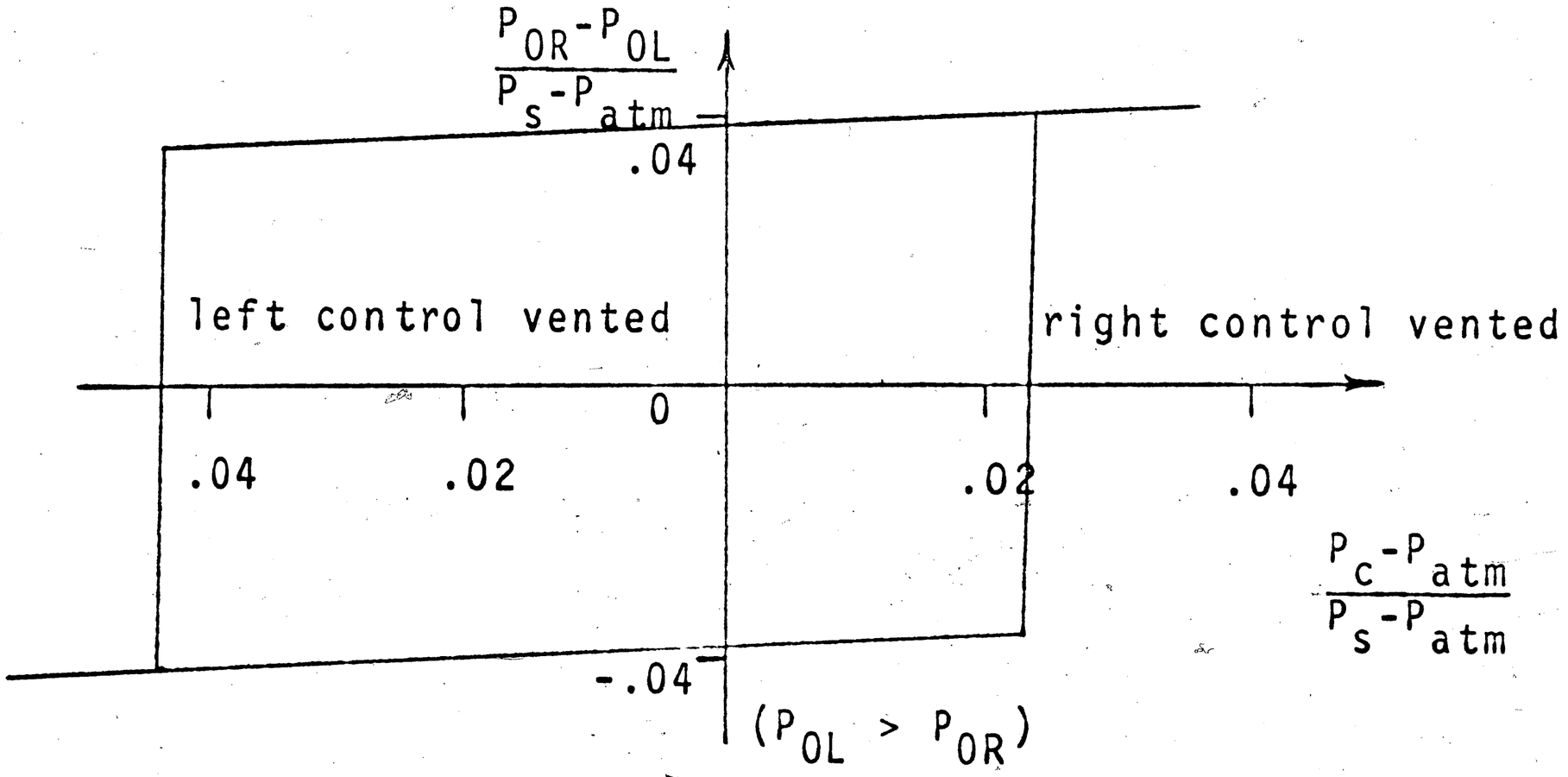

Figure 21(a). Supply pressure = 3.0 psig

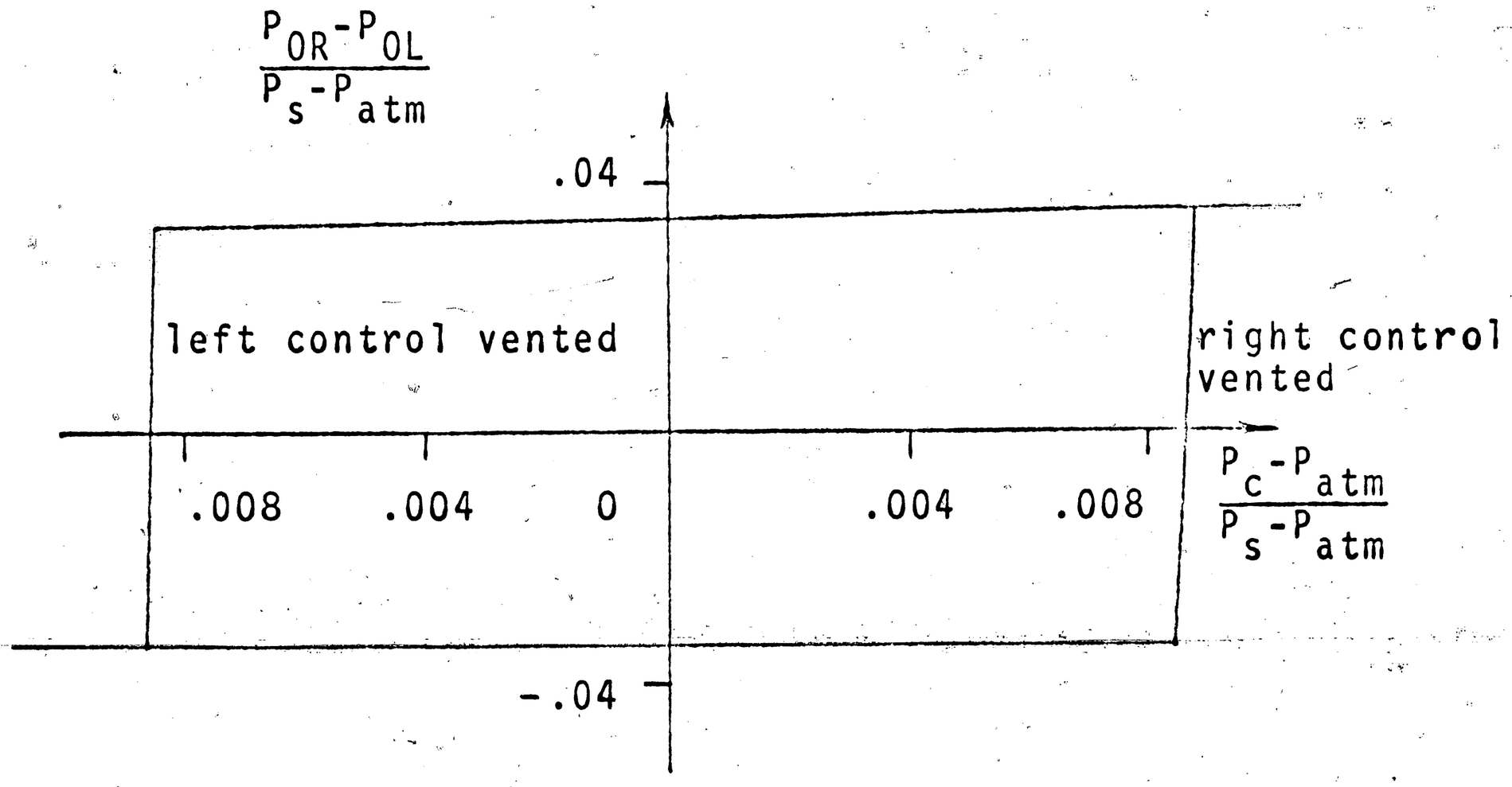

Figure 21(b). Supply pressure P_s = 5.0 psig

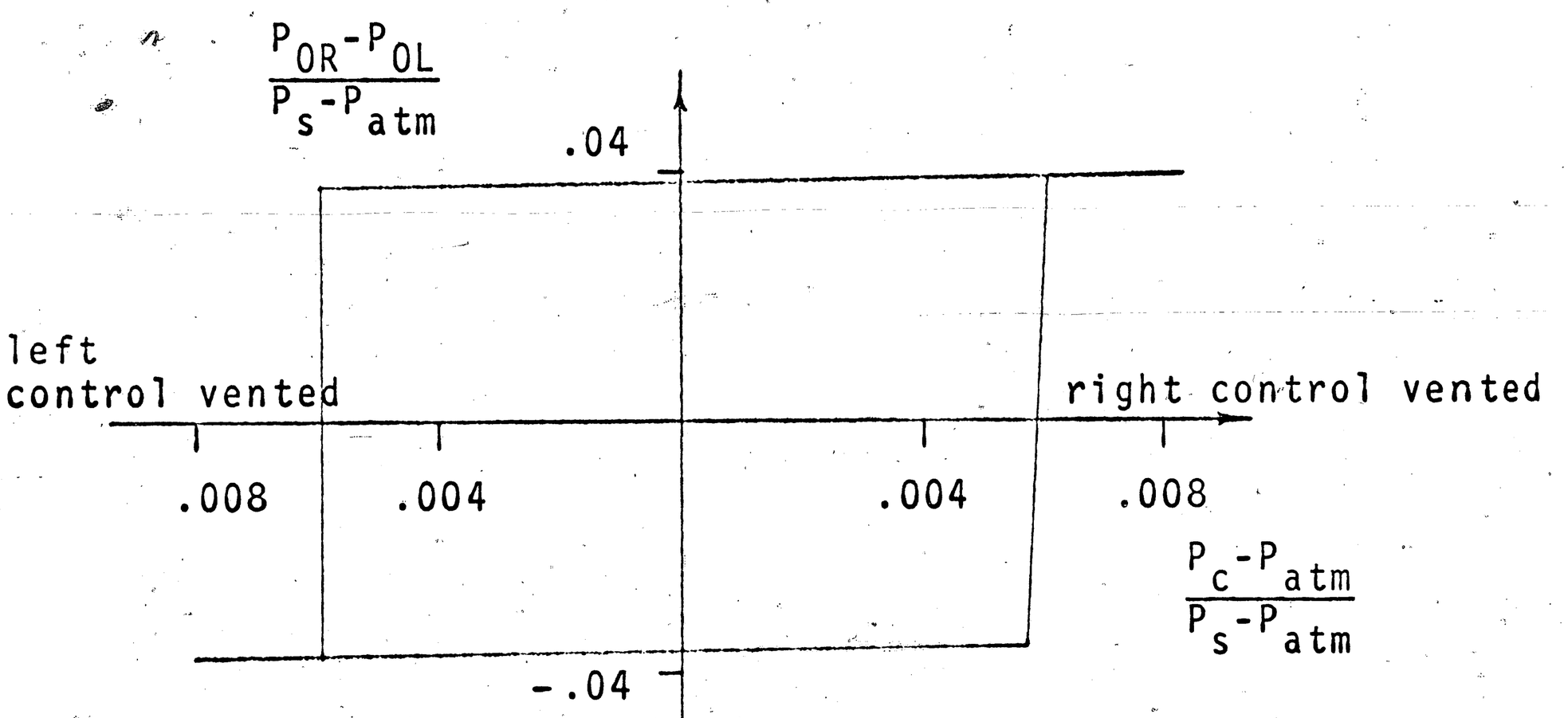

Figure 21(c). Supply Pressure P_s = 8.0 psig

Differential input-output characteristics at no load conditions. Amplifier No. 2.

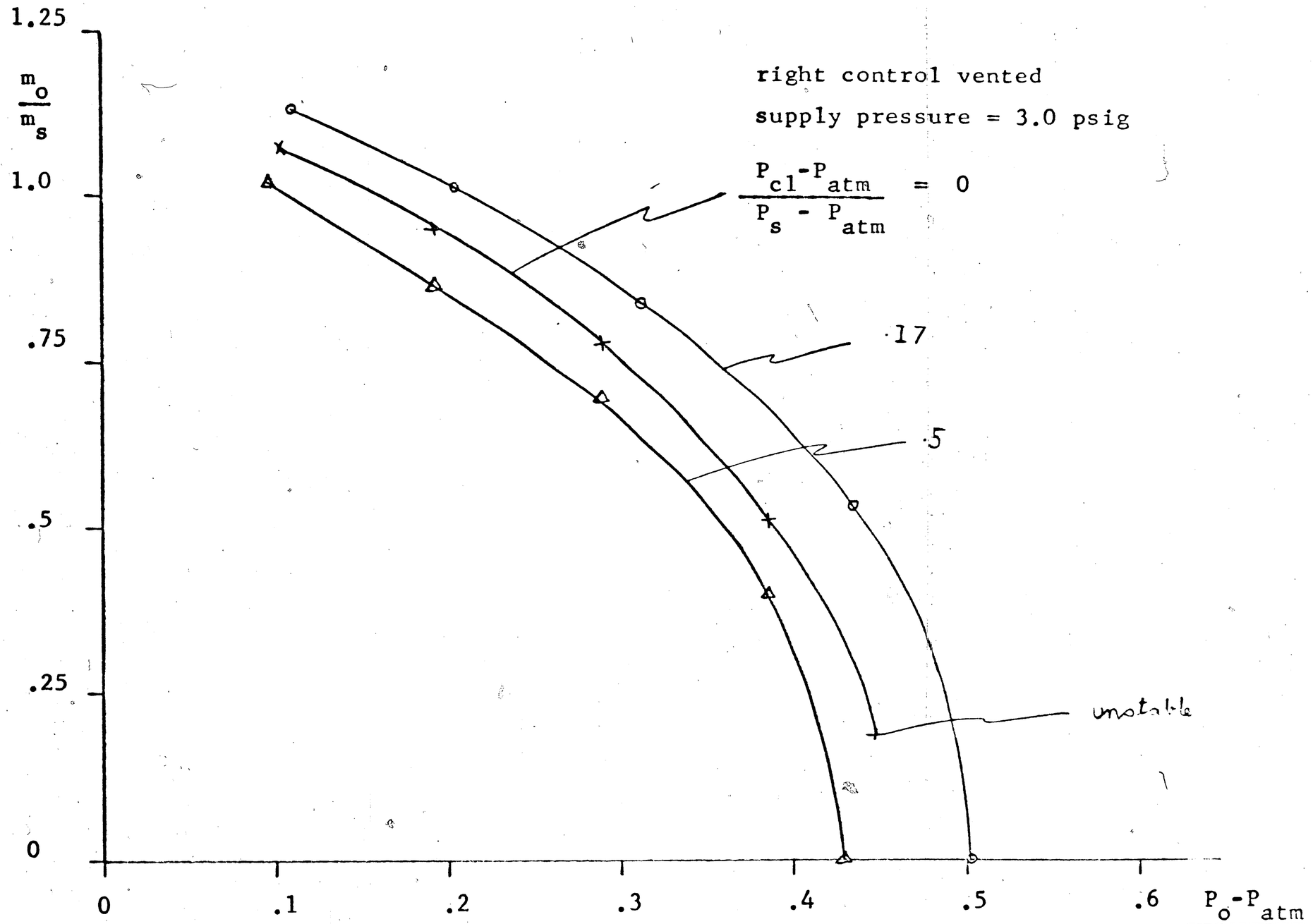

Figure 22 (a) Right output characteristics

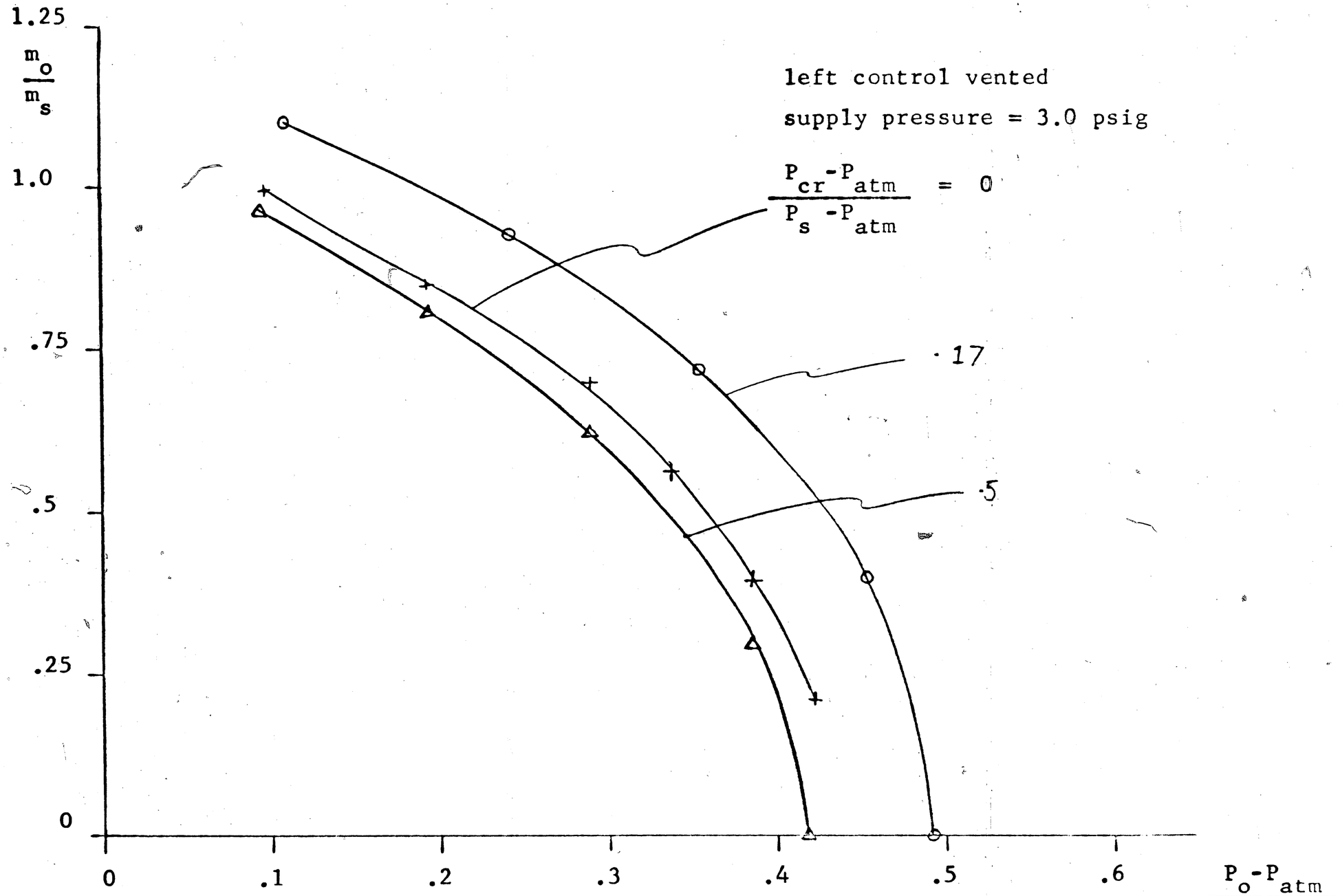

Figure 22 (b) Left output characteristics

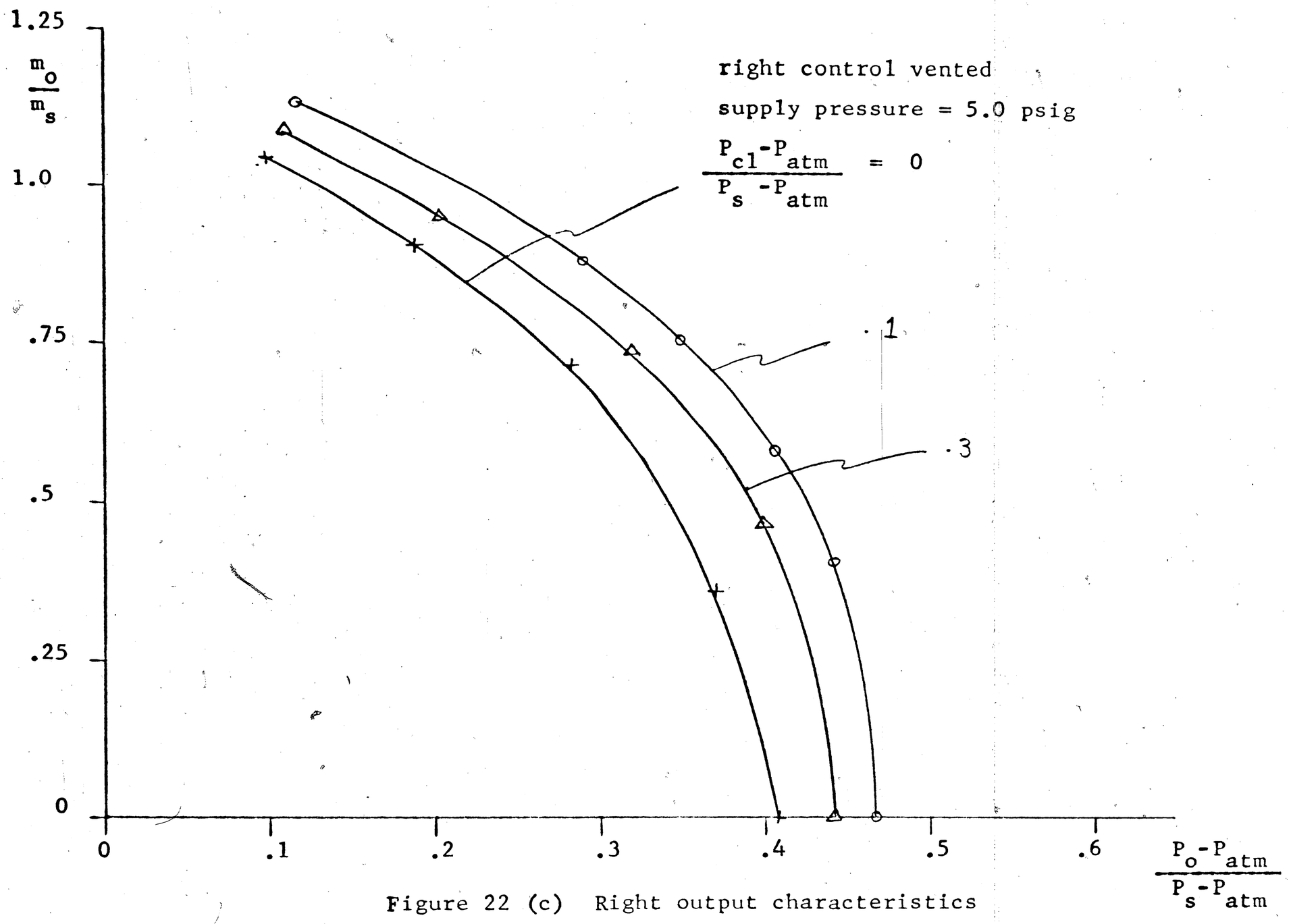

Figure 22 (c) Right output characteristics

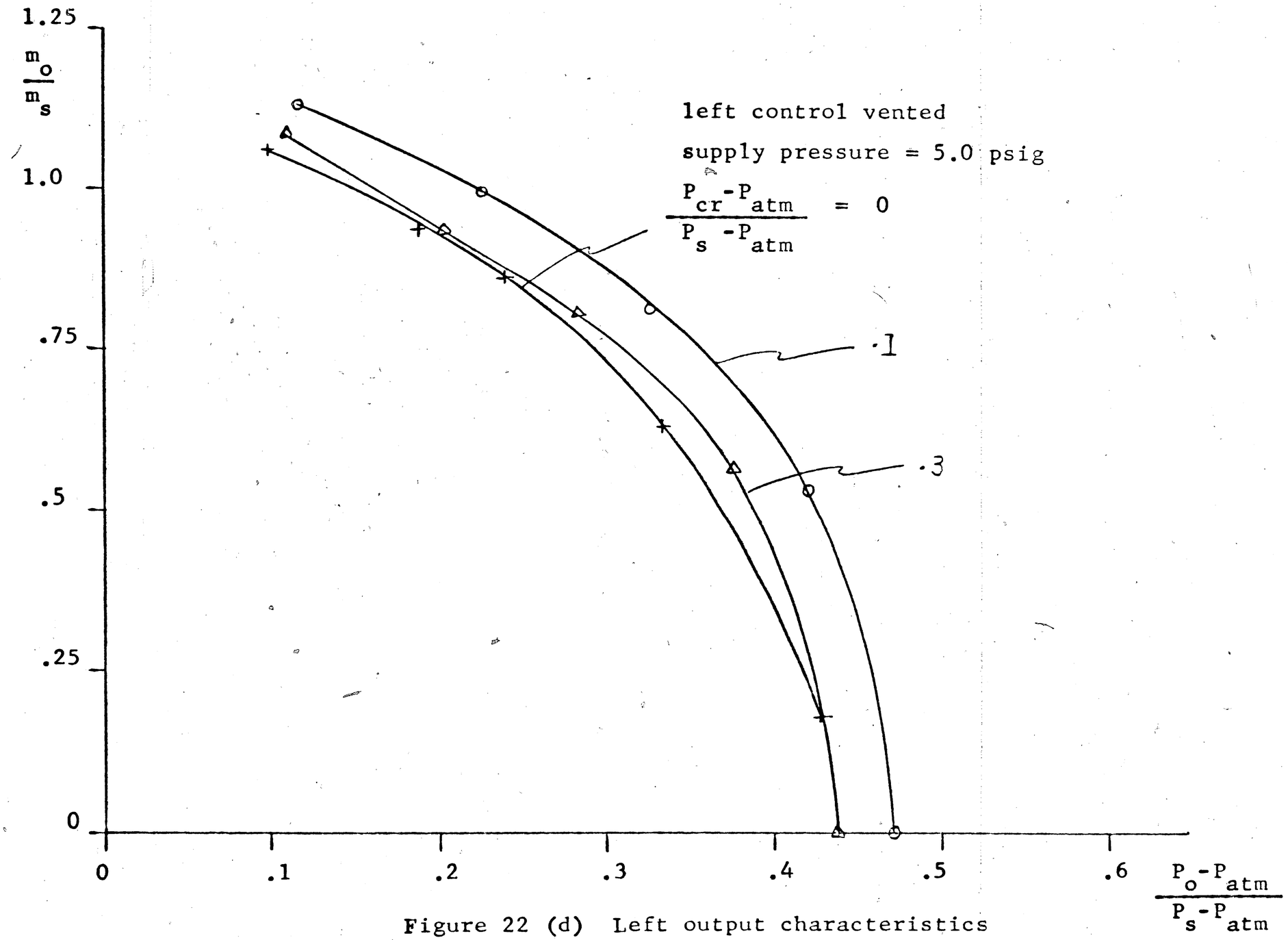

Figure 22 (d) Left output characteristics

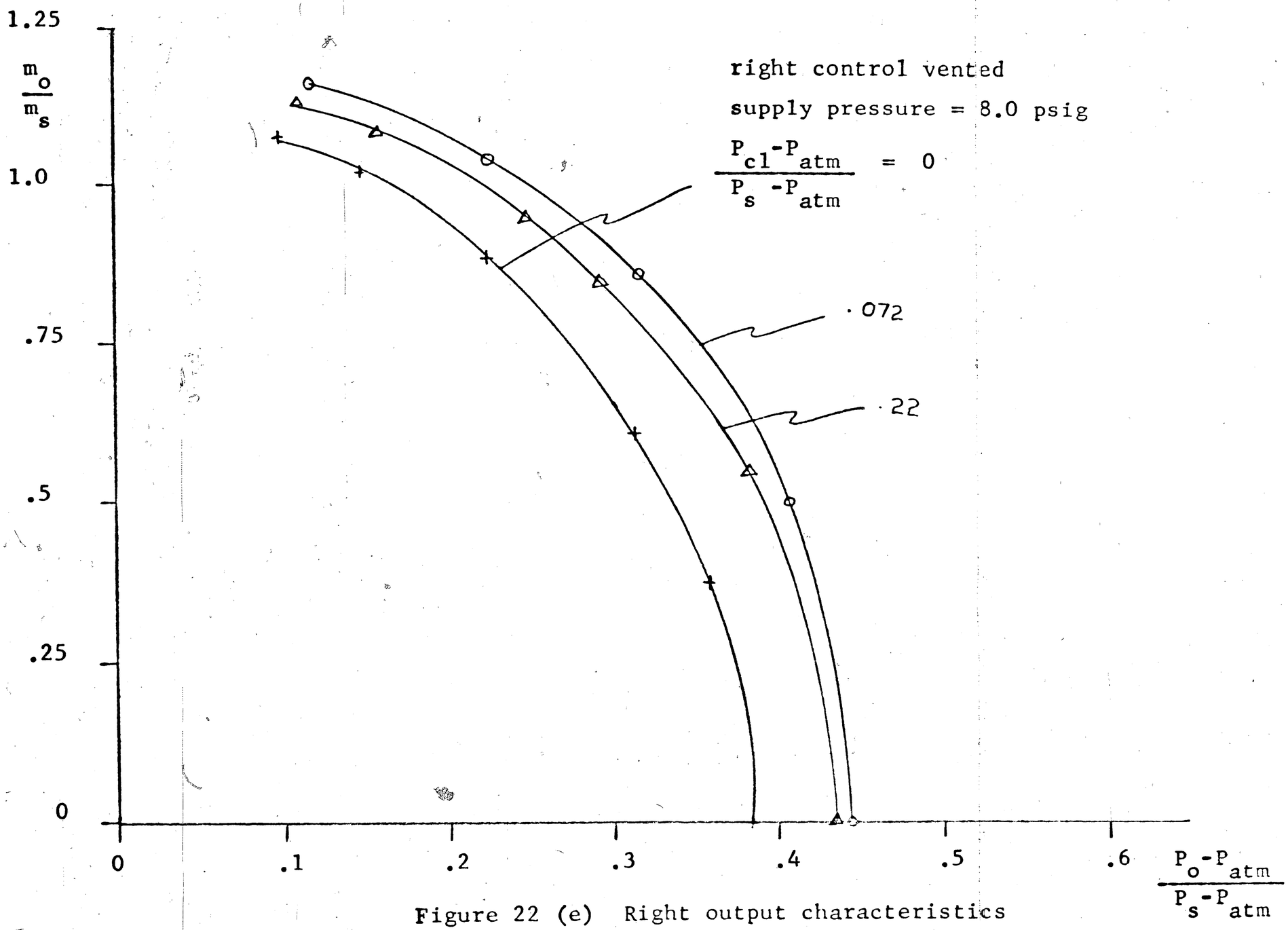

Figure 22 (e) Right output characteristics

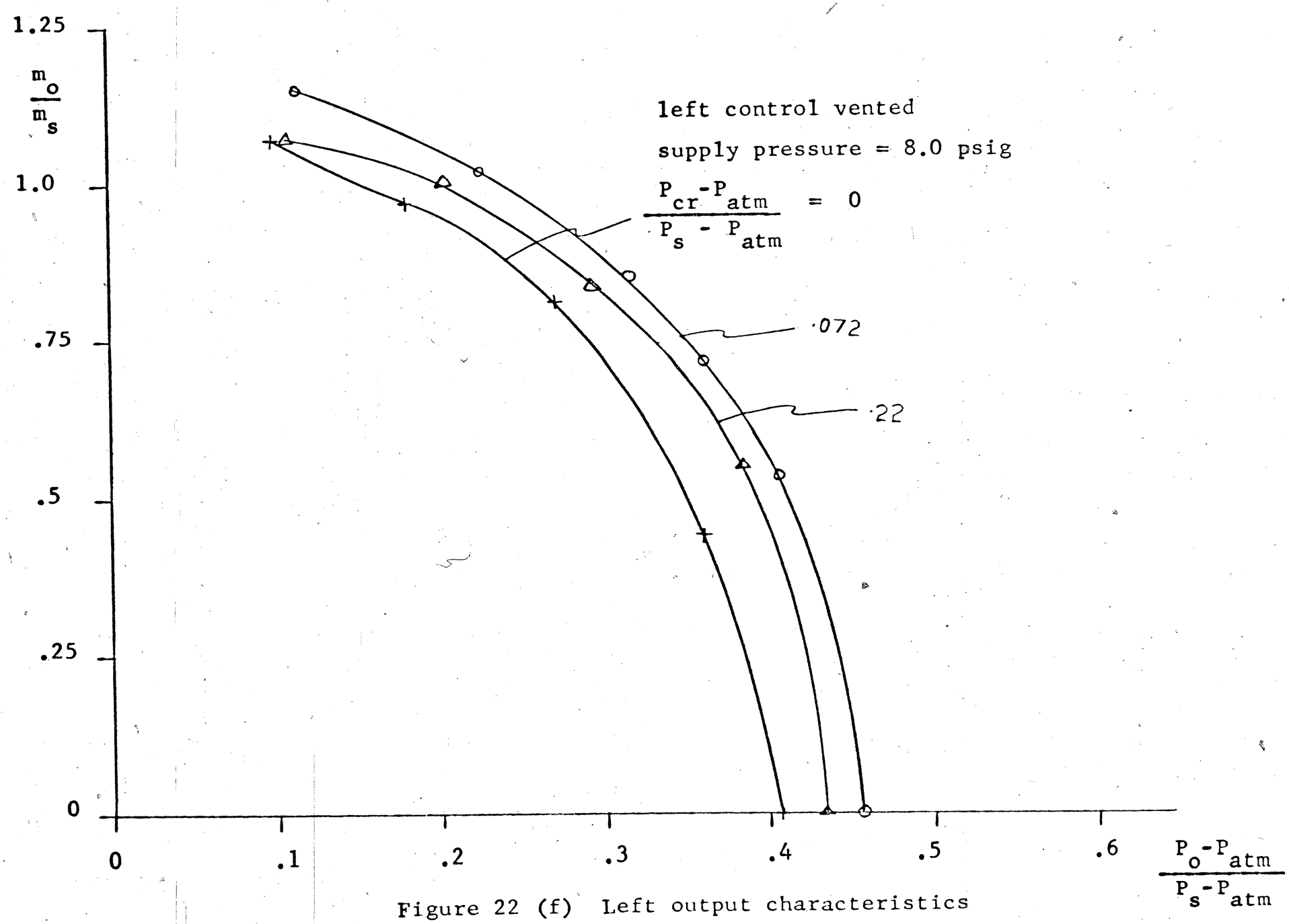

Figure 22 (f) Left output characteristics

Output characteristics. Amplifier No. 2

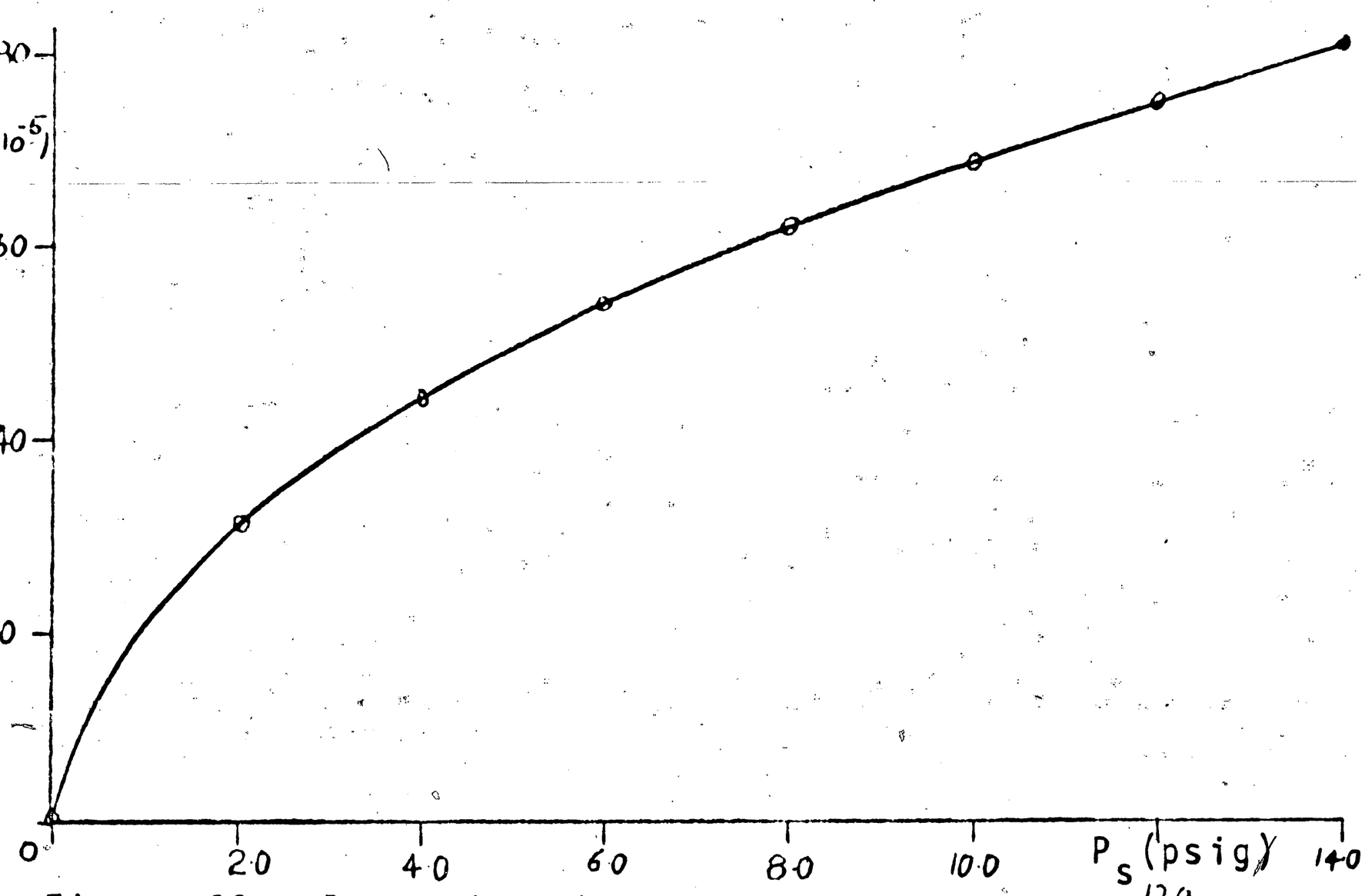

Figure 23. Power jet characteristics
Proportional amplifier

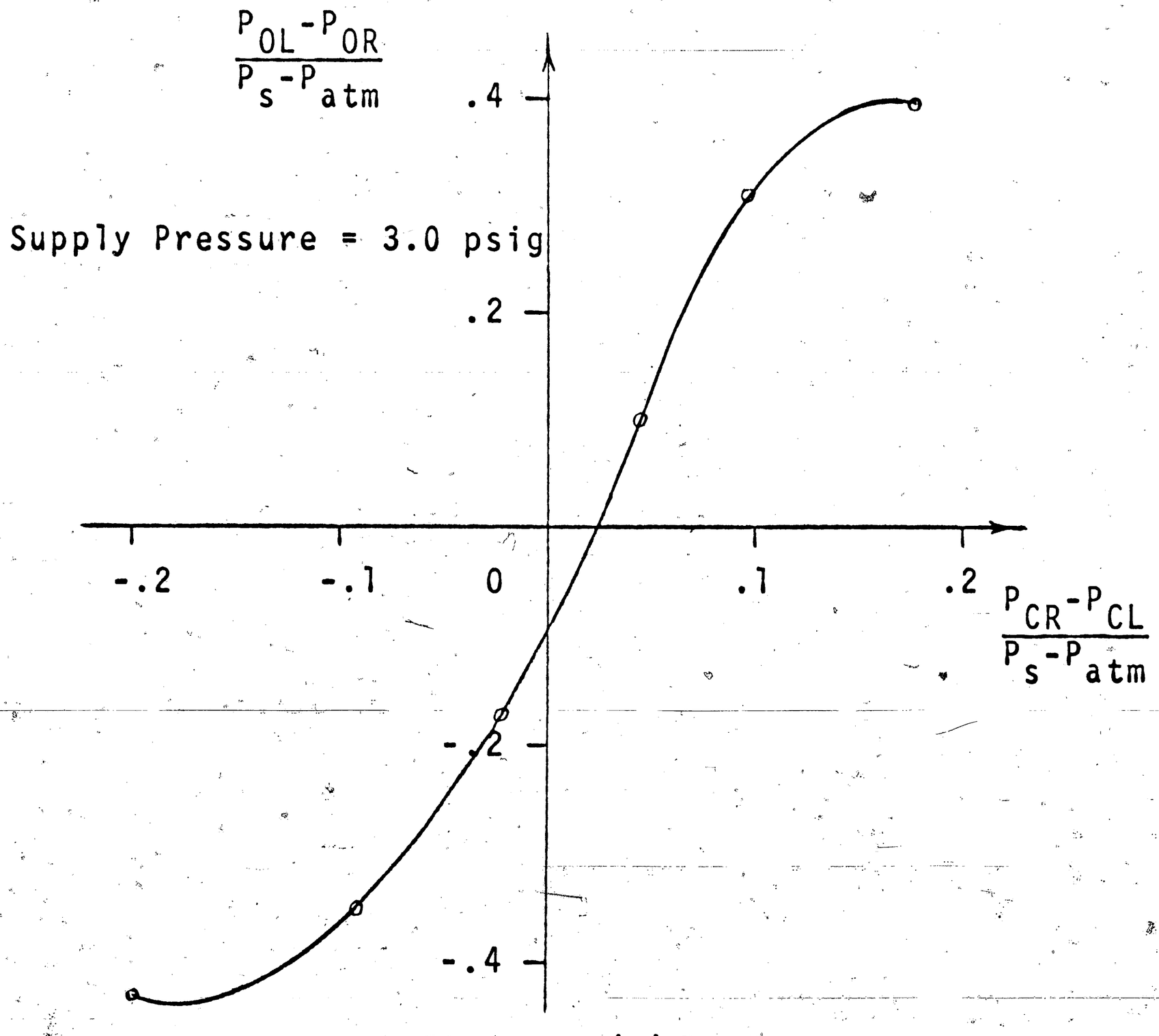

Figure 24(a)

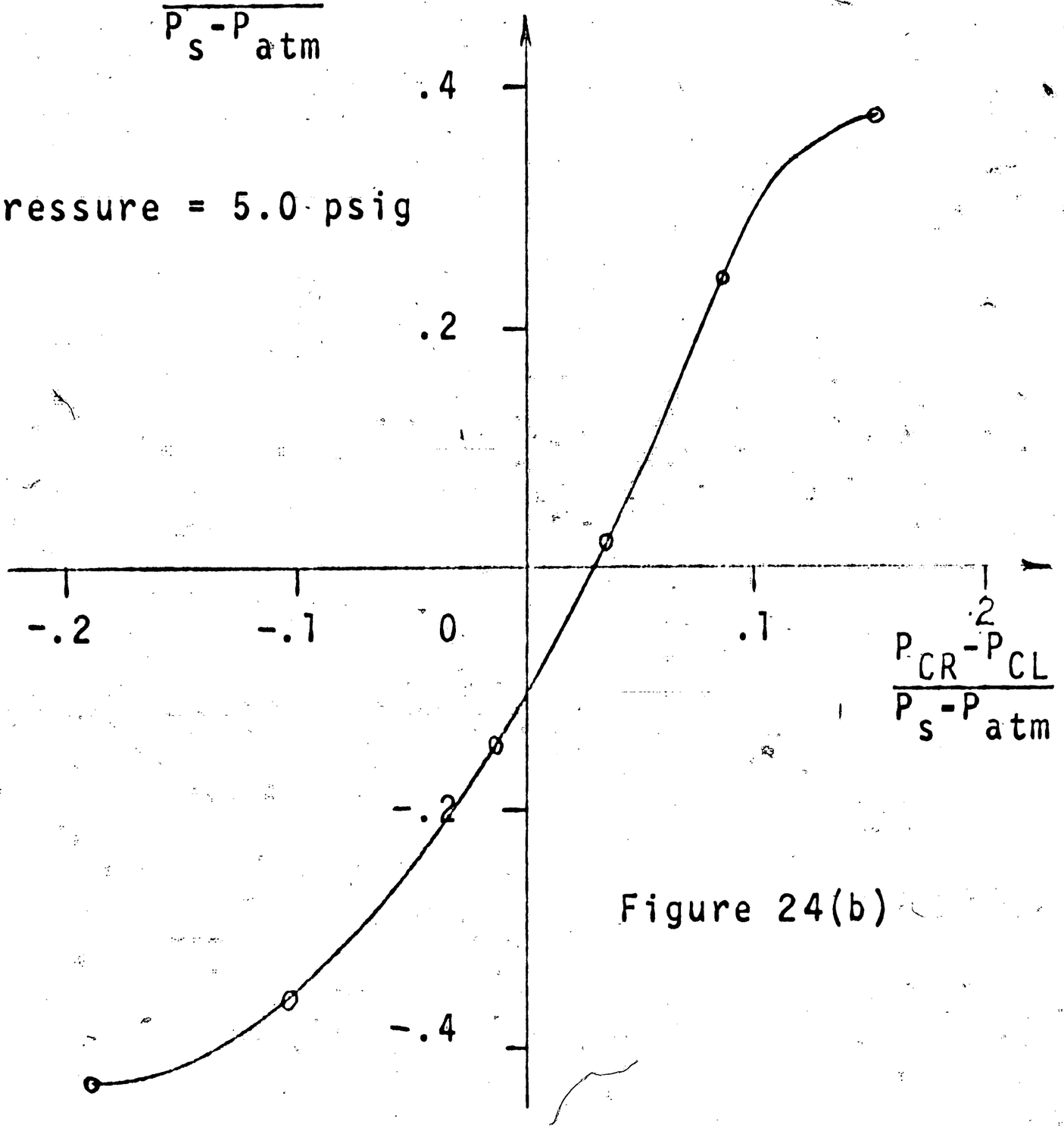

Figure 24(b)

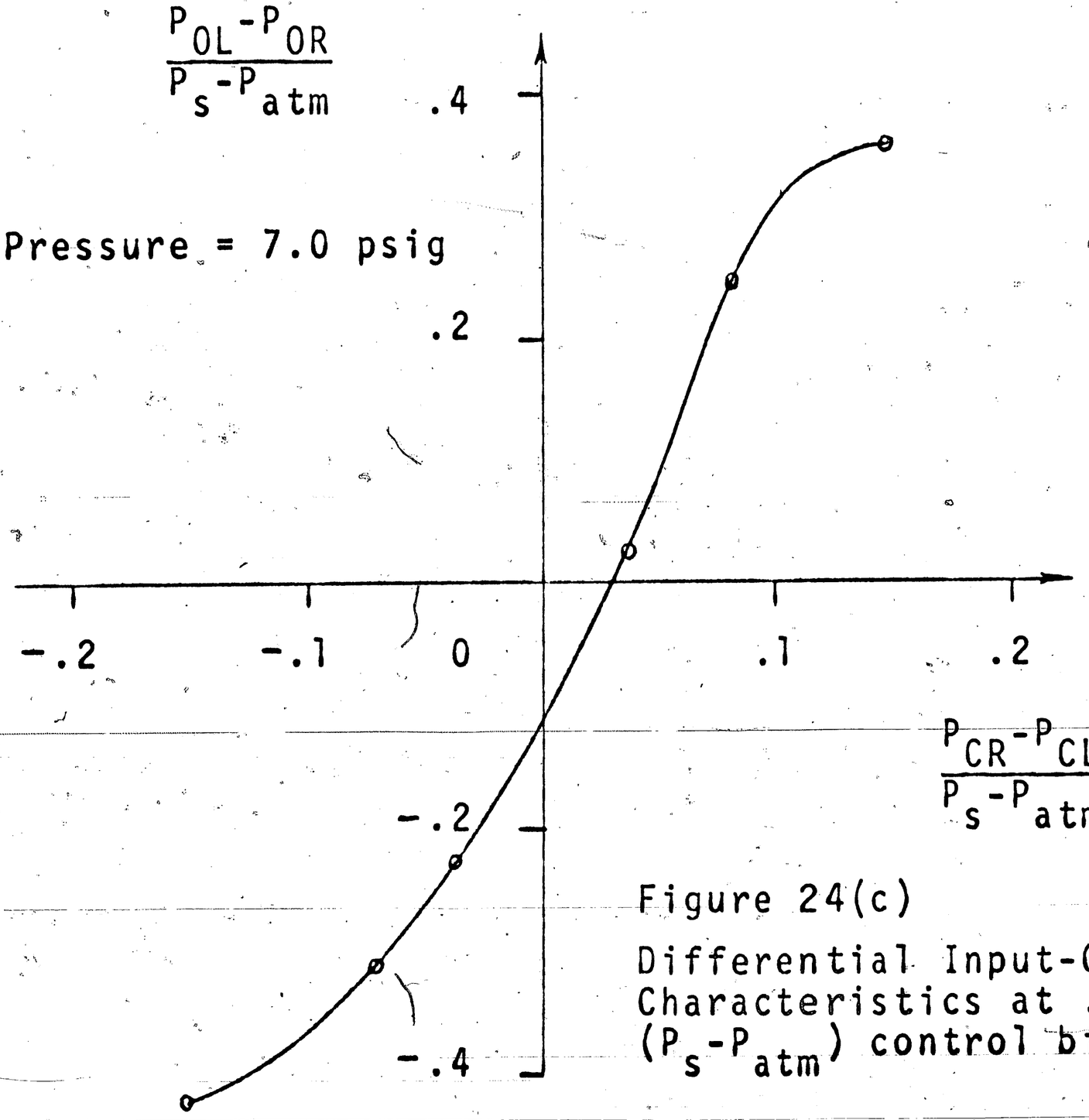

Figure 24(c)

Differential Input-Output-Characteristics at .2 (P_s-P_{atm}) control bias

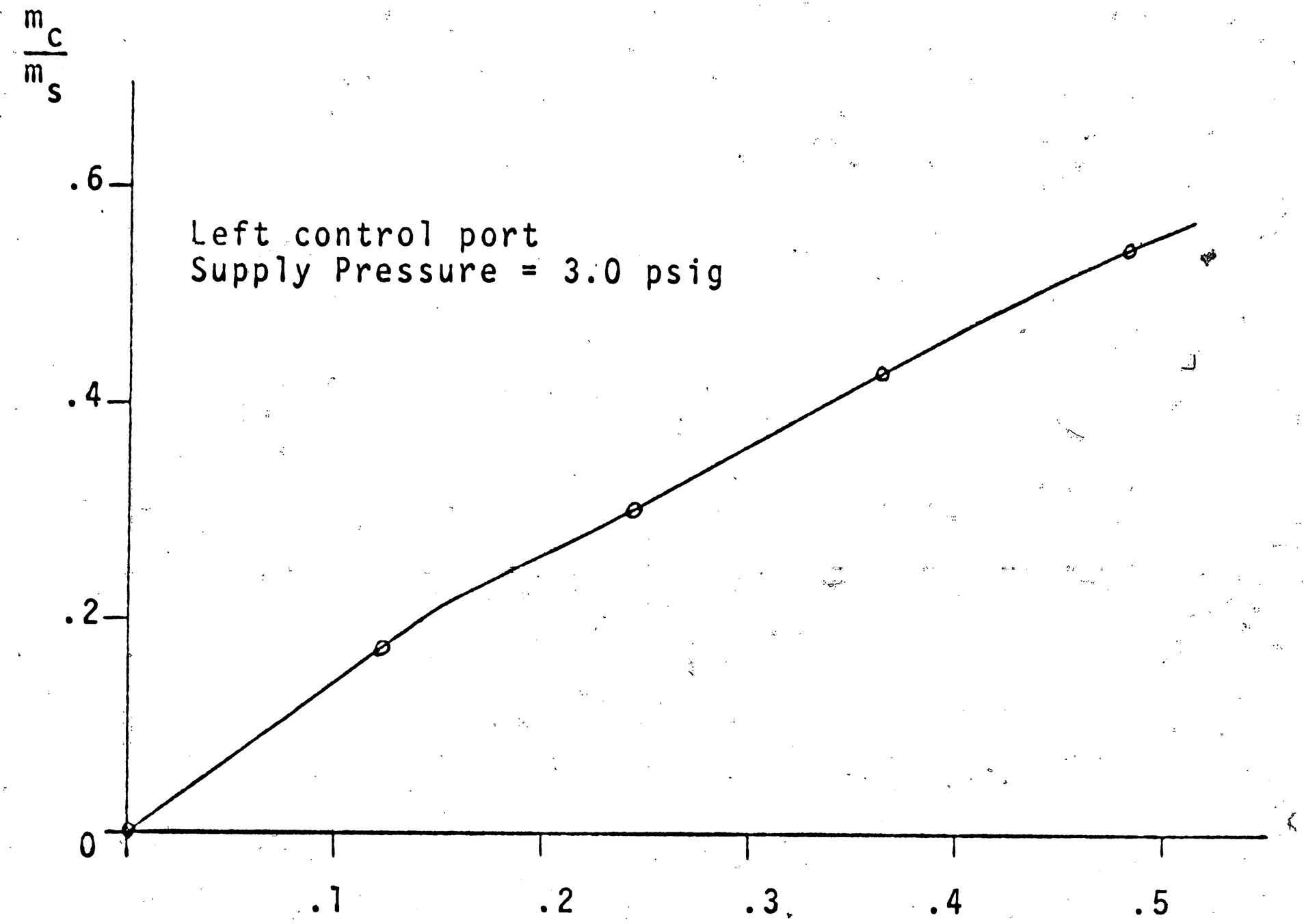

Figure 25(a)

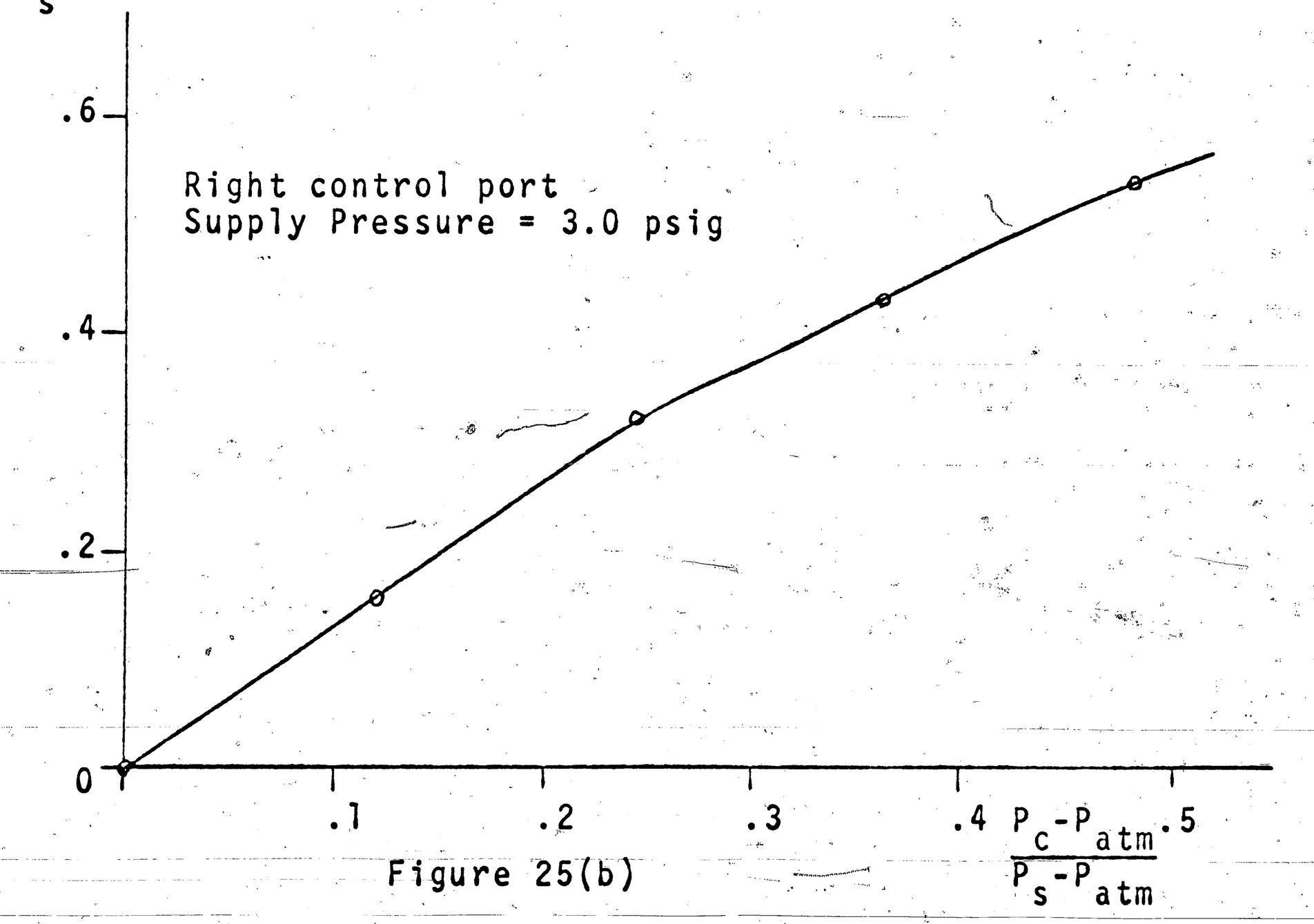

Figure 25(b)

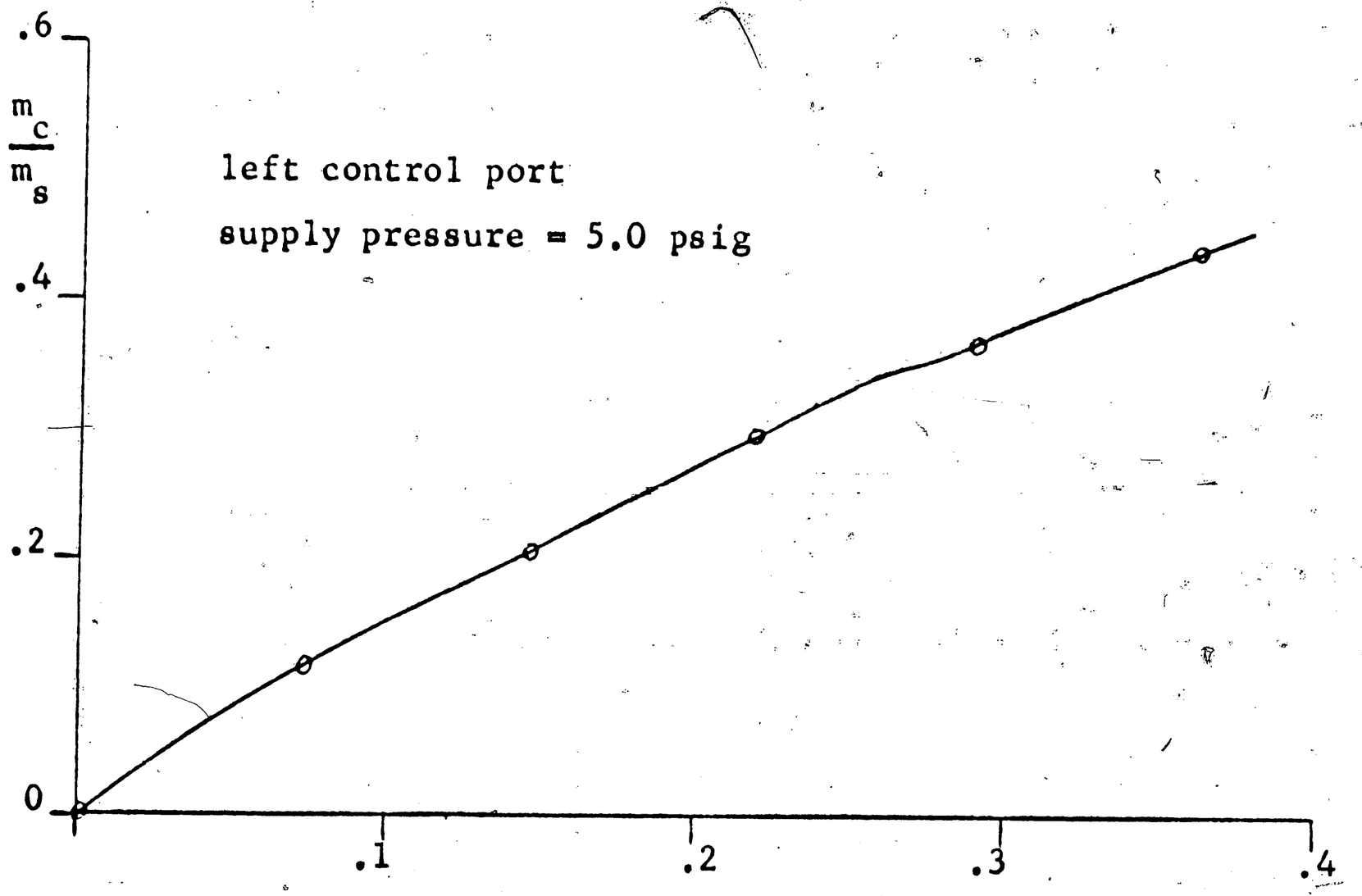

Figure 25 (c)

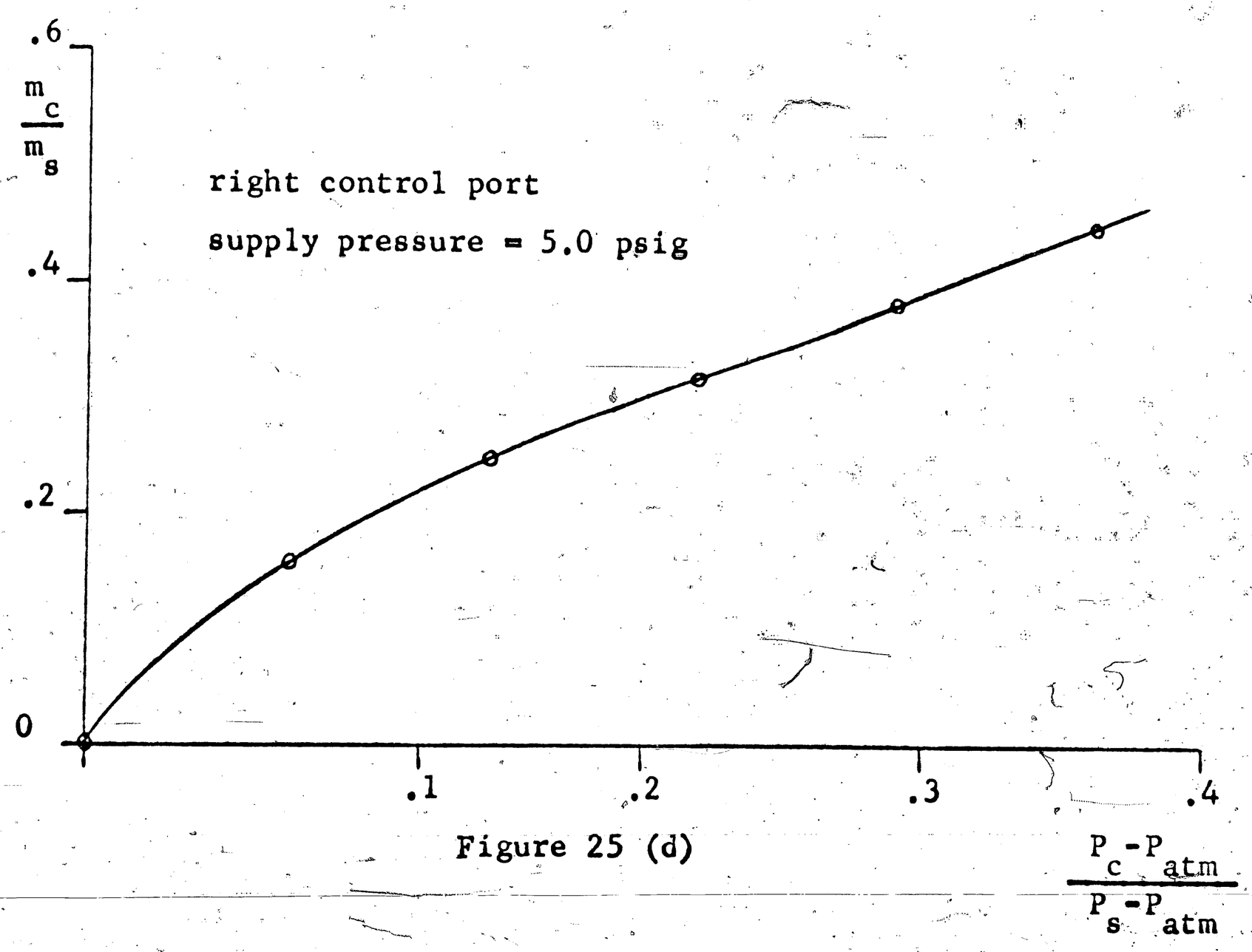

Figure 25 (d)

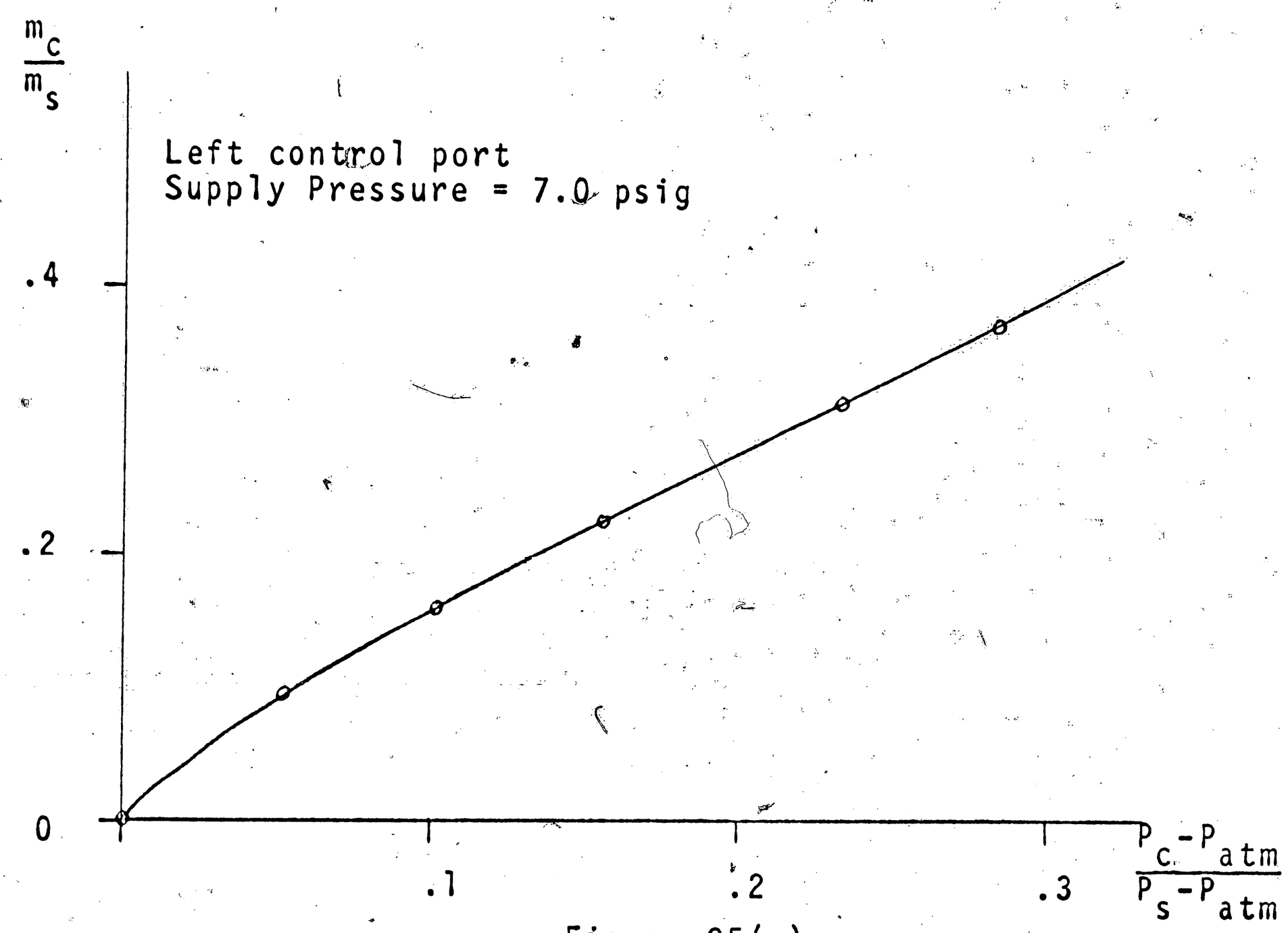

Figure 25(e)

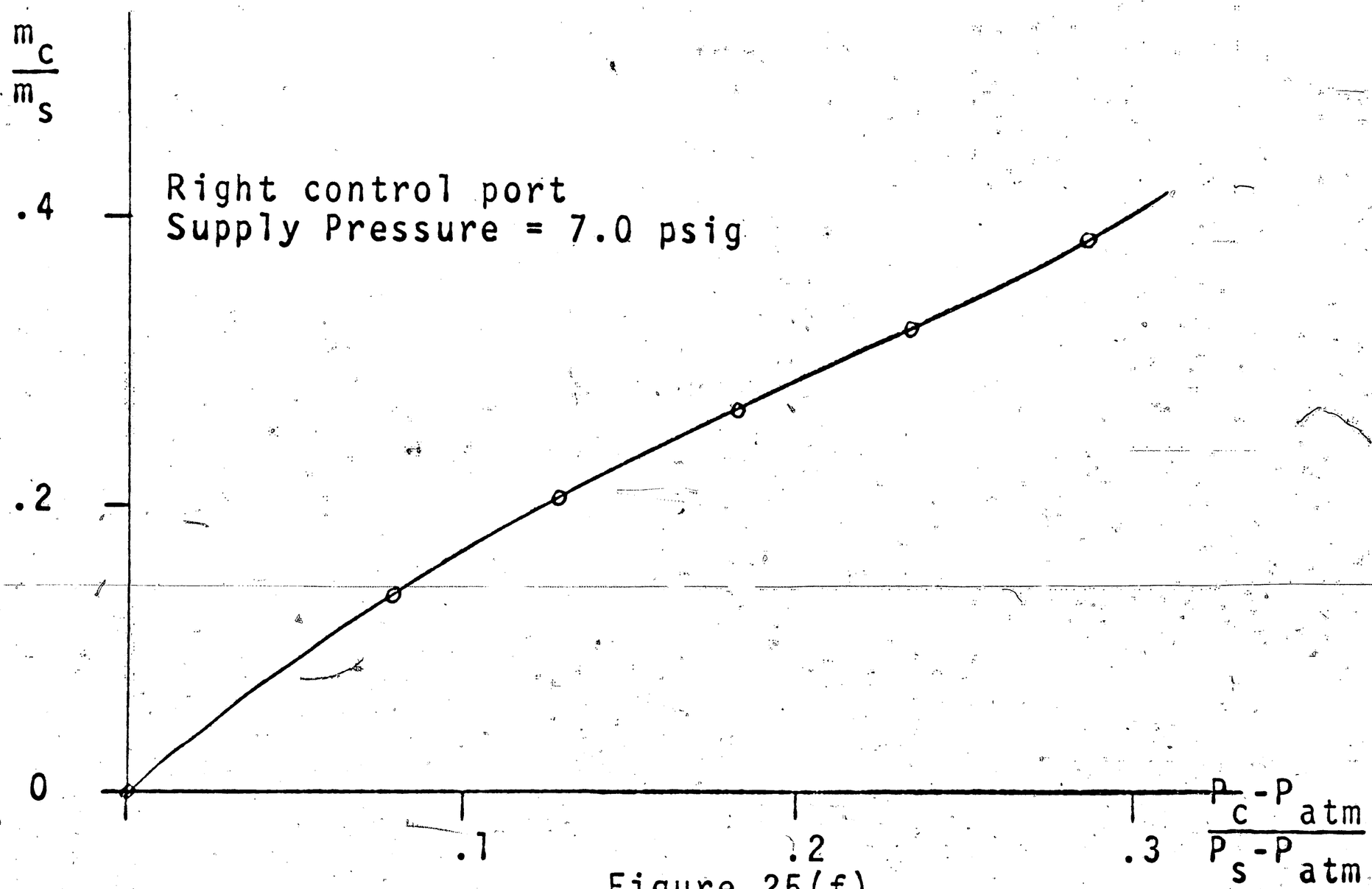

Figure 25(f)
Input characteristics at .2($P_s - P_{atm}$) control bias

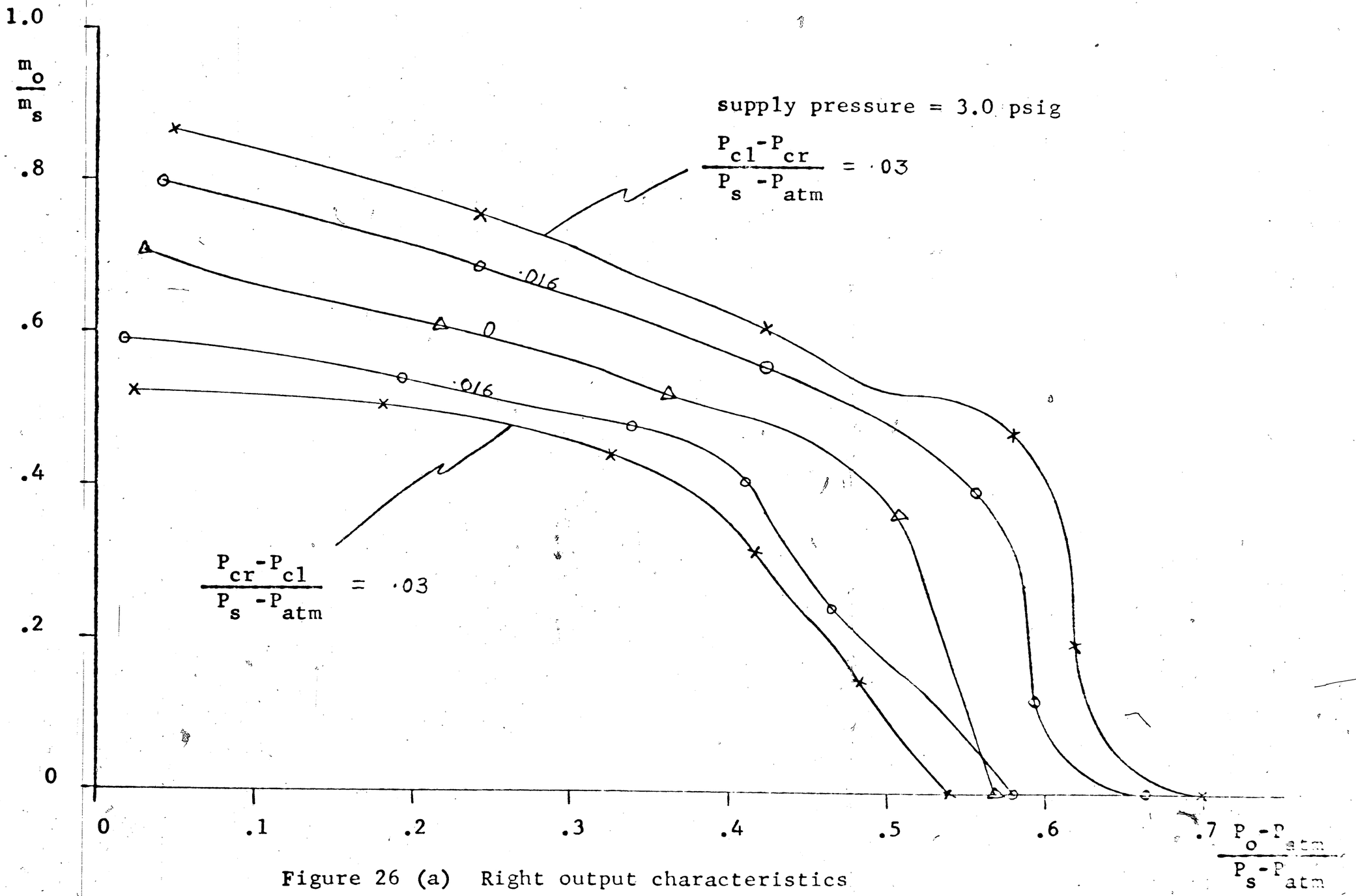

Figure 26 (a) Right output characteristics

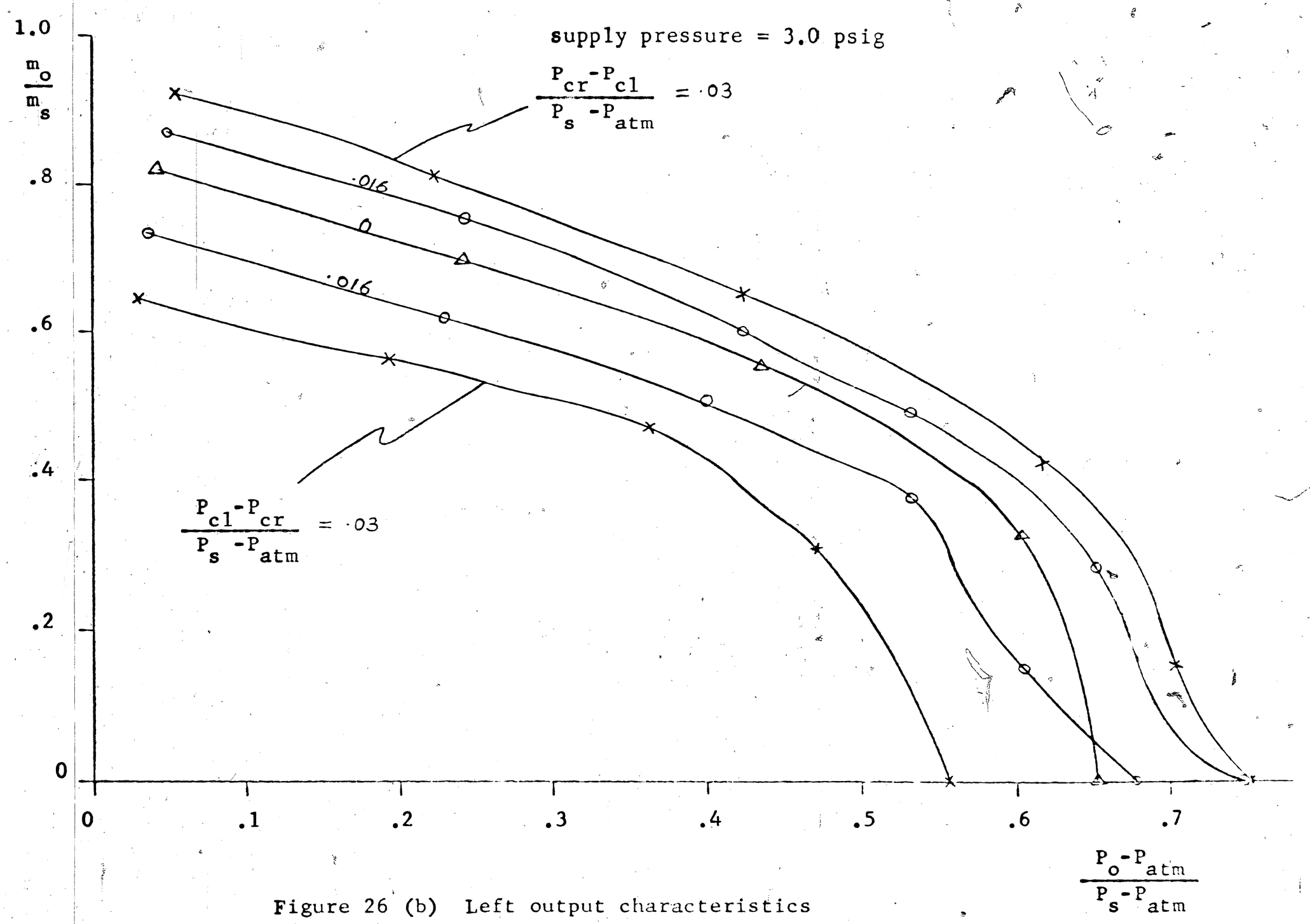

Figure 26 (b) Left output characteristics

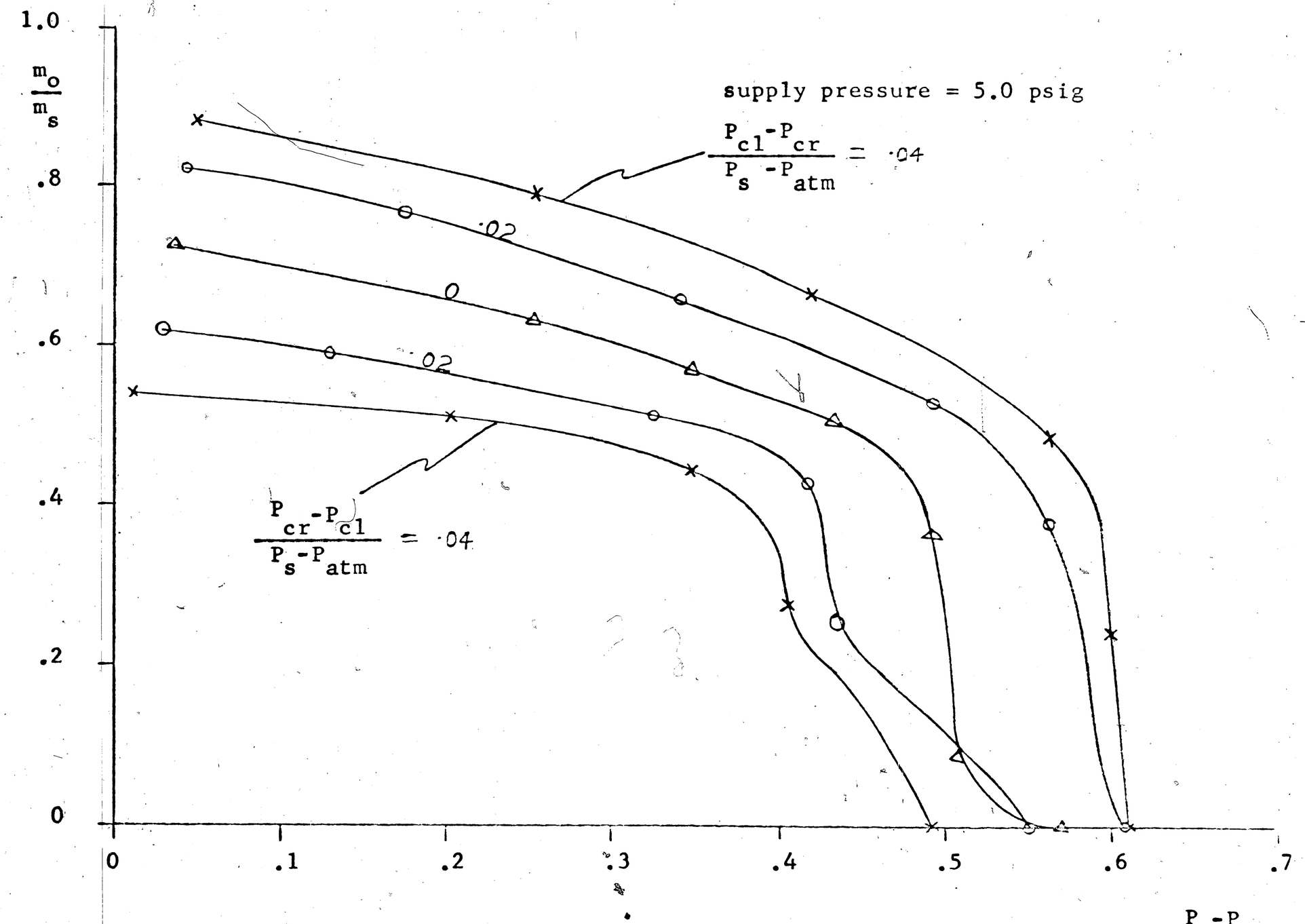

Figure 26 (c) Right output characteristics

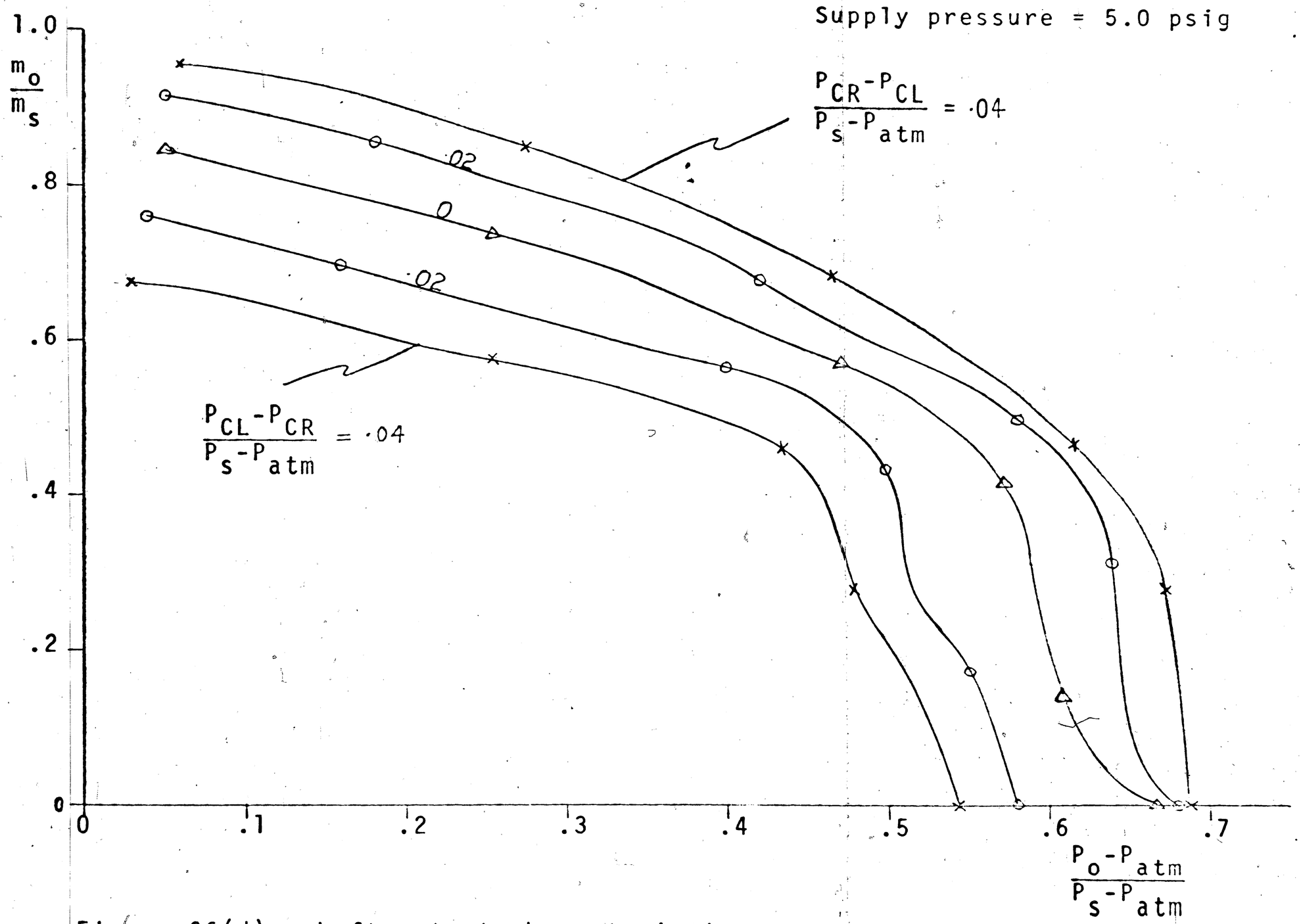

Figure 26(d). Left output characteristic

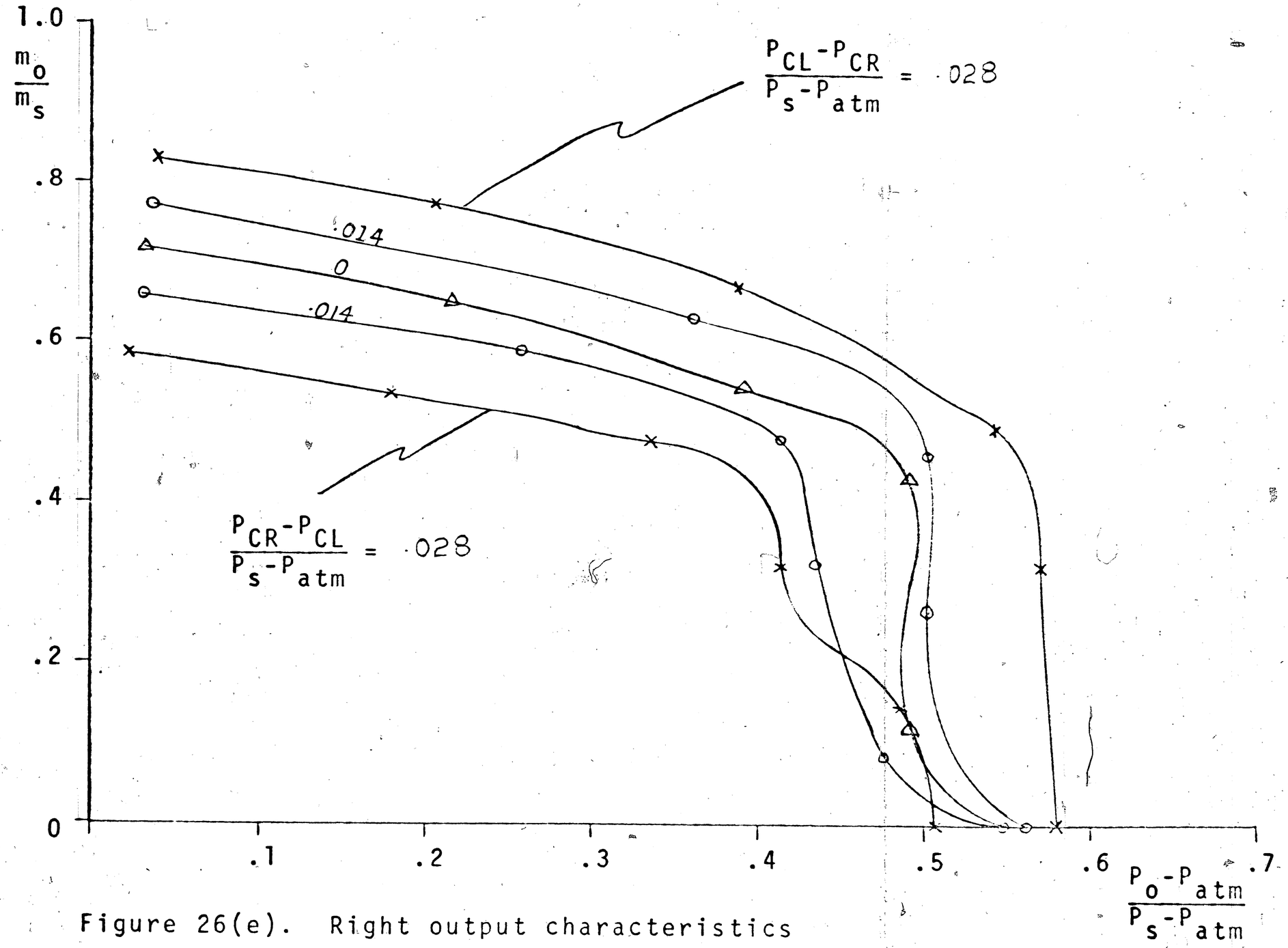

Figure 26(e). Right output characteristics

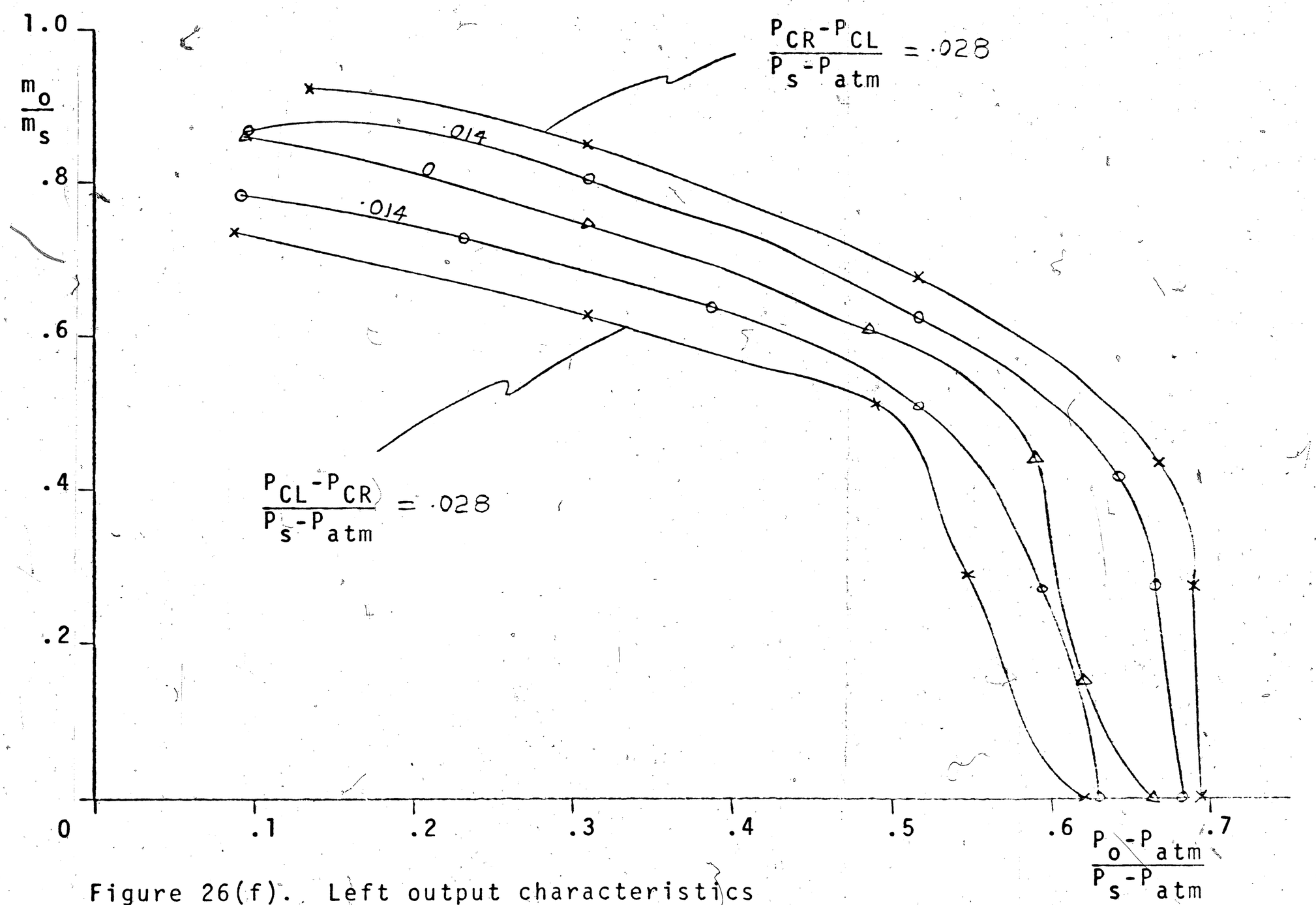

Figure 26(f). Left output characteristics
Output characteristics proportional amplifier

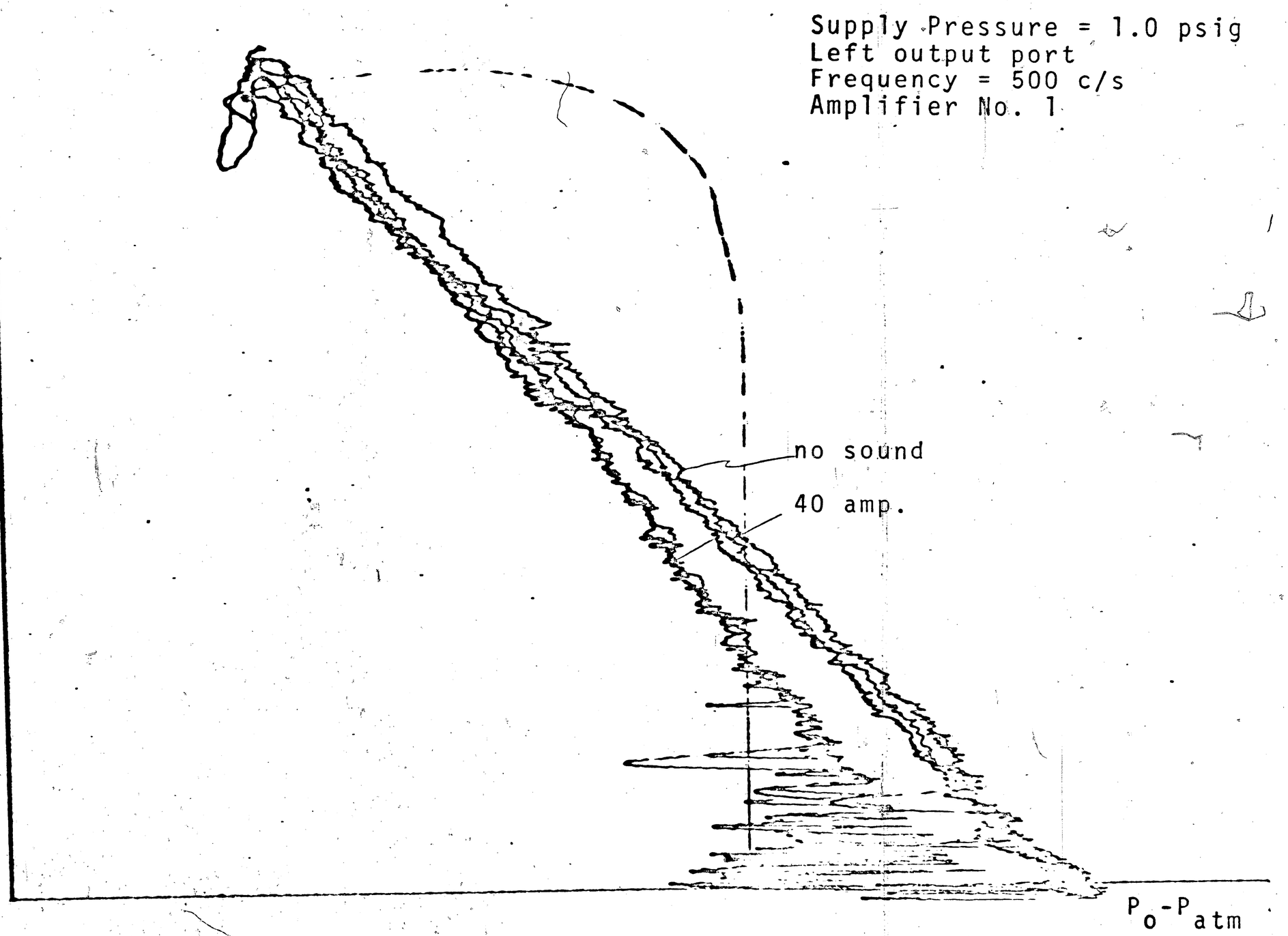

Figure 27. Output port characteristics with sound introduced in power jet

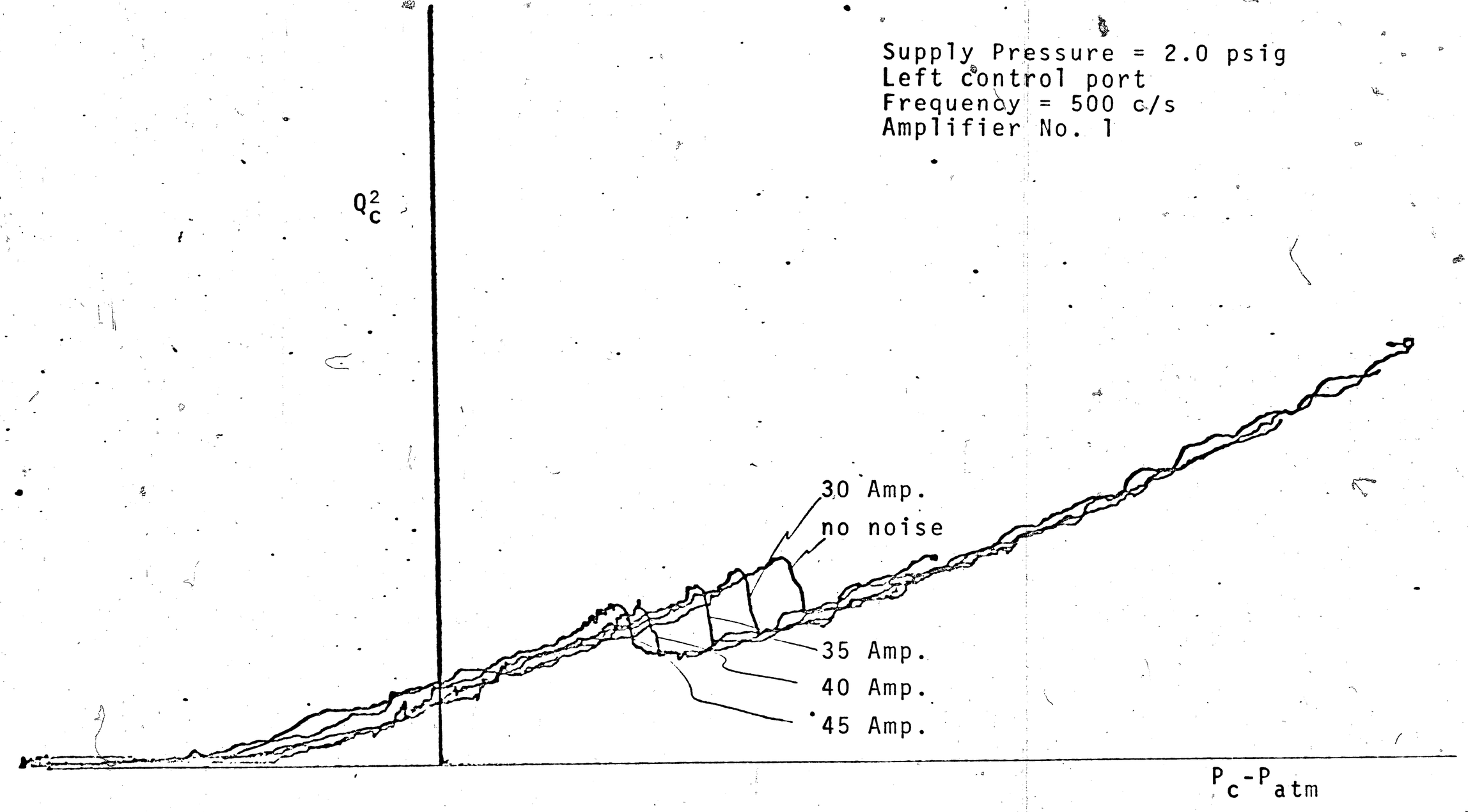

Figure 28. Input characteristics with sound introduced in power jet

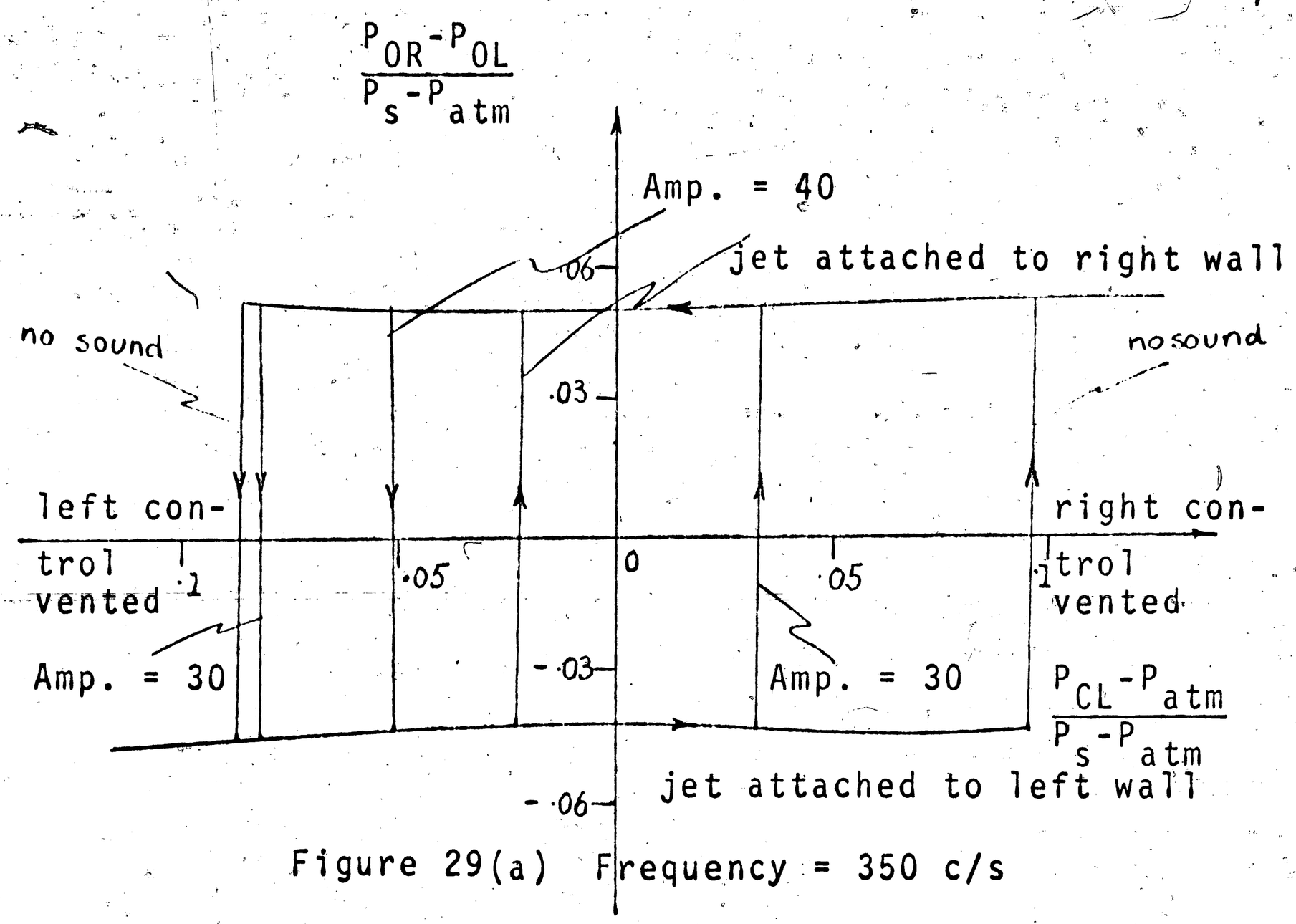

Figure 29(a) Frequency = 350 c/s

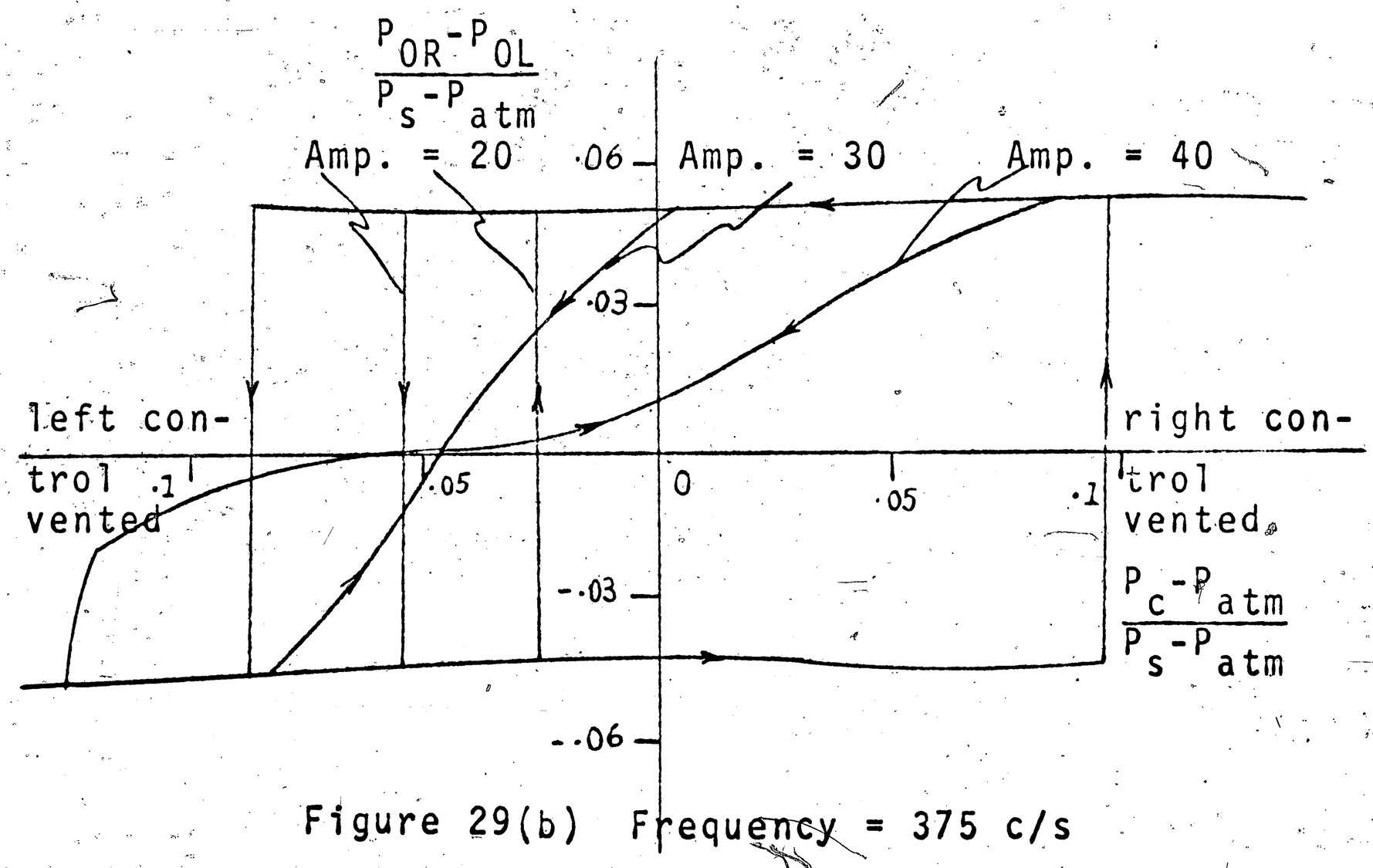

Figure 29(b) Frequency = 375 c/s

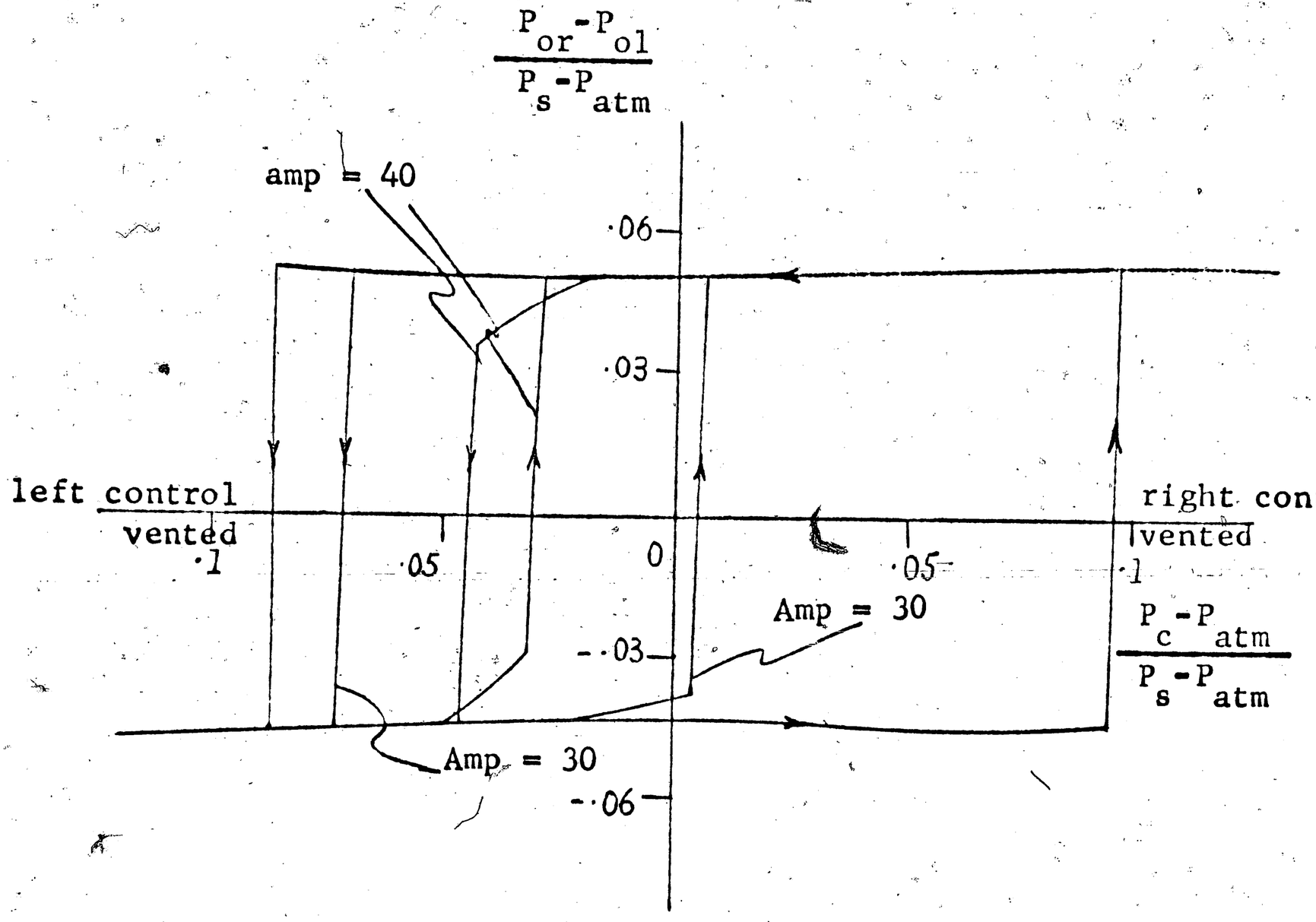

Figure 29 (c) frequency = 400 c/s

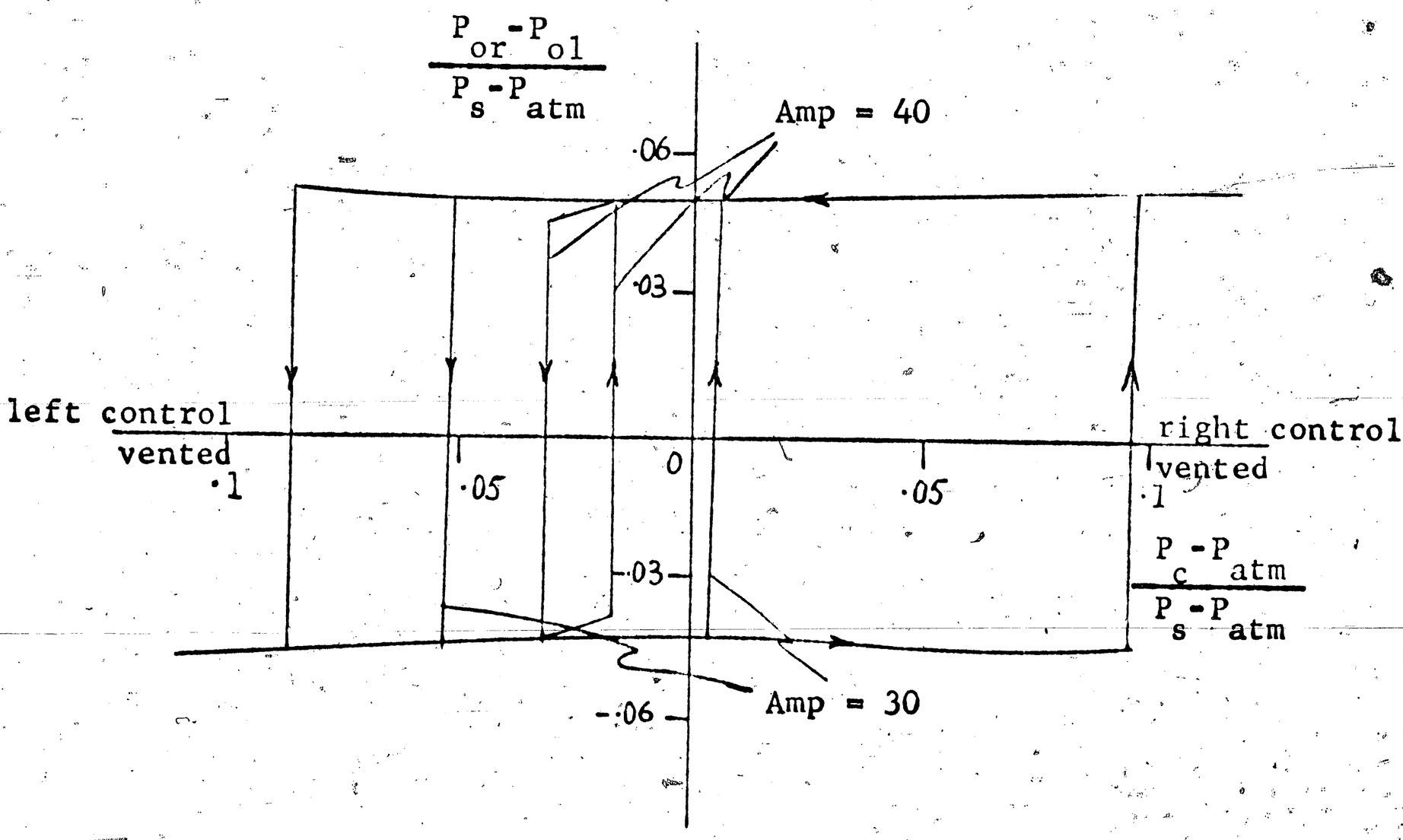

Figure 29 (d) frequency = 500 c/s

Differential input-output characteristics

supply pressure = 2.0 psig

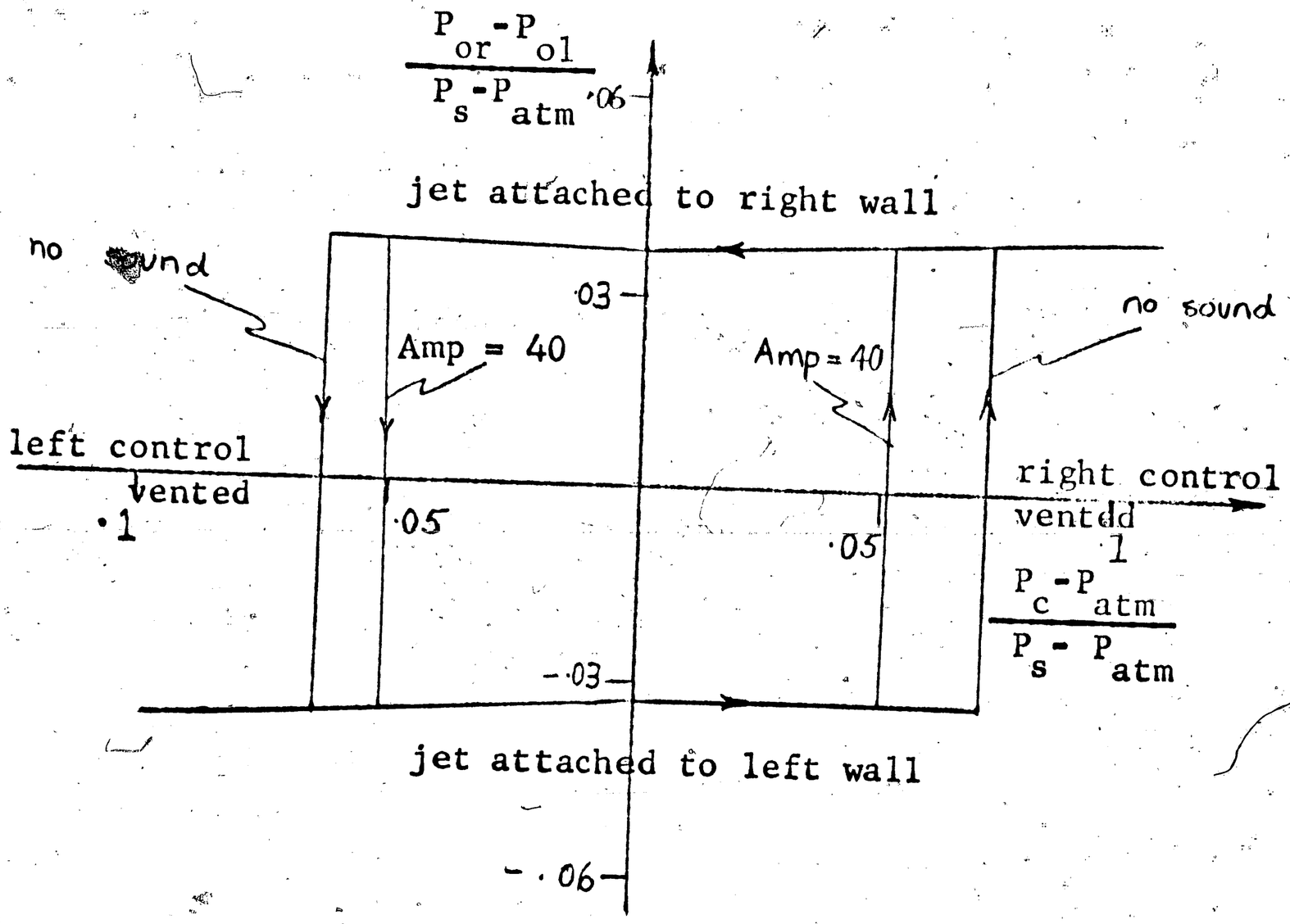

Figure 30 (a) frequency = 330

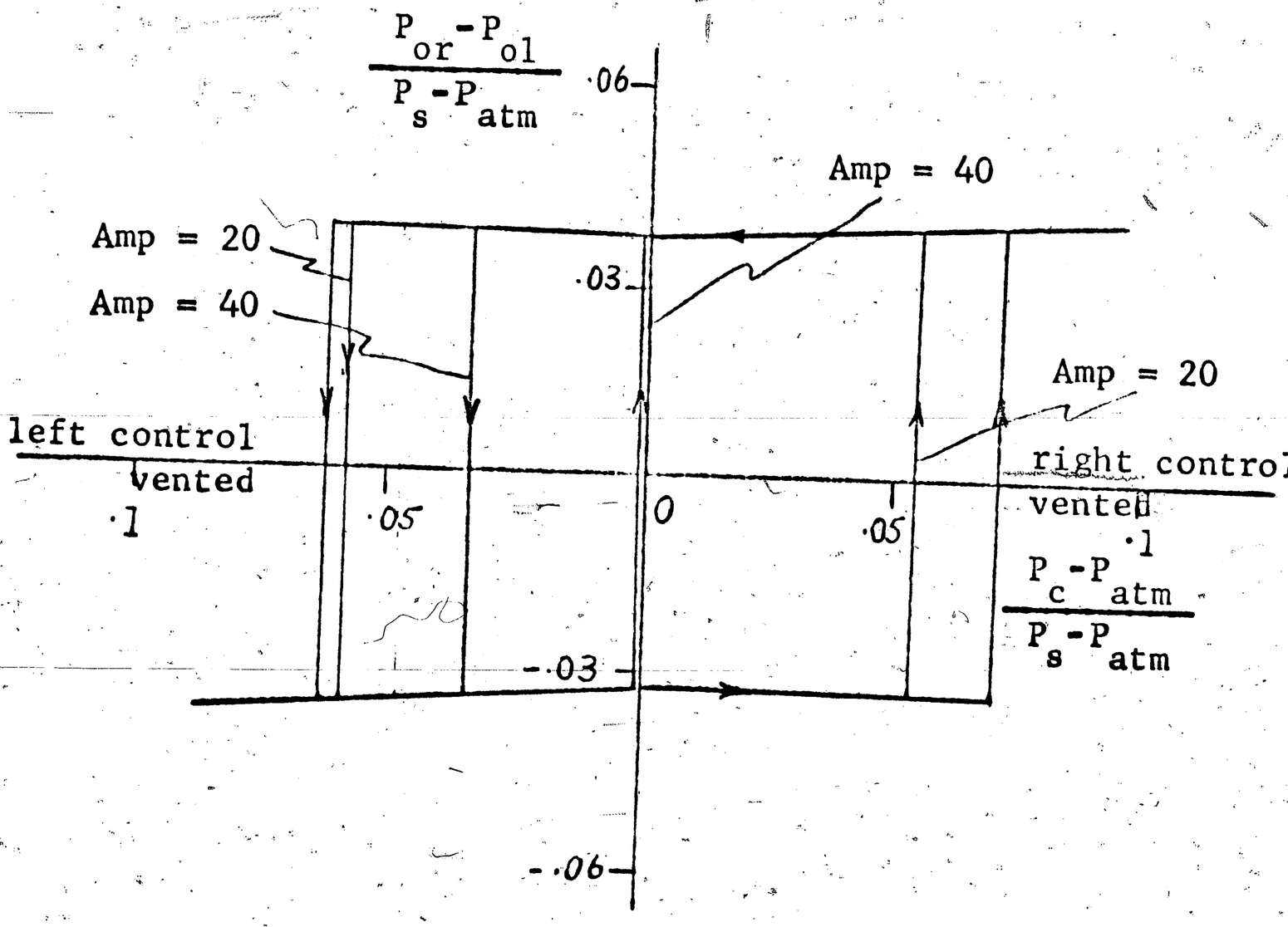

Figure 30 (b) frequency = 400 c/s

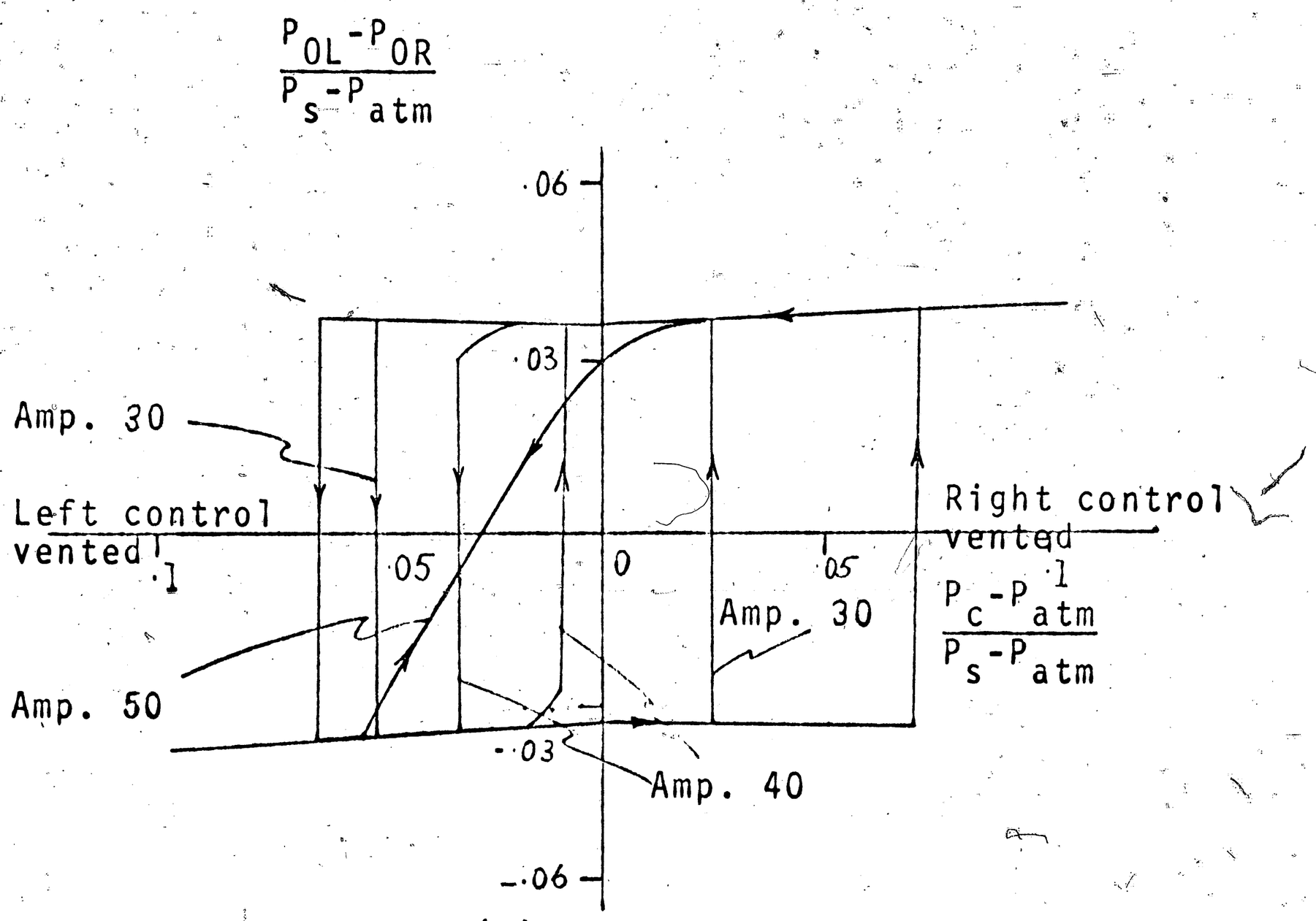

Figure 30(c) Frequency = 500 c/s

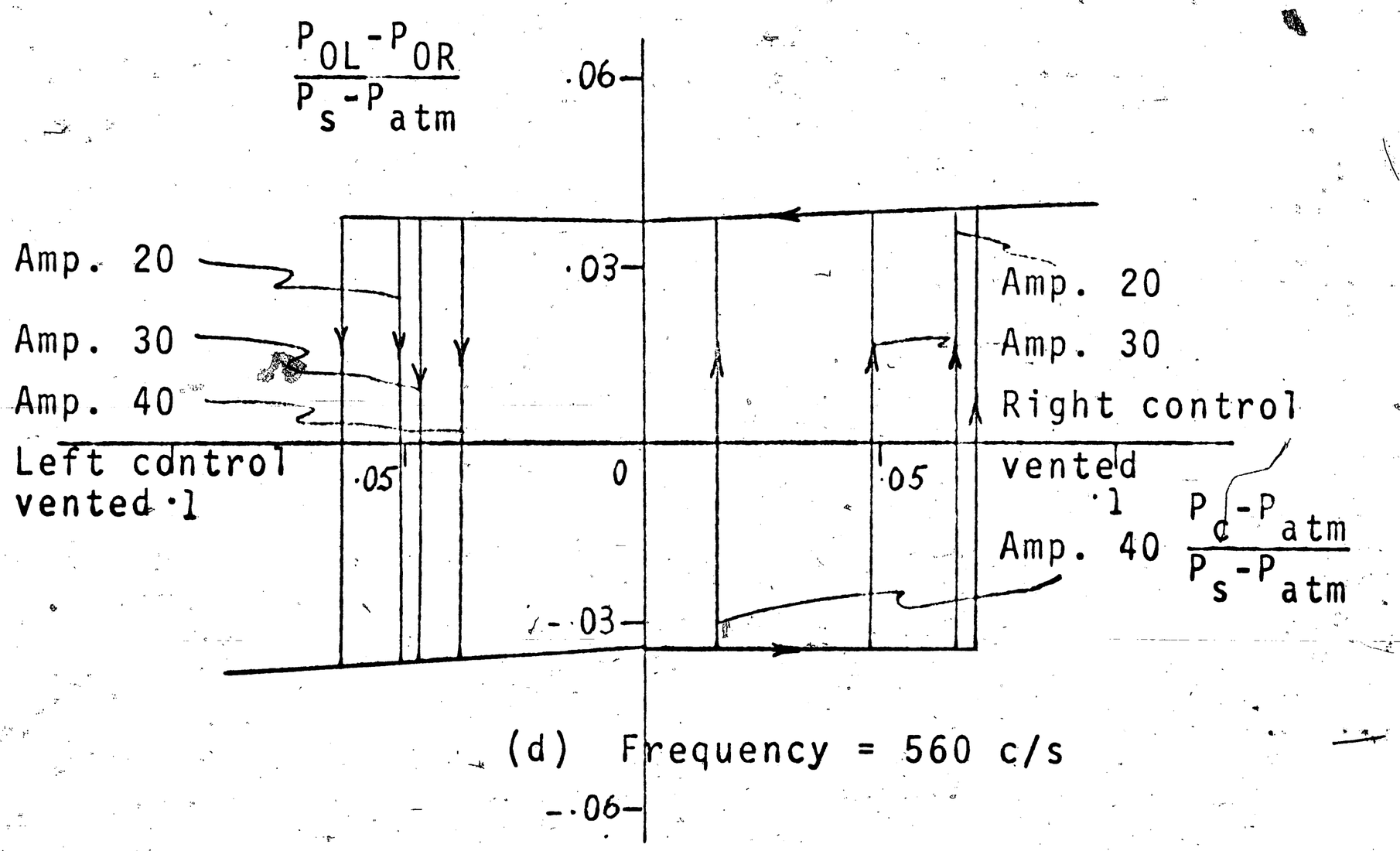

(d) Frequency = 560 c/s

Figure 30. Differential input-output characteristics. Supply pressure 3.0 psig.

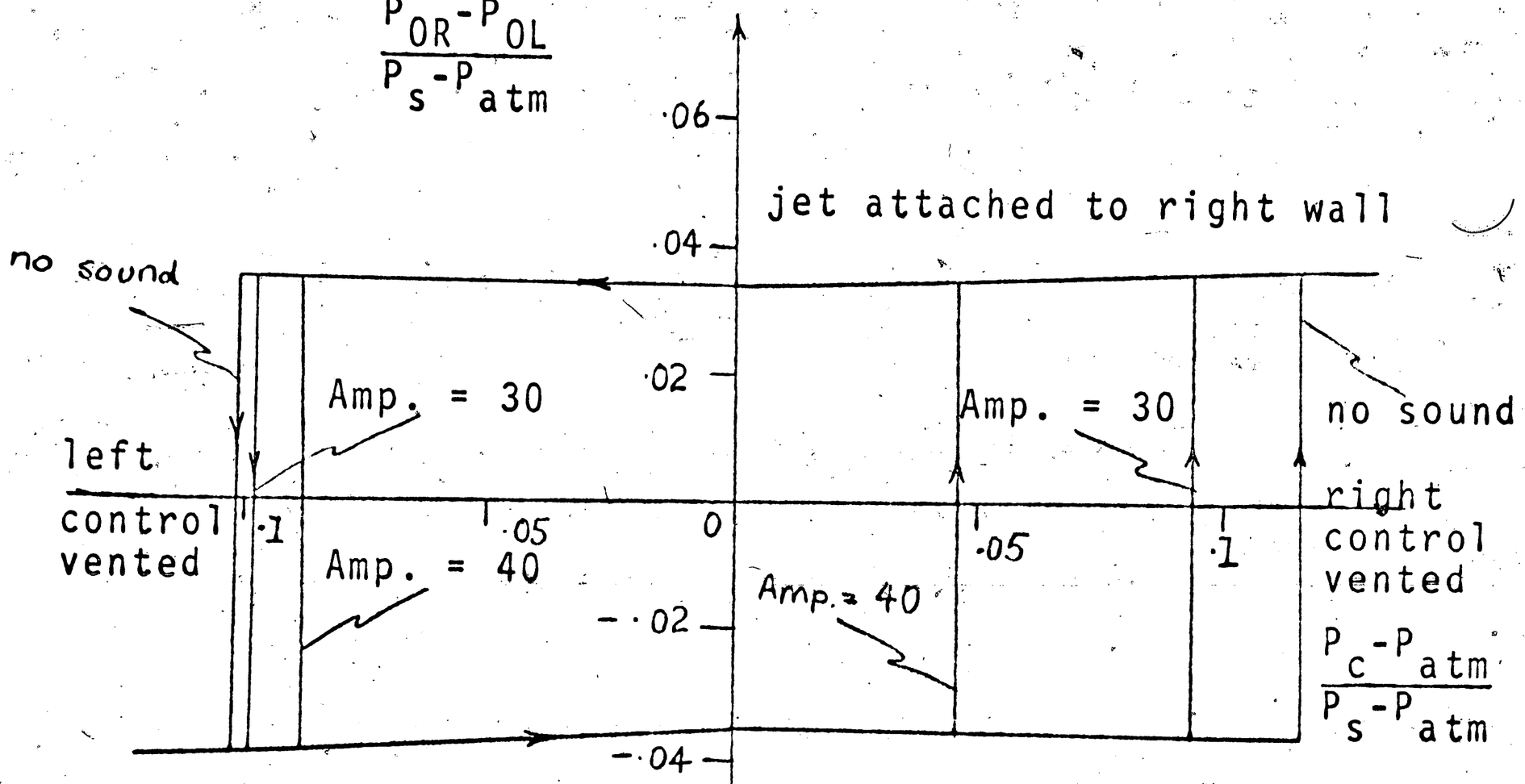

Figure 31(a) Frequency = 350 c/s

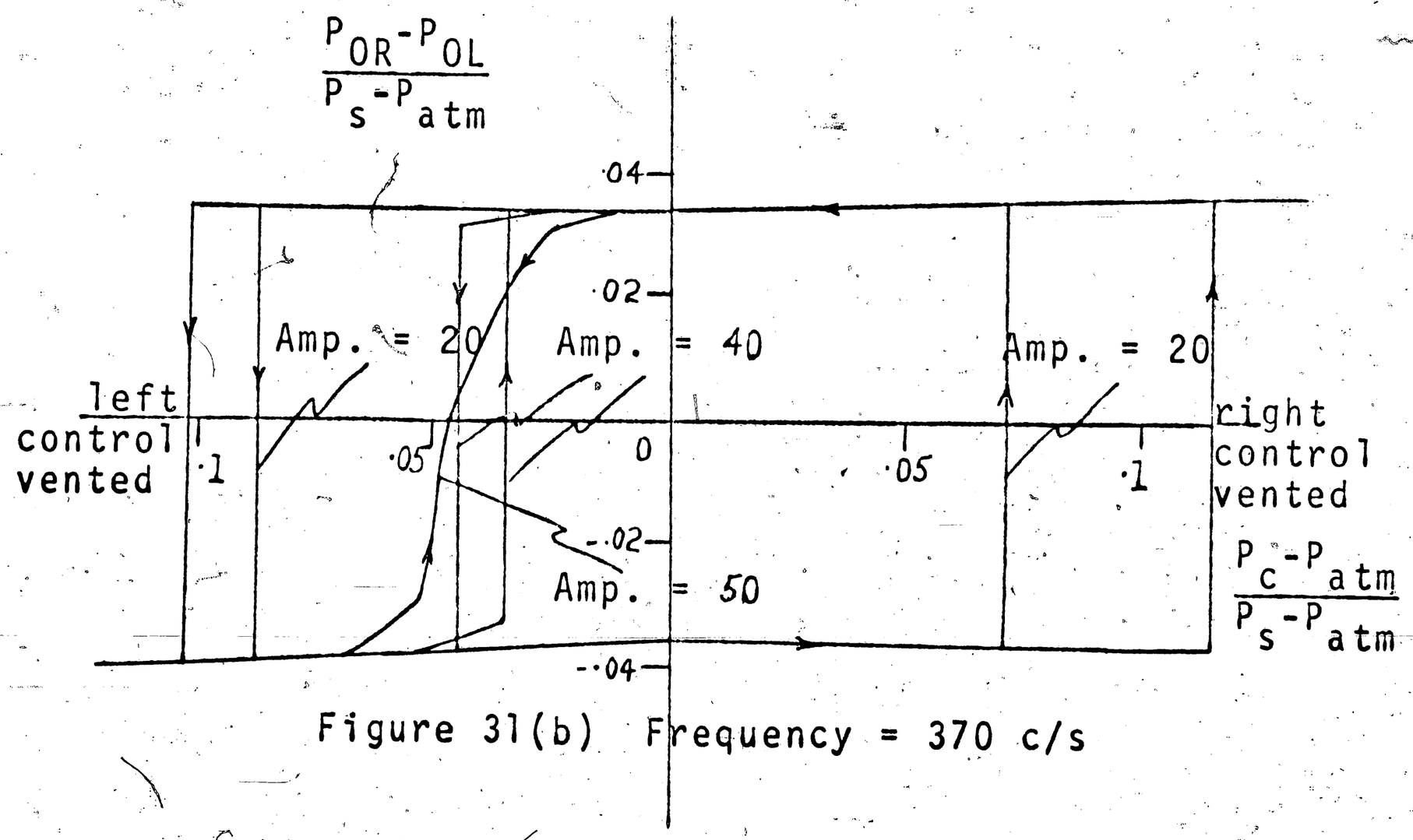

Figure 31(b) Frequency = 370 c/s

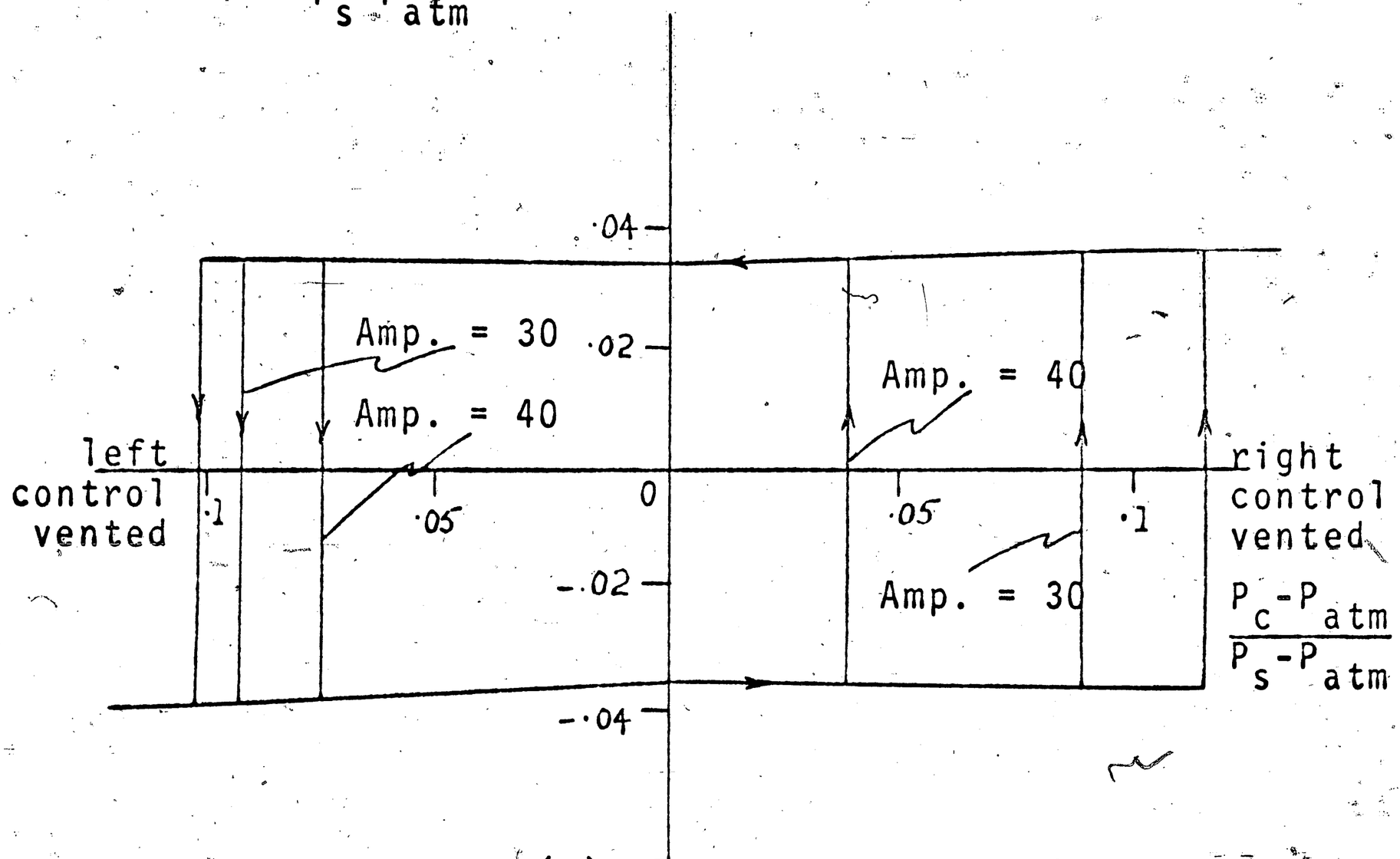

Figure 31(c) Frequency = 390 c/s

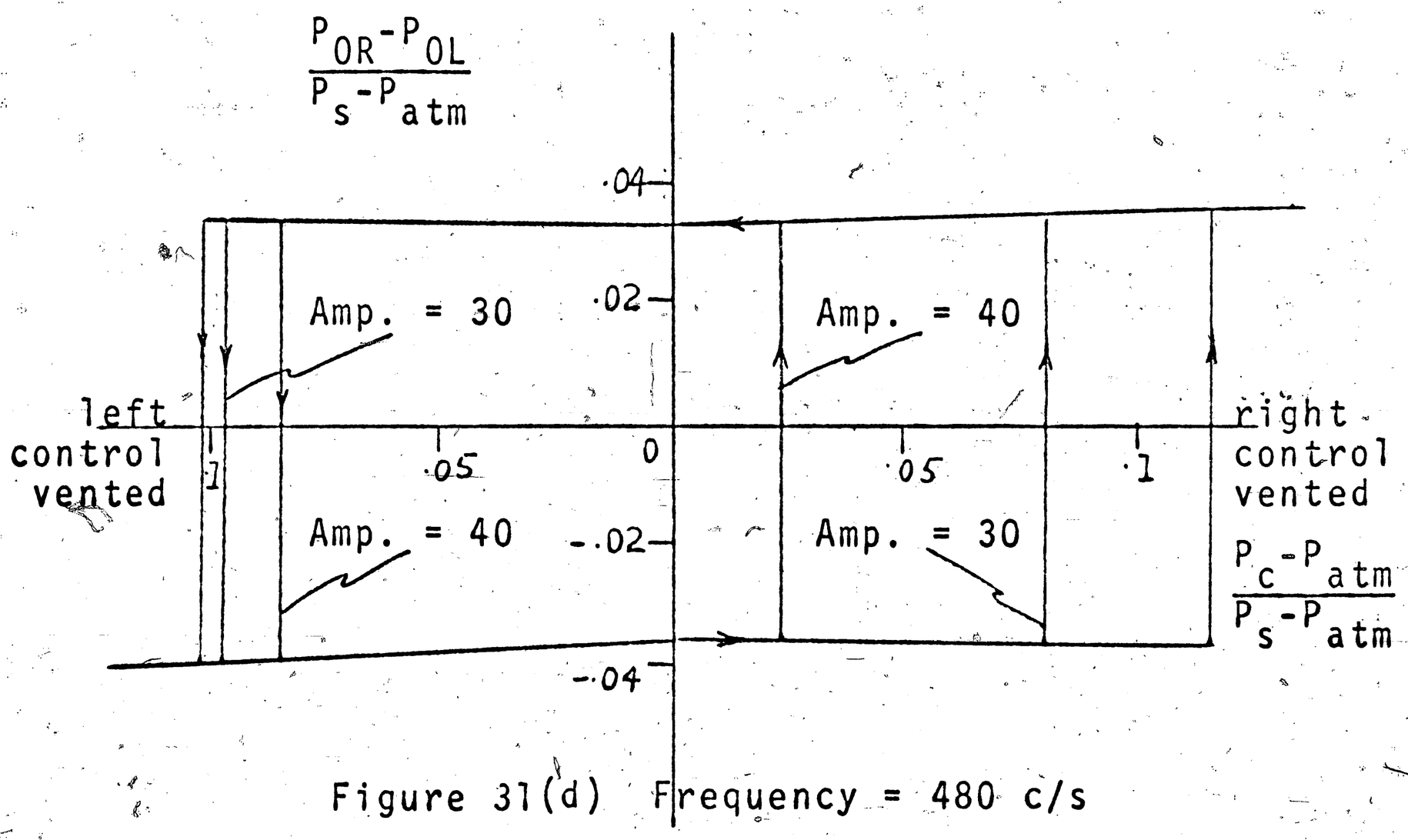

Figure 31(d) Frequency = 480 c/s

Figure 31. Differential Input-Output characteristic
Supply pressure = 5.0 psig

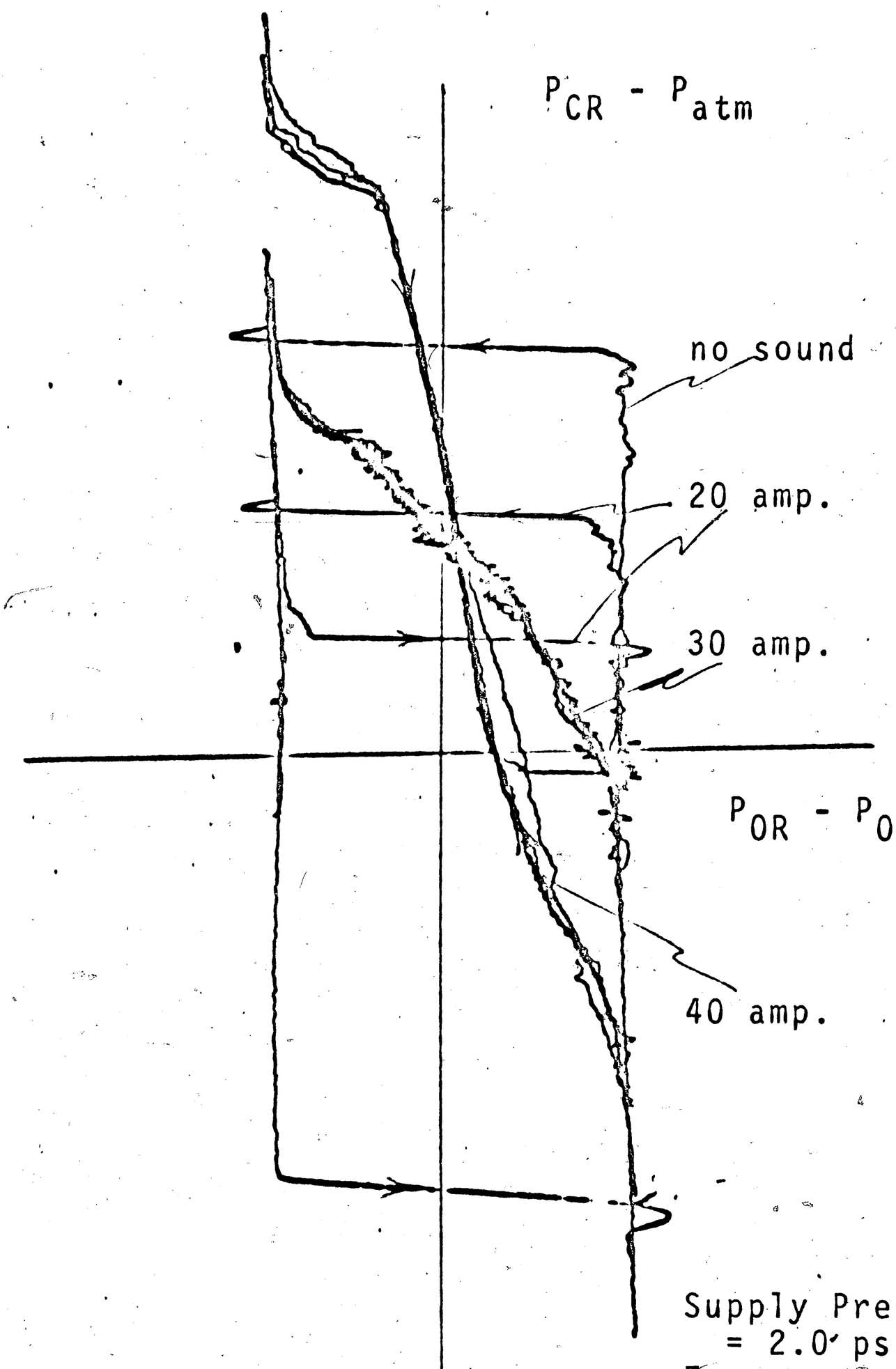
$P_{CR} - P_{atm}$
no sound
20 amp.
30 amp.
40 amp.
$P_{OR} - P_{OL}$
Supply Pressure
= 2.0 psig
Frequency = 375 c/s
Amplifier No. 1

Figure 32(a)

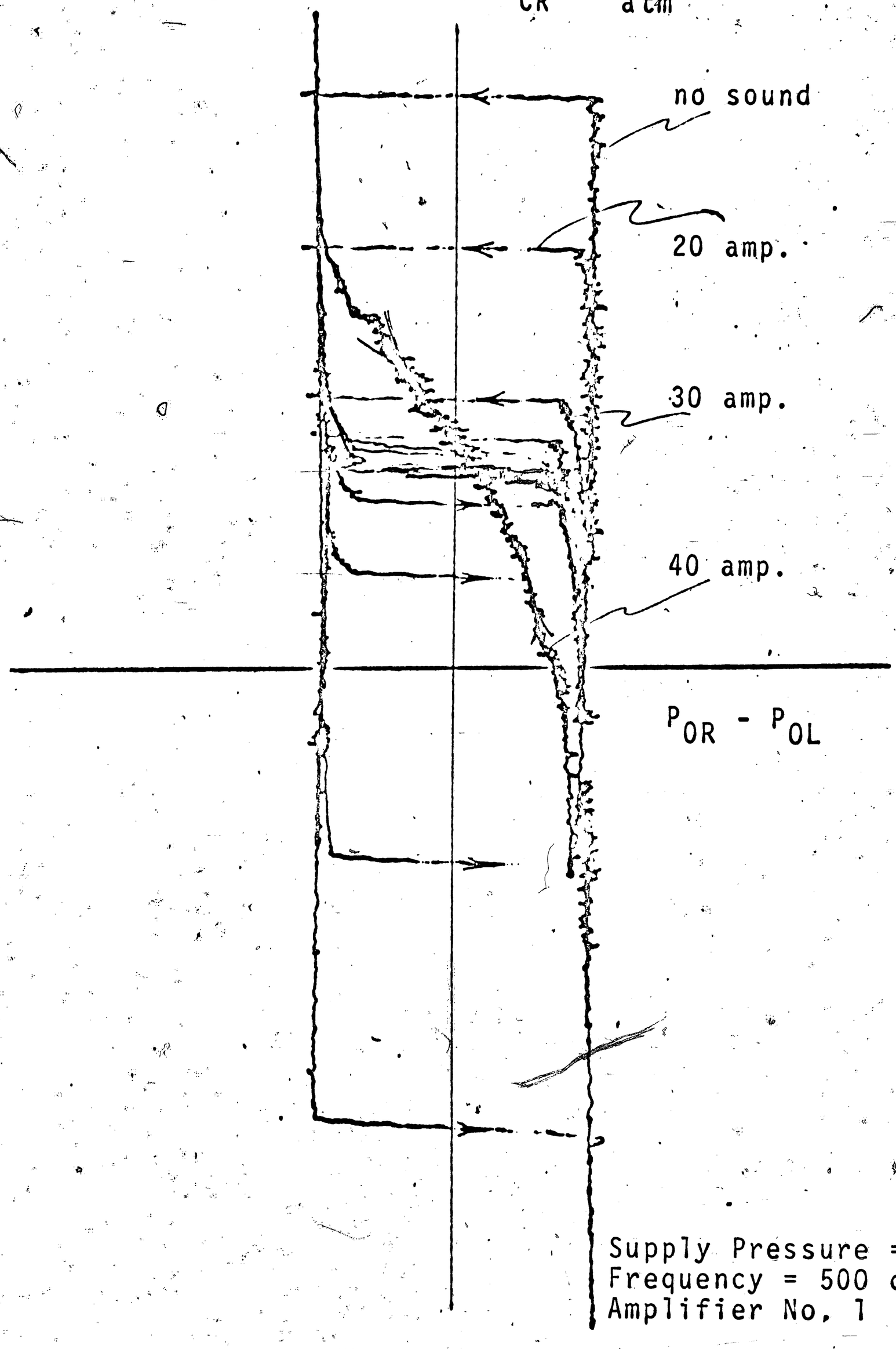
$P_{CR} - P_{atm}$
no sound
20 amp.
30 amp.
40 amp.
$P_{OR} - P_{OL}$
Supply Pressure = 3.0 psig
Frequency = 500 c/s
Amplifier No. 1

Figure 32(b)

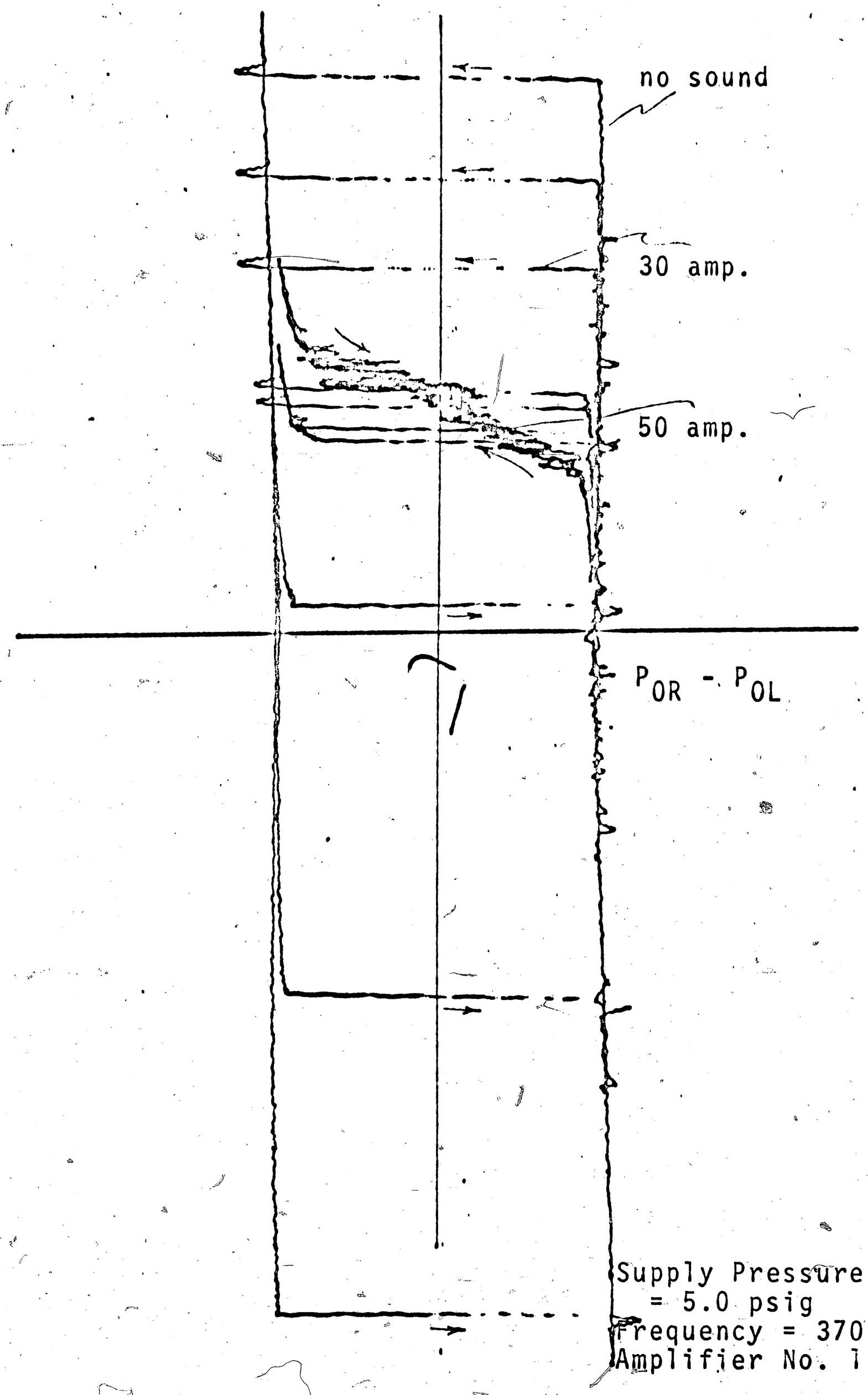

Figure 33(c)

Differential Input-Output Characteristics as obtained on the X-Y Plotter

VITA

Ramesh Gupta, the son of Mr. and Mrs. B. S. Gupta, was born on September 22, 1947, in Nairobi, Kenya. He attended elementary and high schools in Nairobi and graduated in December 1965. In April 1966, he entered University College, Nairobi, one of the three colleges forming the University of East Africa. He graduated in June 1969, with a Bachelor of Science with honors in Mechanical Engineering.

He received a fellowship from the African-American Institute and entered Lehigh University in September 1969, as a graduate student in the Mechanical Engineering Department.